

**REPORT  
42**



# **THE WOONGARRA RHYOLITE — A GIANT LAVALIKE FELSIC SHEET IN THE HAMERSLEY BASIN OF WESTERN AUSTRALIA**

**by A.F.Trendall**



**GEOLOGICAL SURVEY OF WESTERN AUSTRALIA  
DEPARTMENT OF MINERALS AND ENERGY**



**GEOLOGICAL SURVEY OF WESTERN AUSTRALIA**

**REPORT 42**

**THE WOONGARRA RHYOLITE —  
A GIANT LAVALIKE FELSIC SHEET  
IN THE HAMERSLEY BASIN OF  
WESTERN AUSTRALIA**

by  
**A. F. Trendall**

**Perth 1995**

**MINISTER FOR MINES**  
The Hon. George Cash, JP, MLC

**DIRECTOR GENERAL**  
K. R. Perry

**DIRECTOR, GEOLOGICAL SURVEY OF WESTERN AUSTRALIA**  
Pietro Guj

Copy editor: J. H. Thom

**REFERENCE**

The recommended reference for this publication is:

TRENDALL, A. F., 1995, The Woongarra Rhyolite — a giant lavalike felsic sheet in the Hamersley Basin of Western Australia: Western Australia Geological Survey, Report 42.

**National Library of Australia Card Number and ISBN 0 7309 6500 7**

Trendall, A. F. (Alec Francis).

The Woongarra Rhyolite — a giant lavalike felsic sheet in the Hamersley Basin of Western Australia

Bibliography.

ISBN 0 7309 6500 7.

1. Geology, Stratigraphic — Precambrian — Western Australia — Hamersley Basin.
2. Rhyolite — Western Australia — Hamersley Basin.
3. Hamersley Basin (W.A.).
  - I. Geological Survey of Western Australia.
  - II. (Series: Report (Geological Survey of Western Australia); 42).

ISSN 0508-4741

**Cover photograph:**

View to the east across the pool at the mouth of Woongarra Gorge showing the darker, rocky slopes of the steeply dipping Boolgeeda Iron Formation overlying the uppermost part of the Woongarra Rhyolite.

# Contents

Summary .....	1
Introduction .....	2
Purposes and scope of this report .....	2
Nomenclature .....	3
Regional setting .....	4
Previous investigations .....	4
Geochronology .....	6
Descriptions of main components .....	7
The basal contact .....	7
Lower unit .....	7
Median raft complex and other rafts .....	14
Upper unit .....	15
The rocks about the upper contact .....	18
Problems of definition .....	18
Peperite .....	18
The immediately overlying strata .....	22
The type and reference sections .....	22
Woongarra Gorge .....	22
Coondiner Gorge .....	25
Duck Creek .....	26
Fish Pool .....	28
Kalgan Creek area .....	29
Mount Maguire .....	30
Nallanaring Creek .....	31
Silver Grass Syncline .....	33
Wylloo Dome .....	35
Yeera Bluff .....	35
Geochemistry .....	36
Data available .....	36
Principal features .....	37
General character and homogeneity of composition .....	37
Peperite composition .....	39
Chemical effect of autobrecciation .....	39
Differences between the upper and lower units at Woongarra Gorge .....	40
Discussion .....	40
Salient features to be explained .....	40
Lavalike lithology .....	40
Shape and dimensions: area, thickness, volume .....	41
The upper and lower units .....	41
The median raft complex .....	41
The lower contact .....	41
The upper contact .....	41
Chemical composition .....	46
Relationship to sills of the Weeli Wolli Formation .....	46
Emplacement .....	47
Alternative hypotheses .....	47
Evaluation of the hypotheses .....	47
Antithetic thickness relationship .....	50
Formation of a tabular lava flow by eruption in deep water .....	50
Vesicularity .....	51
The upper margin .....	51
Intrusion: a preferred model .....	52
Tests of the proposed hypothesis .....	63
The Kaapvaal connection .....	63
Acknowledgements .....	65
References .....	66

## Figures

1. Geological map of the Pilbara Craton .....	4
2. Aerial photograph showing the outcrop expression of the Woongarra Rhyolite in the Kalgan Creek area .....	8
3. General view of the uppermost part of the Woongarra Rhyolite and the overlying Boolgeeda Iron Formation at Woongarra Gorge .....	9
4. The basal contact of the Woongarra Rhyolite exposed in cliffs in the axial area of the Brockman Syncline .....	10
5. Photograph of the lowermost rhyolite of the lower unit .....	10
6. Weathered surface of rhyolite of the lower unit from the Silver Grass area .....	12
7. Typical thin-section appearance of rhyolite of the lower unit .....	12
8. Thin section of rhyolite of the lower unit showing quartz-feldspar spherulites .....	13
9. Thin section of rhyolite of the lower unit showing quartz paramorphs after tridymite .....	13
10. Thin section of rhyolite of the lower unit showing microcrystalline chlorite .....	14
11. Embayed $\beta$ -quartzes from rhyolite of the lower unit .....	14
12. Disrupted rocks of the median raft complex of the Woongarra Rhyolite .....	15
13. Phenocrysts of rhyolites of the upper unit .....	16
14. Granophyric corona on plagioclase phenocryst in rhyolite of the upper unit .....	16
15. Typical thin-section appearance of rhyolite of the upper unit .....	17
16. Brecciated material from rocks of the upper unit .....	19
17. Plastic fold of laminar structure in rhyolite of the lower unit .....	20
18. Flow banding in rhyolite of the upper unit .....	20
19. Photomicrographs and macrophotos of thin sections of peperites associated with the upper contact .....	21
20. Comparative stratigraphic sections of the Woongarra Rhyolite in selected locations .....	23
21. Comparative sections of the upper contact of the Woongarra Rhyolite in selected locations .....	24
22. The upper contact of the upper unit at Woongarra Pool .....	25
23. Vertical cliffs, about 80 m high, cut in massive rhyolite of the upper unit on the west bank of Coondiner Creek .....	26
24. Banded peperite at the top of the median raft complex in the Duck Creek reference section .....	27
25. Thin-section photographs of the 'stratified' tuffs of the Duck Creek reference section .....	28
26. The upper contact of the Woongarra Rhyolite at the Kalgan Creek South locality .....	30
27. Composite photograph and explanatory sketch of the upper contact of the Woongarra Rhyolite at Kalgan Creek West location .....	33
28. Peperite lens at the locality of Figure 27 .....	34
29. Peperite lens, about one metre thick, dipping gently south at the locality of Figure 27 .....	34
30. Silica/total alkalis plot for groups 1, 2 and 3 .....	40
31. Jensen and AFM diagrams for groups 1, 2 and 3 .....	41
32. Harker plots of major oxides for groups 1, 2 and 3 .....	42
33. Harker plots of selected minor elements for groups 1, 2 and 3 .....	43
34. Spidergrams for groups 1, 2 and 3 .....	44
35. Various components against stratigraphic height for Woongarra Gorge section .....	45
36. Rb/K <sub>2</sub> O for all samples .....	46
37. Sr/Na <sub>2</sub> O for all samples .....	47
38. Cartoon sequence summarizing the suggested emplacement mechanism of the Woongarra Rhyolite .....	54
39. Hypothetical deep crustal cross sections depicting pressure and stress conditions within and adjacent to a rising column of magma .....	55
40. Relationship between radial velocity and length of major axis in a sill which has a uniform thickness of 200m and is an ellipse with a 5:1 elongation in plan .....	61
41. Simplified lithostratigraphic equivalence of part of the Precambrian supracrustal successions of the Pilbara and Kaapvaal Cratons .....	64

## Tables

1. Thicknesses of the Woongarra Rhyolite in the type and reference sections .....	11
2. Chemical composition of selected samples from the Woongarra Rhyolite .....	37

# The Woongarra Rhyolite — a giant lavalike felsic sheet in the Hamersley Basin of Western Australia

by

A. F. Trendall

## Summary

*Introduction.* The name giant lavalike felsic sheet (GLFS) is here proposed for very large concordant bodies of silicic rock that have the shape and extent of ash-flow tuffs but the lithology of lavas; GLFSs are widespread in time and space, and the origin of many is unclear. The Woongarra Rhyolite (previously Woongarra Volcanics) is a GLFS within the Precambrian Hamersley Group of Western Australia. This group is one of three that make up the Mount Bruce Supergroup, which was deposited in the Hamersley Basin between ~2.8 and ~2.4 Ga. The basin unconformably overlies a basement of granite–greenstone terrane that formed between ~3.5 and ~2.9 Ga. The Mount Bruce Supergroup and the underlying granite–greenstone terrane jointly make up the Pilbara Craton. The oldest (Fortescue) group of the Hamersley Basin consists of up to 7 km of mainly mafic lavas, with smaller felsic, pyroclastic, and epiclastic components; its stratigraphy is laterally variable. The overlying Hamersley Group is about 2.5 km thick, and is characterized by the presence of banded iron-formation (BIF) units, whose stratification displays remarkable continuity at all scales; the present outcrop area of the group is ~60 000 km<sup>2</sup>, with a maximum linear dimension of over 500 km. The Woongarra Rhyolite is a regionally concordant formation within the upper part of the Hamersley Group. It is underlain by the Weeli Weeli Formation and overlain by the Boolgeeda Iron Formation, the topmost formation of the group. An envelope enclosing outcrops of the Woongarra Rhyolite has an area of about 37 500 km<sup>2</sup>. The rhyolite has an average thickness of ~400 m. The *minimum* initial volume was  $15.4 \times 10^3$  km<sup>3</sup>, and may have been twice this. There has been surprisingly little previous study of this major felsic unit, although its extent has been well mapped at a scale of 1:250 000.

*Geochronology.* Reported conventional multigrain U–Pb zircon ages of  $2470 \pm 30$  Ma (Compston et al., 1981) and  $2439 \pm 10$  Ma (Pidgeon and Horwitz, 1991) lie within error, and the latter, which includes single-grain analyses, provides the best estimate for the crystallization age of the Woongarra Rhyolite. Extensive earlier Rb–Sr work yielded ‘anomalous’ ages up to ~500 m.y. too young.

*Descriptions of main components.* In spite of significant variations in total thickness and relative thicknesses of internal subdivisions, the Woongarra Rhyolite is consistently divisible into three main components: a lower unit, a median raft complex, and an upper unit. Both the lower and upper units consist mainly of massive, homogeneous rhyolite. The lower contact of the lower unit is rarely visible; in the only well-exposed section found, the contact is sharply defined against lithified BIF, and only a narrow chilled zone is present. Typically, the rhyolite of the lower unit is pale green, with a rough fracture, and a granular appearance due to abundant spherulites. Thin sections commonly show quartz paramorphs after tridymite, as well as a relatively coarse micropoikilitic texture. It is not conspicuously porphyritic. In contrast, the rhyolite of the upper unit is commonly porphyritic and dark grey, with a subconchoidal fracture. Although planar-flow texture, locally plastically folded, and brittle autobrecciation occur in both units, folds formed during magma flow are relatively abundant in the lower unit, whereas autobrecciation is more typical of the upper unit. The median raft complex is a stratigraphically impersistent sheet separating the upper and lower units, and consists variously of BIF, dolerite, and shale. All these rocks show evidence of disintegration or strain in situ. In most sections examined, a band of mixed breccia (peperite) of rhyolite and sedimentary clasts, often highly compacted, lies between the uppermost massive rhyolite and the overlying sedimentary rock. Sills of similar peperite, locally lenticular, occur within those rocks above the upper contact. Inconclusive evidence suggests that this is stratigraphically discordant.

*The type and reference sections.* The type section first proposed by MacLeod et al. (1963) for the Woongarra Volcanics at Woongarra Gorge is retained and redescribed as the type section for the Woongarra Rhyolite. Comparison with nine widely distributed reference sections (at Coondiner Gorge, Duck Creek, Fish Pool, Kalgan Creek, Mount Maguire, Nallanaring Creek, Silver Grass Syncline, Wyloo Dome, and Yeera Bluff) shows substantial regional thickness variations in the median raft complex, the lower unit, and the upper unit. The nature of the upper contact also shows considerable variation.

*Geochemistry.* Considering its large volume and areal extent, relatively few chemical analyses of rocks from the Woongarra Rhyolite exist. The available data include: 10 major-oxide and (in part) trace-element analyses of the upper unit, of which 7 are newly reported here and 3 previously published; 11 major-oxide and (in part) trace-element analyses

of the lower unit, of which 10 are new and 1 previously published; 4 major-oxide and (in part) trace-element analyses of peperites, of which 3 are new and 1 previously published; Rb, Sr, K and Na analyses of 43 samples from the Woongarra Gorge section; and 4 published Rb and Sr analyses (Leggo et al., 1965). The main conclusions from these data are: (i) all upper and lower unit samples lie within, or only just outside, the rhyolite field in the  $\text{SiO}_2/\text{total alkalis}$  plot internationally recommended for the chemical classification of volcanic rocks; (ii) no consistent chemical discrimination using major or trace elements is possible between rhyolites of the upper unit, rhyolites of the lower unit, and peperites with low sedimentary contents; (iii) major-element compositions are generally comparable with other rhyolites, but the  $\text{MgO}/\text{CaO}$  ratio tends to be unusually high, and  $\text{Al}_2\text{O}_3$  low; (iv) slight chemical differences exist between the upper and lower units at Woongarra Gorge, where there is also evidence that autobrecciation increases mobility of alkalis.

*Discussion.* Models for the emplacement of the Woongarra Rhyolite must account for its lavalike lithology, its vast areal extent and volume, its regionally consistent subdivision into two lithologically distinct units having the same chemical composition, the presence of the median raft complex, and the peperites associated with an upper contact, which seems to show slight stratigraphic discordance. Emplacement as subaerial lava flows would require at least one, and possibly two, associated tectonic events involving exposure and resubmergence of the Hamersley Basin floor. The sheet-like form of both rhyolite units of the Woongarra Rhyolite would also require physical behaviour of the lava inconsistent with experimental and observational evidence. Such an emplacement mechanism is not credible. The problem posed by the sheet-like form is overcome by supposing that the rhyolite units are secondarily remelted ash-flow tuffs. Although these would be substantially larger than any ash-flow tuffs so far recorded, this possibility is hard to refute, but it still requires the coupled tectonic exposure and resubmergence events.

Deep-water extrusion of silicic magma has been proposed elsewhere as a mechanism for forming extensive stratiform silicic bodies, but the evidence for the only published example seems inconclusive; and it is hard to conceive how such gravity-driven lava flows could extend evenly throughout a basin. Emplacement by ash-flows that penetrated below the basin water following massive subaerial eruptions on the adjacent land overcomes this gravitational objection, but remains inconsistent with the lavalike lithology of the rhyolites. In any case, none of the preceding hypotheses provides a natural explanation of the peperites associated with the upper contact, or accommodates the possibility of stratigraphic discordance.

A hypothesis involving emplacement by intrusion of both the upper and lower rhyolite units as sills, injected via a comparatively small feeder pipe in the central part of the outcrop area, is consistent with all the described features of the Woongarra Rhyolite. The upper unit was injected first. When the rising rhyolitic magma ( $2.2\text{g}/\text{cm}^3$ ) reached the base of the zone of diagenesis ( $\sim 200\text{--}300\text{ m}$  below the sediment/water interface) immediate vapourization of water in the wet but lithified BIFs led to their explosive disruption, and formation of a chaotic fluidized breccia of BIF and magma fragments ('proto-peperite') which was injected laterally along the fissile stratification to initiate a sill. Rhyolitic magma (at  $\sim 1000^\circ\text{C}$ ) followed close behind, and gradually spread as a sill of elliptical plan (elongate 5:1), forcing the proto-peperite against the roof and compacting it to form the present peperite. Proto-peperite was also injected up tension cracks to form sills in the overlying strata as the rim of the sill advanced; this is both a predicted and observed phenomenon associated with the dynamics of sill emplacement.

At an assumed constant magma supply rate of  $10^3\text{ m}^3/\text{s}$  the radial velocity of the 200 m-thick sill declined exponentially, and reduced to  $\sim 1.6 \times 10^{-5}\text{ m/s}$  after  $\sim 7.5 \times 10^9\text{ s}$ , or about 240 years; the major axis of the ellipse was then about 500 km long. Cooling models for tabular intrusions are consistent with a viscosity ( $< 10^{13}$  poises) low enough to accommodate these flow parameters. Sill injection formed a corresponding 'blister' on the basin floor. After emplacement of the upper unit sill there was an interval ( $\sim 500$  years) before further rise of identical magma up the same feeder pipe. This was unable to penetrate the partially cooled upper unit sill, and again spread laterally to form a second, thinner sill (the lower unit) in the hot ( $\sim 400^\circ\text{C}$ ) and dry sedimentary rocks below. Lithological, and other, differences between the chemically near-identical upper and lower units are explained by resultant differences in emplacement and cooling conditions. The intrusion model proposed is the only one consistent with the common presence of peperite sills above the top of the Woongarra Rhyolite, and with stratigraphic discordance of the upper contact.

The geological evolution of the Pilbara Craton and the Kaapvaal Craton of southern Africa have many analogous features, and from available descriptions the Rooiberg Felsite of the Transvaal Supergroup shows a number of similarities to the Woongarra Rhyolite.

**KEYWORDS:** GLFS, giant lavalike felsic sheet, Hamersley Basin, Pilbara Craton, rhyolite, sill emplacement, volcanology, Western Australia

## Introduction

### Purposes and scope of this report

A number of concordant stratiform felsic volcanic units of vast areal extent occur in the Precambrian stratigraphic record of Australia. Examples, in order of increasing age, include the  $\sim 1600$  Ma Yardea Dacite of the Gawler Range Volcanics, the  $\sim 1850$  Ma Whitewater Volcanics of the

Kimberley Basin, the  $\sim 2440$  Ma Woongarra Rhyolite, and the  $\sim 2760$  Ma Bamboo Creek – Spinaway Porphyry, both of the Hamersley Basin.

A recent paper on the Yardea Dacite (Creaser and White, 1991) has highlighted an unresolved problem presented by many of these bodies: their combination of the very large areas and low aspect ratios typical of ash flows with the lithologies of lavas. Henry et al. (1988) have drawn attention to the identical problem in the

Tertiary Trans-Pecos volcanic field of Texas and, following Ekren et al. (1984), applied the term 'lavalike' to the rocks of the extensive silicic sheets they described. The problem has also been identified in southern Africa (Twist and Bristow, 1990). In this report such bodies are called giant lavalike felsic sheets (GLFS).

Neither Creaser and White (1991) nor Henry et al. (1988) offered a resolution of the GLFS paradox, and it remains an open question whether any GLFS really flowed as a liquid lava, or whether they were all emplaced as ash flows (i.e. as hot fluidized ash clouds), and acquired their lavalike characteristics during subsequent processes, which also destroyed all trace of a pyroclastic origin. In the case of the Woongarra Rhyolite, a GLFS of the Hamersley Basin, an alternative resolution of the paradox lies in an intrusive, rather than an extrusive, emplacement mechanism.

The first purpose of this Report is to bring together sporadic field and petrographic observations on the Woongarra Rhyolite made at intervals by the author over a period of nearly 30 years, and integrate them with the published results of others in a systematic way. The second purpose is to review these data in relation to the GLFS paradox, and assess their relevance to Woongarra Rhyolite emplacement.

The observations on which this Report is based are mainly confined to the type locality and a small number of regionally distributed reference sections (Staines, 1985, p. 99) in locations where part or all of the thickness of the Woongarra Rhyolite is known to be well exposed. A number of major outcrop areas, such as those of the Brockman and Turner Synclines, were visited only briefly, and no sections in these areas were systematically examined. The distribution of reference sections over the total outcrop area is indicated in Figure 1. A general description of the internal structure of the Woongarra Rhyolite, based largely on the type and reference sections, is first presented. This is followed by individual reference section descriptions, which maintain a systematic sequence of subheadings. A brief account of the limited geochemical data available follows. In the final section headed **Discussion** it is concluded that the total available evidence is consistent with an intrusive origin, and hypotheses involving extrusion of the Woongarra Rhyolite either fail to account for some of its features or require implausible concepts of basin evolution.

## Nomenclature

The rocks of the Woongarra Rhyolite have hitherto been generally accepted as extrusive. This has been implicit in the name 'Woongarra Volcanics', which has been mainly used for the unit. The Australian Code of Stratigraphic Nomenclature (1973) recommends application of the term 'Volcanics' only to 'assemblages of volcanic rocks consisting of lavas and pyroclastic rocks of different kinds', a usage whose continuation is endorsed by Staines (1985). This description can no longer be

considered to apply to the Woongarra Rhyolite, and the name 'Woongarra Volcanics' is therefore discontinued. The section in the vicinity of Woongarra Pool, originally designated by MacLeod et al. (1963) as the type section of the 'Woongarra Dacite', is retained as the type section of the Woongarra Rhyolite. The name Woongarra Rhyolite is preferred to 'Woongarra Formation' since the Australian Code of Stratigraphic Nomenclature (1973, Article 19) recommends that 'the term "formation" should be used as part of the name only where the lithology of the beds cannot be described by one lithological term ... because ... it does not consist mainly of one lithological type'; the Woongarra Rhyolite consists predominantly of rhyolite. Although Staines (1985) has drawn attention to special problems in applying stratigraphic nomenclature to igneous rocks, the effective regional concordance of the Woongarra Rhyolite throughout its outcrop area makes it appropriate to continue to regard it as a component formation within the Hamersley Group.

Cas and Wright (1987, p. 224–5) have discussed the nomenclature of pyroclastic flow deposits and noted a preference by the 'English school' for the term ignimbrite (Marshall, 1935) for the rock usually referred to in American literature as ash-flow tuff (Ross and Smith, 1961). For consistency the latter term is used throughout this Report, largely because of the convenient distinction between an ash flow (the dynamic phenomenon) and an ash-flow tuff (the lithified result of an ash flow). There is no implication of a restriction of grain size.

The term peperite was used by Scrope (1862) for basaltic tuffs and breccias of the Limagne area of central France. The genesis of the originally described speckled 'pepper rocks' is now controversial (Jones, 1967; Fisher and Schmincke, 1984, p.264), and the name was little used through the early part of the present century. Its use was revived by Smedes (1956, 1966), and Schmincke (1967) used the term for breccias formed by the invasion of wet sediments by lavas flowing over them. More recently the name has been commonly applied to mixed rocks formed during the intrusion of magma into wet sediments, mostly at relatively shallow depth (e.g. Brooks et al., 1982; Hanson and Schweickert, 1982; Kokelaar, 1982; Busby-Spera and White, 1987; Branney and Suthren, 1988). Peperite is used here as a non-genetic term for a clastic rock composed of an intimate mixture of fragmented magmatic and sedimentary material, formed during, and due to, the emplacement of the magma. However, it so happens that the peperites here described are also believed to result from the interaction between intrusive rhyolitic magma and the wet sediment with which it came into contact at shallow depth. The proportion of sedimentary material in peperites is highly variable, and usually impossible to quantify without chemical analysis. It is therefore convenient to apply the word to a gradational sequence of rocks in which the sedimentary component may vary from about half to virtually nil, rather than use the more correct terms hyaloclastite or hydroclastite (according to genesis) for those that consist almost entirely of comminuted glass resulting from the marginal chilling of magma.

## Regional setting

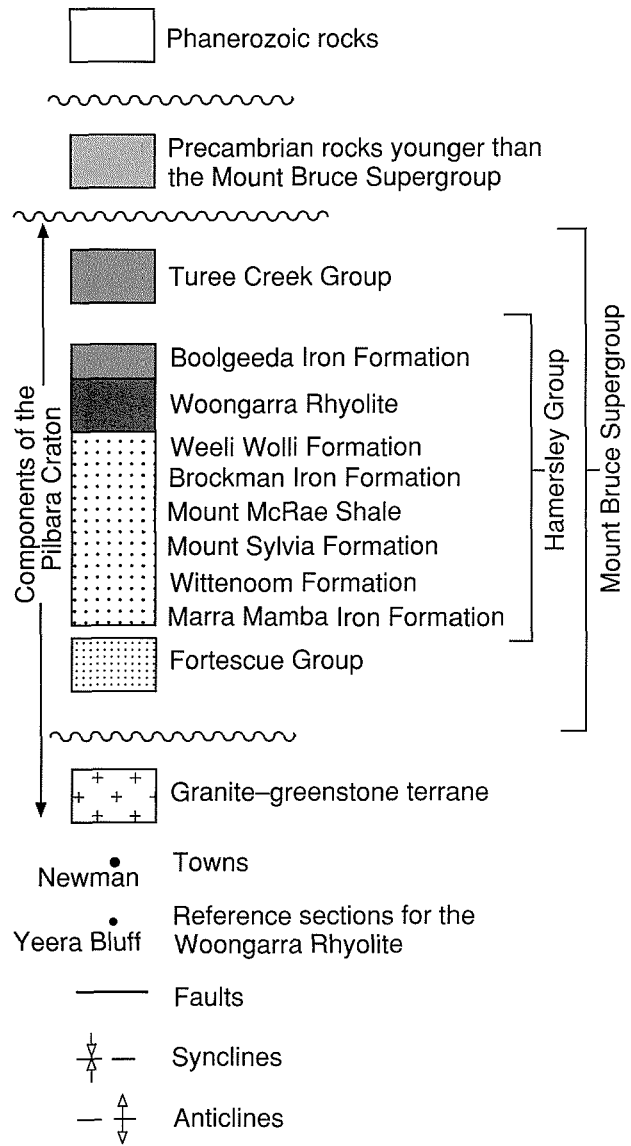
The Hamersley Basin is the younger of the two main components of the Precambrian Pilbara Craton, in the northwestern part of Western Australia (Geological Survey of Western Australia (GSWA), 1990; Fig. 1). The older component of the craton, the north Pilbara granite-greenstone terrane, has the classical features of such a terrane: extensive domal granitoid complexes are marginally intrusive into, and separated by, tightly folded and broadly synclinal greenstone belts. Both the dominantly volcanic greenstone sequences and the contiguous granitoids have similar age ranges, of about 3.5–2.9 Ga, and evolved as tectonically and petrogenetically related components of an episode of primary crustal generation.

The Hamersley Basin developed during the approximate interval 2.8–2.4 Ga as a supracrustal basin over this granite-greenstone terrane, after it had become relatively stable and had undergone extensive denudation. The rocks laid down in the basin are collectively called the Mount Bruce Supergroup; this group has three component groups called, from oldest to youngest, the Fortescue Group, Hamersley Group, and Turee Creek Group. Apart from locally strong tectonism close to the edges of the Pilbara Craton, the rocks of the Mount Bruce Supergroup have undergone relatively little deformation or metamorphism since their deposition. Broad regional uplift of the Pilbara Craton has resulted in the development of excellent exposures of all three component groups in the southern part.

The ~2.4 km-thick Hamersley Group, which conformably overlies the basal and dominantly volcanogenic Fortescue Group, is characterized by abundant banded iron-formation (BIF), whose presence has led to the development of major high-grade iron orebodies. These currently support an annual production of more than 100 000 000 tonnes. In addition, a significant part of the thickness of the group, locally exceeding 30% (Trendall and Blockley, 1970, table 1), consists of stratigraphically concordant, felsic, igneous rocks. These rocks, lithostratigraphically defined as the Woongarra Rhyolite (Fig. 1), are the subject of this Report. The open regional folding associated with the rise of the Pilbara Craton has led to generally excellent exposure of the Woongarra Rhyolite; exposures are present in a number of structurally controlled outcrop areas (Fig. 1), separated either by anticlinorial or domal areas from which the Woongarra Rhyolite has been stripped by erosion, or by synclinal areas where it is concealed by younger rocks.

## Previous investigations

In spite of their vast areal extent and excellent exposure, as well as the challenge presented by the problem of their mode of emplacement, the rocks of the Woongarra Rhyolite have received remarkably little geo-scientific attention. The Woongarra Rhyolite was first recorded in the eastern part of the Ophthalmia Range by H. W. B. Talbot (1920). He described bands of porphyry

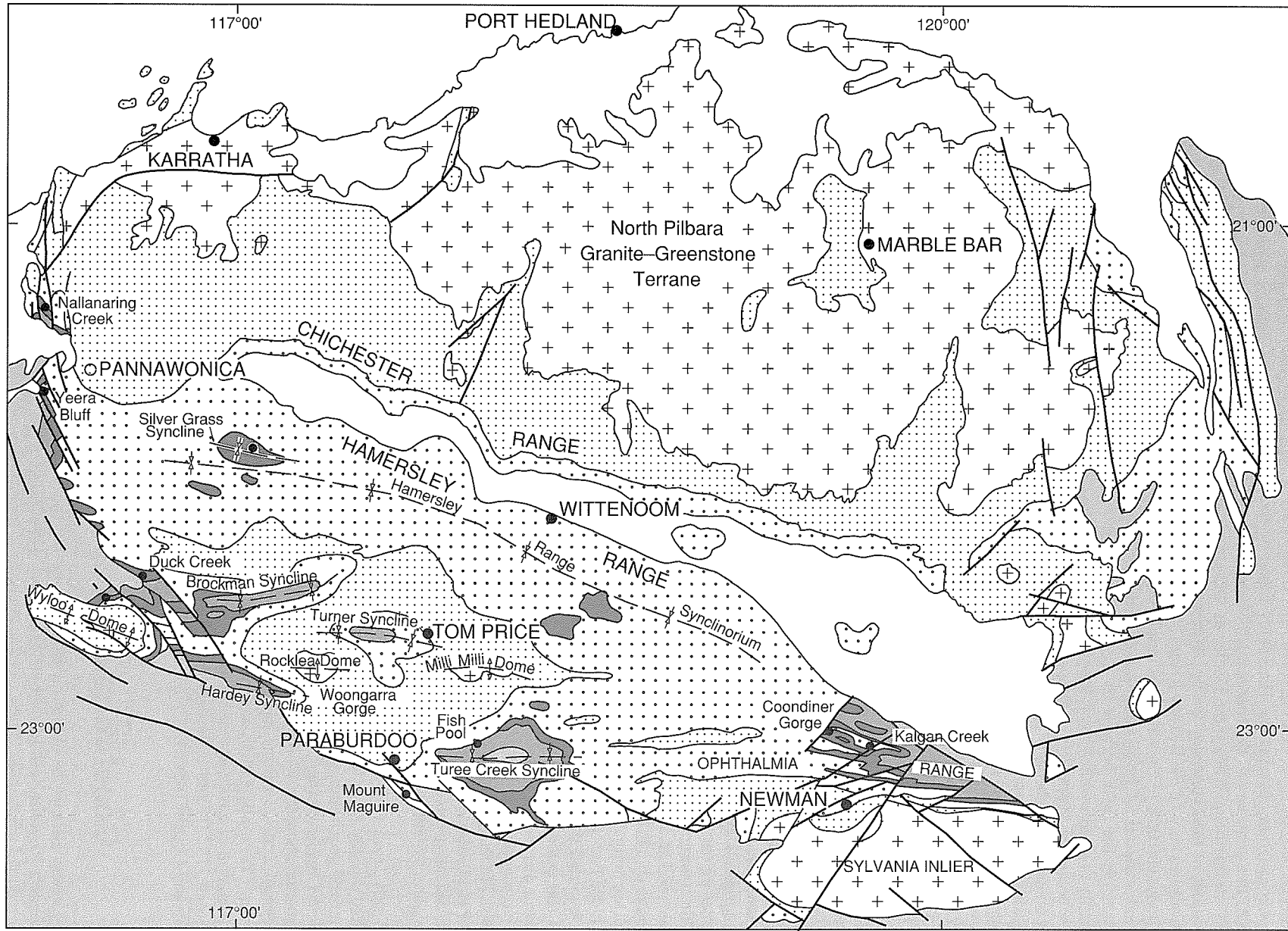


AFT114A

01.08.95

**Figure 1.** (facing page, with Reference above) Geological map of the Pilbara Craton, showing outcrop areas of the Woongarra Rhyolite, the locations of the type and reference sections, major structural features, and the location of towns and selected physiographic features. The thickness of the Woongarra Rhyolite is shown in correct proportion within the 2.5 km-thick Hamersley Group; other parts of the stratigraphic column are purely diagrammatic. Note that units of the Mount Bruce Supergroup above and below the Woongarra Rhyolite are not distinguished. Geological boundaries modified after Myers and Hocking (1988)

in inclined strata of the 'Nullagine Series', 'so that they may be interbedded lavas or intrusive dykes or sills'. Talbot was unable to make a judgement on their status from field evidence, but noted the view of R. A. Farquharson (1920) that they were lavas, an opinion based solely on the petrography of three thin sections of



5

samples collected by Talbot.

No further work was published until after the commencement, in 1962, of a systematic 1:250 000-scale mapping program covering the Hamersley Basin by the GSWA. In a summary of the first results, MacLeod et al. (1963) defined the Woongarra Dacite as one of eight formations of the Hamersley Group, with a type locality at Woongarra Pool on the Beasley River (latitude 22°53'S, longitude 117°06'E). They noted a number of different textural varieties of lava, including one called 'green quartzite' in the field, because of its strong lithological similarity to a sedimentary rock. Brief descriptions of the unit subsequently appeared in the published explanatory notes on individual sheets of the 1:250 000-scale mapping program. De la Hunty (1965) amended the name to Woongarra Volcanics on MOUNT BRUCE\* and this was followed on subsequently published sheets, namely NEWMAN (Daniels and MacLeod, 1965), ROY HILL (MacLeod and de la Hunty, 1966), PYRAMID (Kriewaldt and Ryan, 1967), YARRALoola (Williams, 1968), TUREE CREEK (Daniels, 1968), ROBERTSON (de la Hunty, 1969), and WYLOO (Daniels, 1970). MacLeod (1966), in an early synthesis of the results of the mapping program, described the Woongarra Rhyolite (under the name Woongarra Volcanics) as 'an important cycle of acid volcanism which interrupted the protracted cycle of sedimentation of the Hamersley Group'. He also collated the information available at that time on their thickness and regional extent. He emphasized their basin-wide stratigraphic concordance, and noted that no source vent could be identified, as well as the 'puzzling feature of these rocks that there should be such a wide lateral uniformity in lavas which are normally regarded as very viscous'; he therefore concluded that 'the volcanism was mainly submarine'. He also recorded the presence of 'a tuff bed, up to 30 feet thick and extending laterally for 20 miles, at the top of the lava succession' in the Ophthalmia Range area. Later remapping of WYLOO (Seymour et al., 1988), ROBERTSON (Williams and Tyler, 1989), NEWMAN (Tyler et al., 1991), and TUREE CREEK (Thorne et al., 1991) did not involve major revision of the geology of the Woongarra Rhyolite.

Apart from the publications already noted that resulted directly from the GSWA mapping program, and specialized geochronological papers referred to under the heading **Geochronology**, only a few other papers record information about the Woongarra Rhyolite. These include petrographic descriptions and comments on selected samples (Trendall, 1963), a detailed description and interpretation of a rock associated with the upper contact (Trendall, 1972), and a description of the section at Woongarra Gorge (Trendall, 1976).

## Geochronology

The earliest attempt to obtain an isotopic age for the Woongarra Rhyolite was made by Leggo et al. (1965). They reported whole-rock Rb–Sr isotopic analyses of four samples, collected during the 1:250 000 GSWA mapping

\* Capitalized names refer to standard map sheets.

program from the western end of the Brockman Syncline; sample positions are shown in Leggo et al. (1965). The four samples were widely dispersed on a conventional isochron plot, and gave a poorly fitted isochron of 2060 Ma. The authors argued that a better interpretation of the data was obtained by a 2-point isochron of 2130 Ma joining two of the samples taken from the same exposure (R258, R259), which was not greatly different from the age of 2080 Ma given by a line joining the remaining two points (R255, R656). They concluded that the age of the Woongarra Rhyolite was about 2100 Ma, with the two pairs of samples lying on nearly parallel isochrons with initial  $^{87}\text{Sr}/^{86}\text{Sr}$  ratios of 0.715 and 0.700 respectively.

A comparison of the petrographic descriptions, given by Leggo et al. (1965) of their four Woongarra Rhyolite samples, with descriptions later in this Report leaves no doubt that the two pairs of samples selected by them for independent regression came respectively from the lower unit (R258, R259) and the upper unit (R255, R656) as here defined.

To clarify these inconclusive results, a further 46 samples were collected systematically through the Woongarra Rhyolite section at Woongarra Gorge for Rb–Sr isotopic analysis; the stratigraphic positions of 43 of these samples were shown by Trendall (1976, fig. 22). Although the results were not fully reported by Compston and Arriens (1968, p. 567), they provided an interpretation which gave 'an age of  $2000 \pm 100$  Ma with low  $^{87}\text{Sr}/^{86}\text{Sr}$  for acid lavas'. They (ibid.) also noted that 'regression of data from other stratigraphic zones gives a markedly higher  $^{87}\text{Sr}/^{86}\text{Sr}$  ratio, indicating open chemical system behaviour with regard to Rb and (or) Sr'. Arriens (1975), in a later abstract, reinterpreted the same data in the following terms: 'These data can be resolved into at least three populations with parallel isochrons of 2000 Ma age and separate initial ratios in the range from .70 to .78.' Trendall (1976, p. 23–24) noted a further reinterpretation in the form of a personal communication from Arriens, suggesting that selected data may also indicate a thermal up-dating at about 1700 Ma.

Finally, Compston et al. (1981) summarized a completely revised interpretation of the same Rb–Sr data in which the isochron method was discarded 'in favour of the use of Rb–Sr model ages, in which a realistic, low value for the initial  $^{87}\text{Sr}/^{86}\text{Sr}$  is assumed'. Their interpretation continued: 'For 36 radiogenic samples in which the model age is not sensitive to small uncertainty in the initial  $^{87}\text{Sr}/^{86}\text{Sr}$ , peaks in the model-age frequency distribution are found at ~2370 Ma and ~1950 Ma.'

The stimulus for this further reinterpretation was the need to reconcile the Rb–Sr data with the conventional<sup>†</sup> multi-grain zircon U–Pb age of  $2470 \pm 30$  Ma, which they (Compston et al., 1981) also reported. They therefore

<sup>†</sup> Pidgeon and Horwitz (1991, p. 57) incorrectly referred to this age as 'determined on the ANU ion microprobe'. The Sensitive High Resolution Ion MicroProbe (SHRIMP) at the Australian National University was not in productive operation before 1982, and the work reported by Compston et al. (1981) was on conventional multi-grain zircon fractions split on a Frantz magnetic separator.

continued: 'this bimodal distribution is consistent with an original age for the Volcanics of at least 2370 Ma followed by re-setting of the total-rock ages for many samples at  $\leq 1950$  Ma, so that the Rb–Sr results can be understood in terms of the 2470 Ma zircon age'.

The zircon U–Pb age of Compston et al. (1981) has recently been independently confirmed by Pidgeon and Horwitz (1991) by re-collection from the same locality. They reported analyses of five non-magnetic size fractions and of two single grains from a single sample (W101) from Woongarra Pool, and interpreted the weighted average  $^{207}\text{Pb}/^{206}\text{Pb}$  age of  $2439 \pm 10$  Ma as the best age of the Woongarra Rhyolite. Although Pidgeon and Horwitz (1991, p. 62–63) described this result as dating 'the near-final stages of deposition on the Hamersley Platform' they also cited the view of Horwitz (1978) that the component of the Woongarra Rhyolite from which their sample was taken, and here called the upper unit, is intrusive. If this view is correct, and the final **Discussion** section of this publication supports it, the  $2439 \pm 10$  Ma age of the Woongarra Rhyolite gives only a minimum depositional age for the adjacent sedimentary rocks.

## Descriptions of main components

MacLeod et al. (1963) defined the Woongarra Dacite as conformably<sup>†</sup> overlying the Weeli Wolli Formation, and overlain conformably by the Boolgeeda Iron Formation (Fig. 1). By this definition the rocks form a stratigraphically concordant sheet. Minor stratigraphic discordance would not be easy to detect because the whole of the Boolgeeda Iron Formation consists of BIF, and BIF is also the principal component of the Weeli Wolli Formation (the remainder consisting of dolerite sills). In gross stratigraphic terms there is no doubt that the Woongarra Rhyolite forms a coherent stratigraphic unit that can be confidently identified throughout the outcrop area of the Hamersley Group, like all of its other seven formations. However, the possibility of some stratigraphic discordance, particularly at the upper margin, introduces difficulties in precise definition of the upper contact. These are discussed under the heading **Problems of definition**.

In many of the reference sections, and from airphoto interpretation over most of its outcrop area, the Woongarra Rhyolite is divisible into three components: a lower unit, consisting mainly of compact, even-grained, greenish-grey rhyolite; a median band (here called a raft complex) consisting mainly of BIF; and an upper unit, normally thicker than the lower unit, and typically consisting of dark-grey to black, massive, flinty, porphyritic rhyolite.

<sup>†</sup> MacLeod et al. (1963) in fact noted an exceptional situation 'West of Palra Spring, in the north-western corner of the Mt Bruce Sheet', where 'the Weeli Wolli Formation is missing, and the Woongarra Dacite directly overlies the Brockman Iron Formation.' However, this discordance is neither shown on de la Hunty's (1965) map of MOUNT BRUCE nor mentioned in the accompanying notes, and MacLeod (1966, p. 52) wrote unequivocally that the Woongarra Volcanics 'lie conformably above the Weeli Wolli Formation'. Exposure is generally poor in the area west of Palra Spring, and the originally noted discordance is believed to result from unfamiliarity with the stratigraphy at an early stage of the mapping program.

These components are described in upward stratigraphic sequence.

By comparison with the BIFs of the adjacent units of the Hamersley Group, the rocks of the Woongarra Rhyolite are somewhat more susceptible to weathering, and commonly form lower rubbly areas between sharp strike ridges of BIF. The three-component subdivision is consequently reflected in the topographic expression of the Woongarra Rhyolite in many areas of constant dip and strike; in such areas (Fig. 2) the median raft complex forms a distinct central strike ridge flanked by strike-parallel valleys bounded on their other sides by BIF strike ridges of the overlying Boolgeeda Iron Formation and underlying Weeli Wolli Formation. However, in some places where the stratigraphy is transected by the common superimposed drainage pattern of the area, for example at Woongarra Gorge (Fig. 3), the rhyolite may form a prominent positive topographic feature.

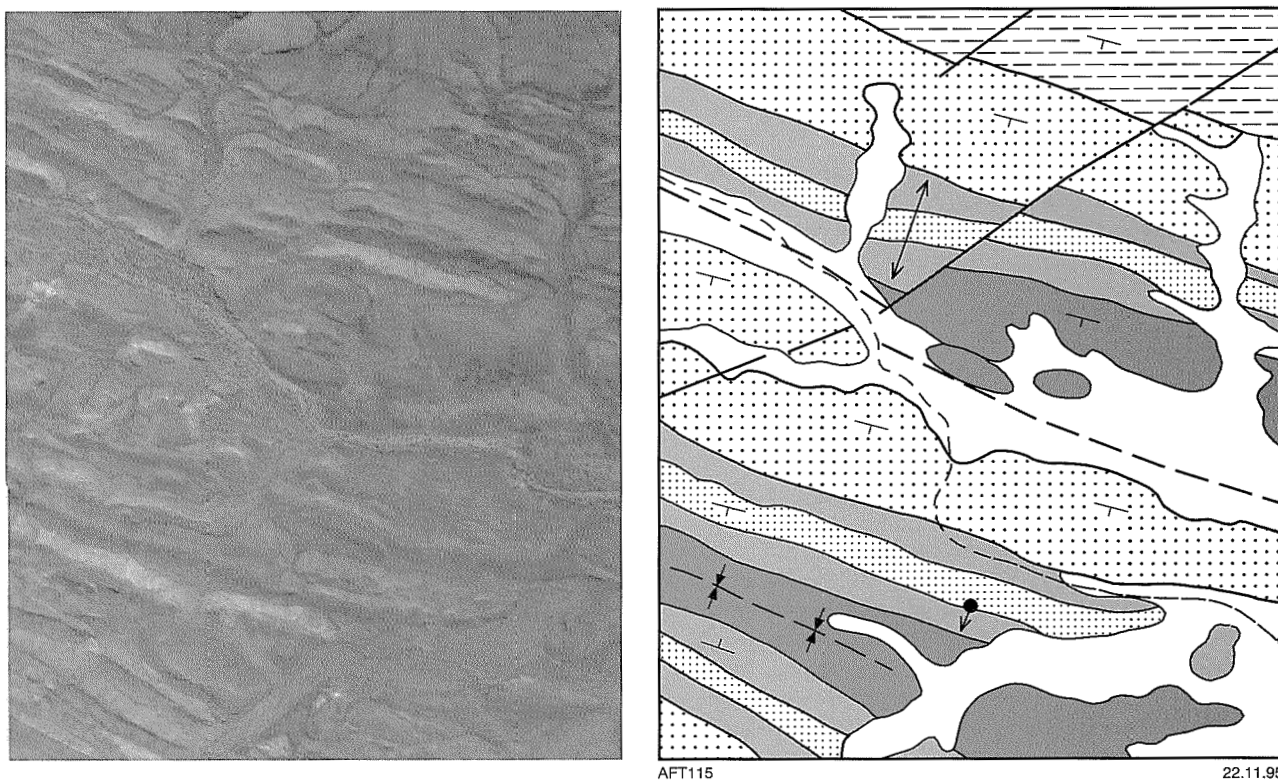
## The basal contact

Although the position of the base of the Woongarra Rhyolite can in many places be identified in the field to within a few metres, the contact with the underlying Weeli Wolli Formation is normally soil covered. The only place found in the course of this study where the contact is well exposed lies in the axial area of the Brockman Syncline (Fig. 1). At that locality the base of the lower unit dips eastwards at about  $3^\circ$ , and is cleanly exposed near the base of a west-facing cliff (Fig. 4). The contact is knife-sharp and perfectly concordant against lithified cherty BIF. At the base of the lower unit, pale-buff, flinty rhyolite, 7–10 cm thick, contains irregularly swirled flow structures (Fig. 5). A fine-grained breccia zone of about the same thickness immediately overlies this flinty rock, and consists of small angular fragments of the marginal material in a matrix of darker, but still fine-grained, rhyolite. At its upper margin the breccia gradationally loses its clastic fabric, and also becomes coarser; within 0.5 m of the base of the lower unit the rhyolite has all the typical attributes of rhyolite within the body of the lower unit (described under the heading **Lower unit**), and has both pseudostratification and spherulitic texture.

No exceptional features within the lower unit have been noted elsewhere in exposures closest to the contact, and similarly there appears to be nothing unusual in the BIF closest to the top of the Weeli Wolli Formation. Thus there is no sign of disturbance of the Weeli Wolli Formation BIF, which must be assumed to have been lithified at the time of emplacement of the rhyolite.

## Lower unit

The lower unit is thinner than the upper unit (Fig. 20; Table 1), and its rocks are typically more susceptible to weathering, and consequently less well exposed, than those of the upper unit. Outcrops tend to be weathered and rubbly, a feature reflecting the common presence of close jointing. In the Duck Creek reference section a strong vertical jointing resembles the columnar jointing of a



↔ Kalgan Creek reference section

● ↓ Figure 26: point photograph taken from and direction of view (Kalgan Creek South)

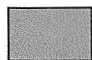
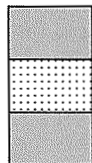
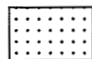
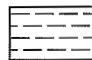
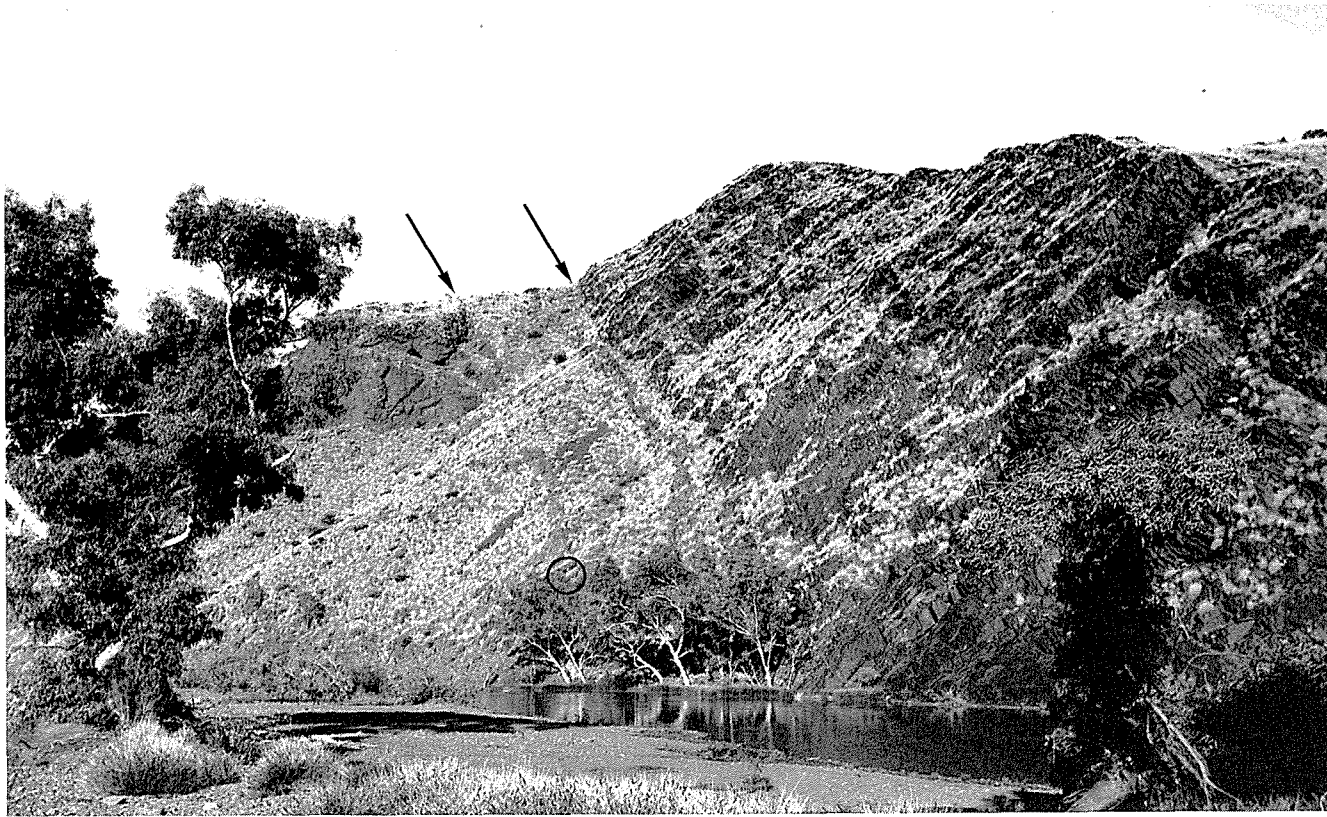
-  Boolgeeda Iron Formation
-  Woongarra Rhyolite, with median raft complex
-  Weeli Wollie Formation
-  Brockman Iron Formation

Figure 2. Aerial photograph and explanatory map showing the outcrop expression of the Woongarra Rhyolite in the Kalgan Creek area. (Part of Newman 1972 Run 4 5058). Note the central strike ridge within the outcrop of the Woongarra Rhyolite formed by the median raft complex



**Figure 3.** General view of the uppermost part of the Woongarra Rhyolite and the overlying Boolgeeda Iron Formation at Woongarra Gorge. The photograph is taken looking easterly across the pool at the mouth of the gorge. The Boolgeeda Iron Formation, dipping steeply south-southwest, forms the dark rocky slopes extending upwards from the pool in the right hand side of the photograph; the lowermost BIF here is typical of the massive, dark, non-microbanded and non-mesobanded type believed to occur only within the Boolgeeda Iron Formation. The paler weathering porphyritic rhyolite of the upper unit of the Woongarra Rhyolite forms the near-vertical cliffs at the top of the ridge immediately right of the tree on the left hand side of the picture; compare Figure 23. Between the sharply defined top of the upper unit and the base of the Boolgeeda Iron Formation, running obliquely down the slope to the trees (ghost gums) along the far edge of the pool, is a ~26 m-thick shale band whose upper and lower boundaries are marked by arrows. Further details of this appear on Figures 21 and 22, and in the accompanying text; the position of Figure 22 is circled.



Figure 4. The basal contact of the Woongarra Rhyolite exposed in west-facing cliffs at trig point JM9, AMG (2252) 773996, in the axial area of the Brockman Syncline. The lower contact of the pale rhyolite dips gently southwards and is perfectly concordant with the stratification of the darker underlying BIF, just above the base of the cliff

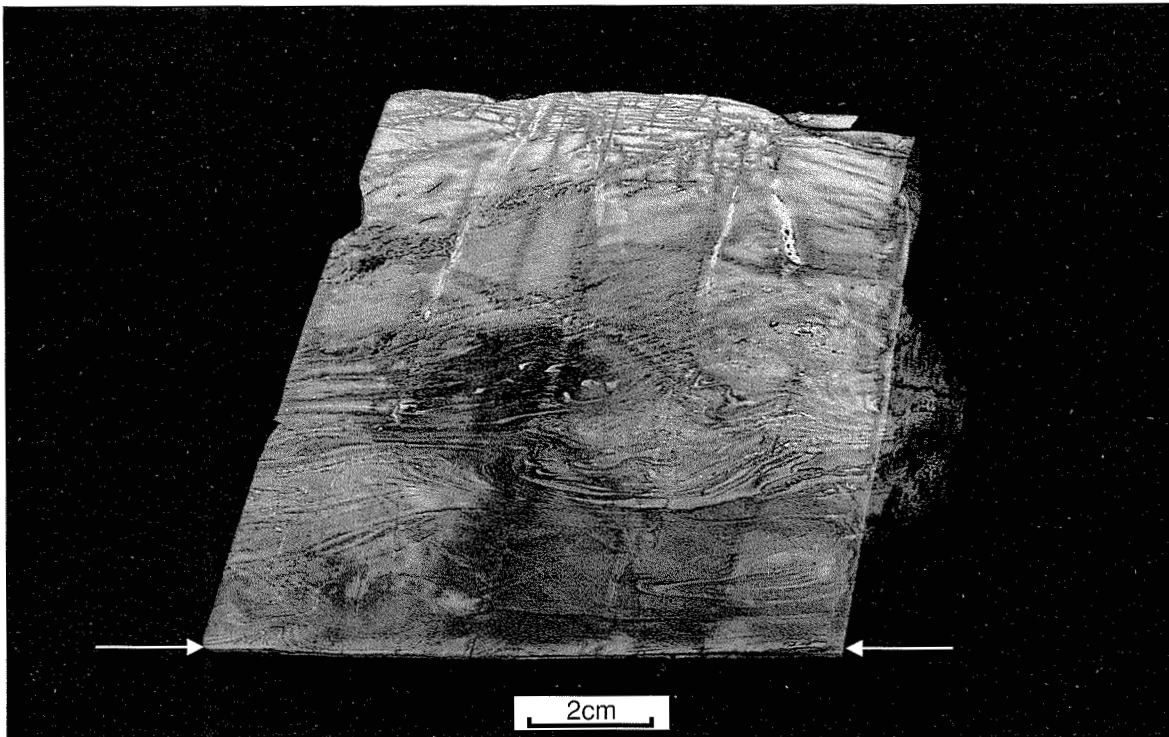


Figure 5. Photograph of the lowermost rhyolite of the lower unit, at the locality of Figure 4. The planar lower edge of the sample (109785), marked by arrows, is knife-sharp and concordant against lithified BIF (a chert mesoband) of the Weeli Wolli Formation. Note the swirled flow banding in the fine-grained and aphanitic marginal rhyolite

**Table 1. Thicknesses of the upper and lower units of the Woongarra Rhyolite in the type and reference sections**

Unit	Thicknesses (m)		Average (a)	Area(km <sup>2</sup> ) (b)	Volume(km <sup>3</sup> )
	Maximum	Minimum			
UPPER UNIT	500	45	245	3.75 x 10 <sup>4</sup>	9.2 x 10 <sup>3</sup>
LOWER UNIT	(c) 350	70	165	3.75 x 10 <sup>4</sup>	6.2 x 10 <sup>3</sup>
Total	750	110	410	3.75 x 10 <sup>4</sup>	15.4 x 10 <sup>3</sup>

**Notes:**

- (a) All averages are of eight sections; Silver Grass Syncline is not used because it is incomplete  
 (b) Area of an envelope enclosing all outcrops  
 (c) Assuming the upper unit is not represented in the Silver Grass Syncline area (see text)

cooling lava, but this is not a common feature. The weathered rubble typical of outcrop areas is orange-brown, but when freshly broken the rock is pale greenish grey, fine grained, tough, compact, and structureless, with a rough fracture resembling that of a quartzite.

Rocks of the unit were called 'green quartzite' during early stages of mapping, and three features of these rocks (the first two of them commonplace) make this misidentification easy to understand. Firstly, a false granularity is commonly present, and is easily discernible with a hand lens as clear to white spheroidal 'grains' of clastic appearance closely packed in a dark-green matrix; the petrographic basis of this appearance is described below. The second feature is a well-developed pseudostratification in outcrop, related to a strong joint-set oriented parallel to the gross stratigraphic orientation of the unit, but not easily identifiable by lithological stratification of any kind in outcrop. The third, less common, feature is a planar textural variation defined by differences in the apparent size and abundance of the spheroidal grains. This last feature provides a particularly compelling simulation of a sedimentary rock (Fig. 6). This banded structure is commonly seen as small- and medium-scale plastic folds, and these are particularly well developed in the Silver Grass Syncline reference section. Autobrecciation is also locally present, but is not common. A good example occurs near the base of the Kalgan Creek West section close to AMG (2851) 751321.

In thin section (e.g. sample 94732, Fig. 7a), typical rocks of this unit have two textural components: quartz-feldspar spherulites in a fine-grained interstitial matrix. The quartz-feldspar spherulites are 1–2 mm across, with a crudely radiate structure resulting partly from scattered straight, in some places discontinuous, dark lines of microcrystalline chlorite, and partly from a fine, radiate, linear pattern of refractive-index variation detectable under high power, probably caused by submicroscopic intergrowth of quartz and feldspar. The spherulites appear generally cloudy with abundant irregular inclusions, probably of chlorite, a few microns across. Under crossed polars (Fig. 7b) they usually extinguish in irregularly shaped patches about 0.5 mm across with indistinct edges that commonly do not bear any relationship to the radiate pattern; a single extinction patch commonly embraces parts

of adjacent spherulites. This is the 'snowflake' texture of Snyder (1962), for which Lofgren (1971b) suggested the alternative term 'micropoikilitic'; its significance is discussed later. More rarely, the spherulites have feathery radial extinction. Coarsely spotted varieties (Fig. 8) have been noted at a few widely separated localities (e.g. samples 15688, Mount Maguire; 30543, Kalgan Creek), in which the spherulites are up to 8 mm in diameter. The spherulites are commonly closely packed, with irregularly interlocking margins, which may be marked by a thin selvage of microcrystalline chlorite.

The second textural component, the interstitial matrix to the spherulites, consists of a fine-grained intersertal intergrowth whose two main constituents are chlorite and feldspar. The pale-green chlorite usually forms irregular microcrystalline patches. The feldspar commonly extinguishes in fan-shaped patterns and is characterized by an internal dusting of sub-micron hematite, which is only absent close to grain edges and internal cleavages. Small, rounded, individual grains of clear quartz or irregular patches of fine mosaic also occur in the interstitial component, as well as irregular clusters of microcrystalline sphene. The geometric relationship of spherulites and matrix is widely variable; in some rocks an evenly reticulate matrix provides a three-dimensional framework in which the spherulites rest without mutual contact, whereas in others tightly packed spherulites form a continuous mass which is interrupted by irregularly scattered, large patches of chlorite-feldspar matrix. These two components produce the false granularity that mimics sedimentary granularity in hand specimen. Lofgren (1971b, fig. 3A; Fig. 7a of this Report) introduced the term 'orb texture' for similar, two-component texture in experimentally devitrified rhyolite.

Many variations exist on the typical two-component texture described above. One common feature is the presence of clear 'needles', about a millimetre long, and with elongations mostly between 100:1 and 50:1, which form a random framework transecting both of the described components (Fig. 9). The needles now consist of quartz that, in several units, extinguishes in sympathy with the extinction of the immediately adjacent part of the rock, rather than integrally with the orientation of the needles. They are believed to represent inverted tridymite,

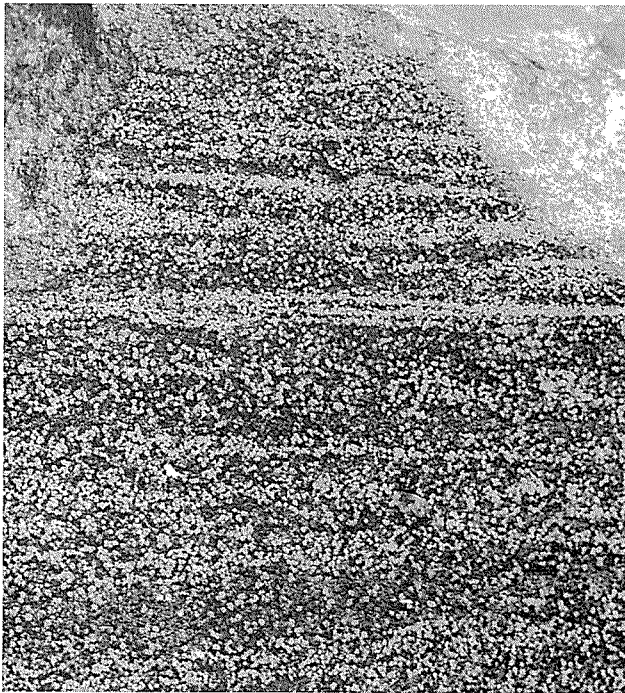


Figure 6. Weathered surface of rhyolite of the lower unit from the Silver Grass Syncline area, showing the pseudostratification and false granularity which simulate the field appearance of a quartzite. The 'grains' are about 1 mm across, and consist of radiate quartz-feldspar spherulites, as shown in Figure 7. Sample 94732

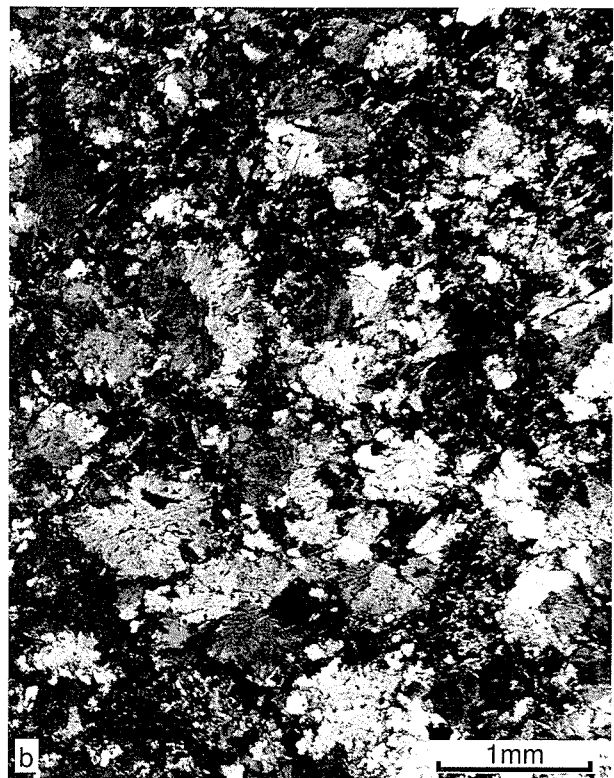


Figure 7. Typical thin-section appearance of rhyolite of the lower unit, under plain light (a) and crossed polars (b). Sample 94732, from the Silver Grass Syncline area. (a) shows clearly the two-component ('orb') texture, with crudely radiate quartz-feldspar spherulites, here about 1mm across, lying in a matrix of similar composition but darkened by microcrystalline chlorite. (b) shows the 'snowflake' extinction pattern, in which vaguely defined, irregularly interlocking areas of common extinction have a general diameter of about 0.5 mm and are unrelated to either the boundaries or internal structure of the spherulites. This pattern should be compared with the finer grained extinction pattern of the upper unit, shown in Figure 15

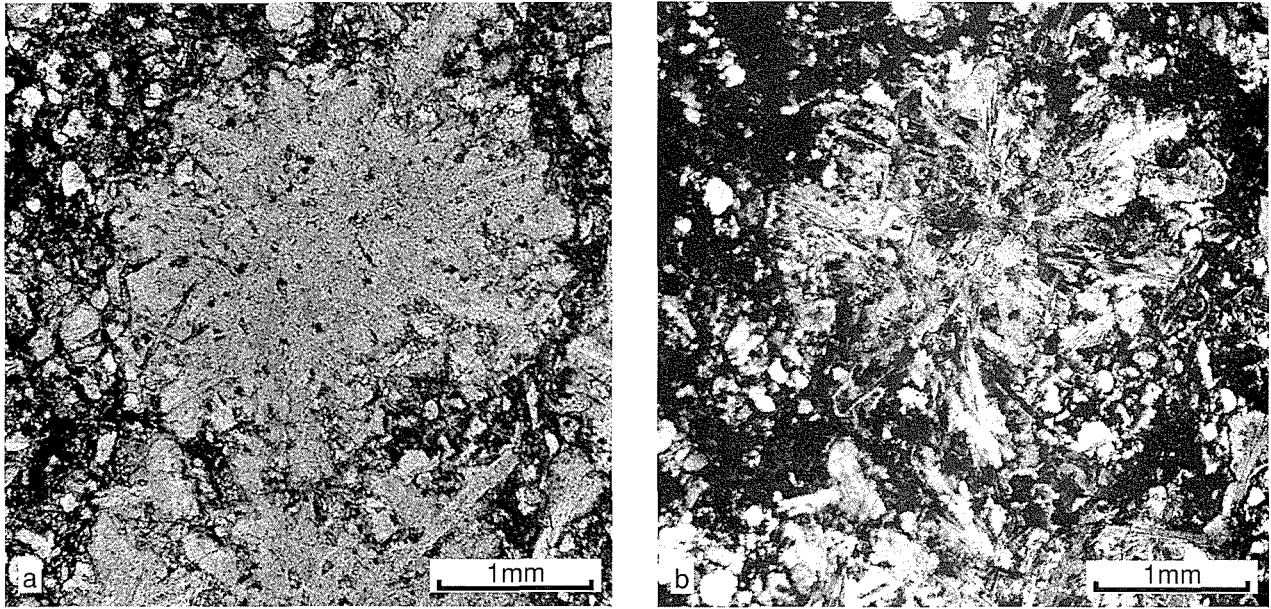


Figure 8. Thin section of rhyolite of the lower unit, under plain light (a) and crossed polars (b), showing exceptionally large quartz-feldspar spherulites. Sample 30543 from the upper Kalgan Creek area. The spherulites in this rock have an average diameter of about 3 mm. However, the areas of common extinction (b) are generally about 0.5 mm across, as in Figure 7(b)

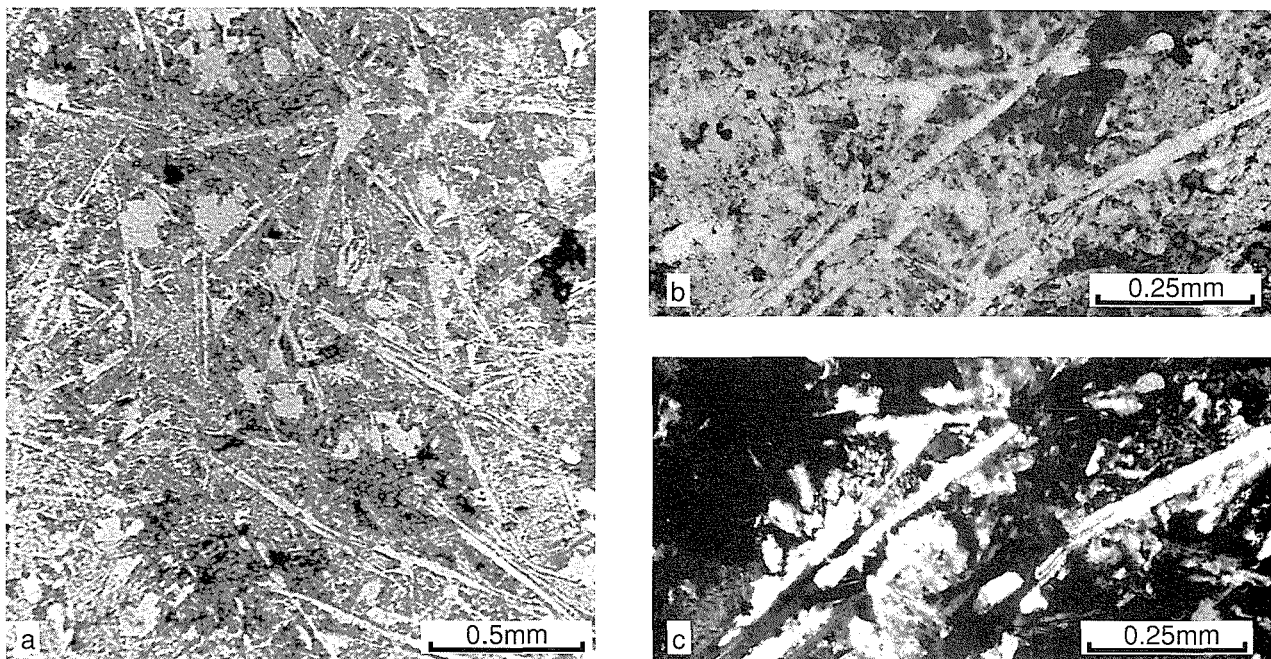
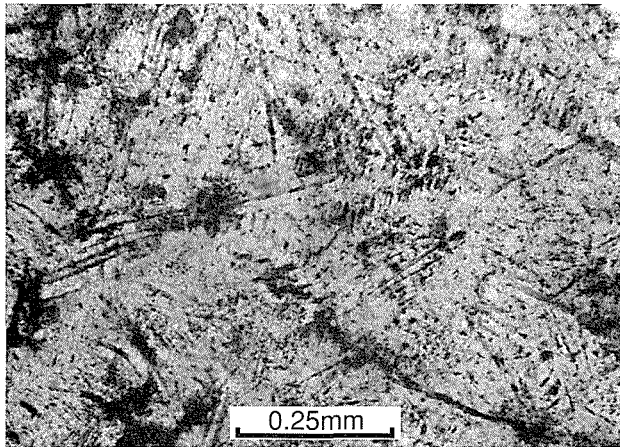


Figure 9. Thin section of rhyolite of the lower unit, showing random framework of polycrystalline quartz paramorphs after tridymite. Sample 94735, from the Silver Grass Syncline area. (a), taken under plain light, shows the randomly interlocking arrangement of the framework, and the total lack of deformation since tridymite crystallization. (b) and (c) show part of the same slide at a higher magnification, under plain light and crossed polars respectively. (c) shows that the boundaries of areas of common quartz extinction are unrelated to the tridymite crystals, and have a general diameter of 0.3–0.5 mm



**Figure 10.** Thin section of rhyolite of the lower unit, showing fine criss-crossing lines of microcrystalline chlorite, giving a pervasive cross-hatched texture. Sample 47236, from Woongarra Gorge

and are texturally very similar to quartz paramorphs after tridymite described by Wager et al. (1953). A possibly related texture of uncertain origin is formed by criss-crossing straight lines of microcrystalline chlorite in an exceptionally fine-grained and irregular quartz mosaic (Fig. 10).

Phenocrysts are not typical in rocks of the lower unit, but both quartz-phyric and feldspar-phyric rock types occur locally. Small ( $\leq 1$  mm) embayed  $\beta$ -quartz phenocrysts form the cores of radiate spherulites in one such rock (sample 30541) from the Kalgan Creek area and are illustrated in Figure 11.

Although considerable attention has been given above to macroscopic and microscopic variation in the rock types of this unit, for the sake of completeness, it is appropriate to conclude this description by emphasizing that these differences are minor relative to the general uniformity of the unit; there is no doubt of its status as a single stratigraphic unit of generally homogeneous composition and appearance.

## Median raft complex and other rafts

The lower and upper volcanic units of the Woongarra Rhyolite are separated by a band consisting mainly of BIF, but with associated components of dolerite, shale, and peperite; the name median raft complex is here applied to it. Its total thickness, and the lithological mix of rocks within it, are highly variable; details are given later in the individual reference section descriptions, and a summary is given in Figure 20. Although the median raft complex commonly forms a distinct topographic feature (Fig. 2) its components are impersistent along strike, and the whole unit does not possess the basin-wide stratigraphic continuity generally characteristic of the Hamersley Group. The stratification of BIFs of the median raft complex is

typically concordant with the gross stratigraphic orientation of the Woongarra Rhyolite at each locality, but it is commonly complicated in detail by a high degree of both brittle and plastic deformation. In its extreme form the BIF gives the impression of almost explosive disruption in situ (Fig. 12), in which the shattered remnants of the more brittle cherty mesobands lie at random in a structureless ferruginous matrix representing the homogenized chert-matrix component. The type of structure illustrated on relatively small scales in Figure 12 is also present on a range of larger scales. Tight, plastically deformed BIF is equally common, also on a range of scales; fold orientations fluctuate greatly, and are clearly unrelated to local tectonics. Thick dolerites within the complex retain the integrity of their igneous textures, but volumetrically smaller dolerite components appear to have suffered the same small-scale disintegration as the BIFs (Fig. 12d).

In spite of its variability, the median raft complex can usually be identified, with confidence, as a band separating

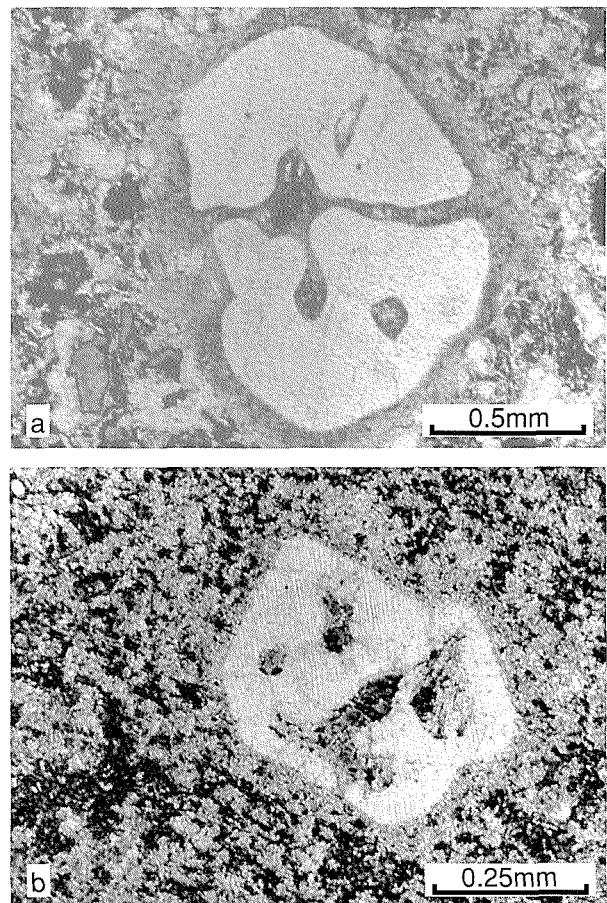


**Figure 11.** Embayed  $\beta$ -quartzes from rhyolite of the lower unit. (a) is from sample 30513, from the Kalgan Creek reference section. (b) is sample 94715, from the Coondiner Creek section. Both phenocrysts show substantial corrosion, but the optical continuity shows no relative displacement of parts. The fine, near-vertical lamellae in (b) are possibly related to cooling stress; they appear to be near-basal

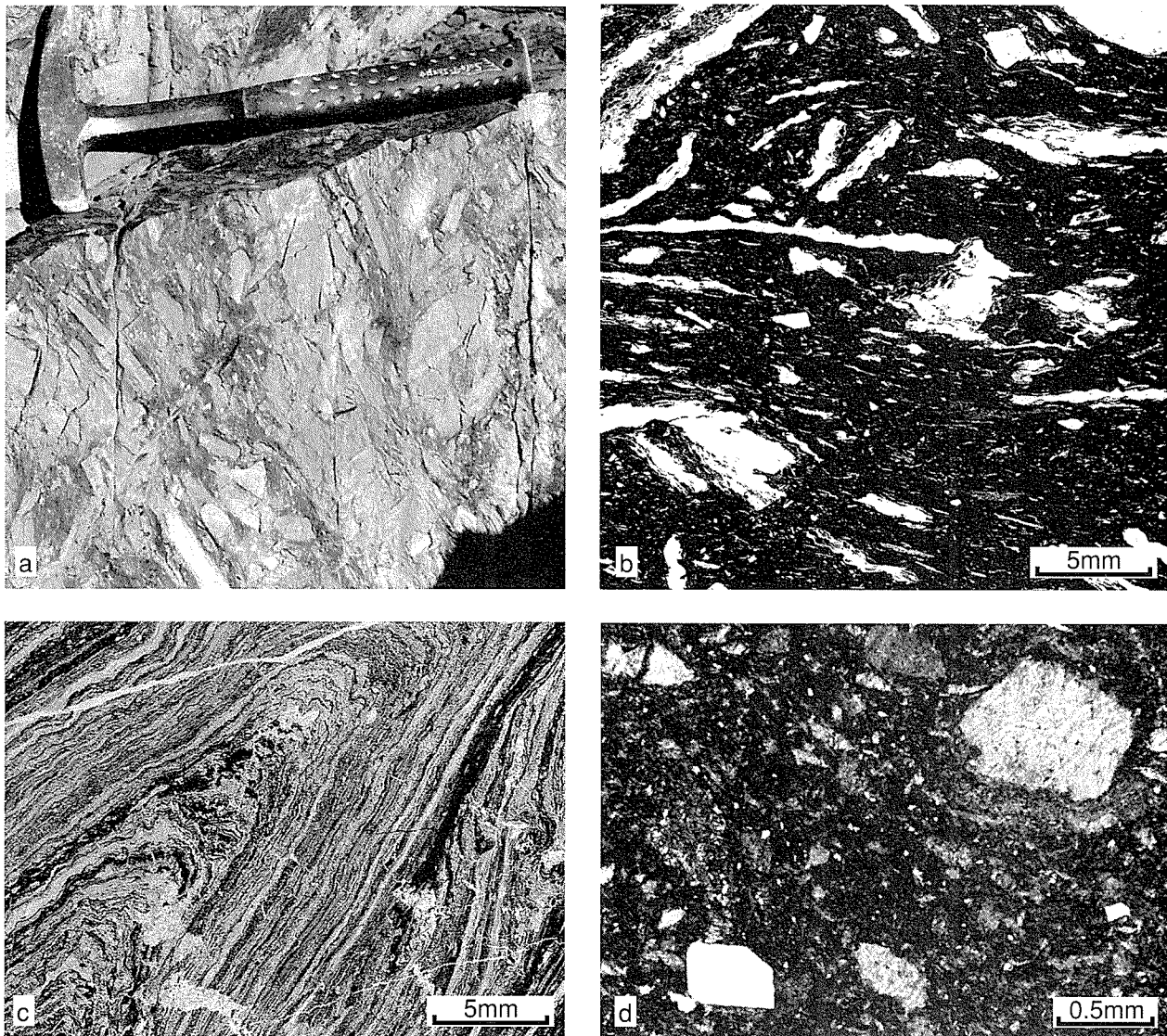


Figure 12. Disrupted rocks of the median raft complex. (a) Ridge-top exposure in the Kalgan Creek West section, at AMG (2851) 746320; hammer for scale. The BIF is broken into angular cherty pieces mainly in the 3–8 cm size range, which are jumbled at random in a dark, iron-rich matrix. (b) Thin section of the matrix material of (a). Sample 94709. The disruption extends continuously downwards in scale, so that what appears as matrix in (a) consists of finer fragments of chert in a fine-grained magnetite–hematite matrix. (c) Tight folding, and associated discordance, within a chert fragment in disrupted BIF of the median raft complex of the Kalgan Creek reference section. Sample 30514. (d) Disrupted dolerite in a sample (94716) from the Coondiner Creek reference section. The rock consists essentially of chloritized mafic debris, but the presence of a euhedral  $\beta$ -quartz (white, lower left) suggests some entrainment of Woongarra Rhyolite material during disruption

the upper and lower rhyolitic units. However, in some of the reference sections additional minor rafts, mostly of BIF but also of shale, are present within both the upper and lower units, but are more common in the latter. Such occurrences are shown in Figure 20, and are described separately under the individual reference section headings.

## Upper unit

The upper unit typically consists of brown-weathering, massive, homogeneous, porphyritic rhyolite, which is dark

grey to black, with a smooth flinty fracture when fresh; it is normally thicker than the lower unit (Fig. 20; Table 1). Peperitic rocks that form a relatively small part of the total thickness of the upper unit are included within it for the purposes of Table 1, but are described separately under the heading **The rocks about the upper contact**.

The common pseudo-granularity of rhyolite of the lower unit has not been seen in that of the upper unit. The unit tends to be less susceptible to weathering and less closely jointed than the lower unit, forming substantial cliffs in well-exposed sections (Fig. 23). Apart from

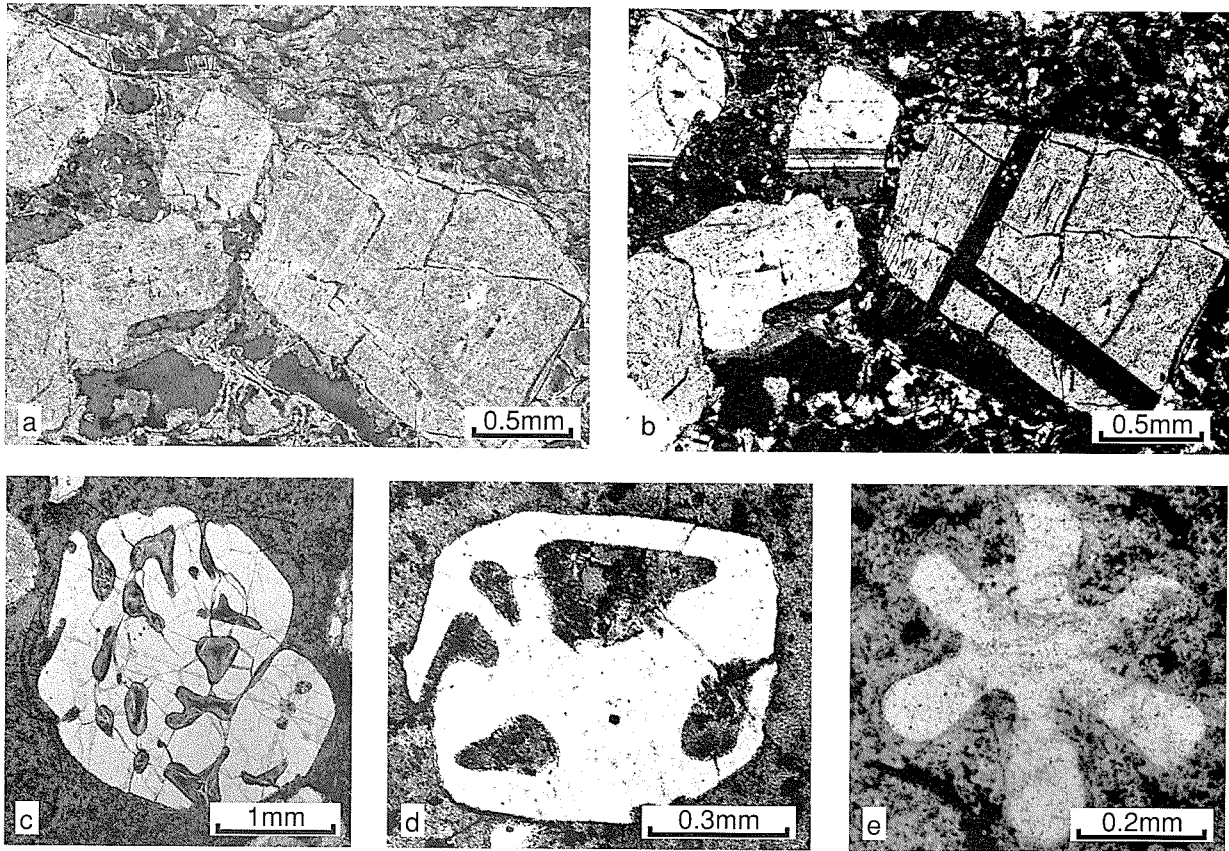


Figure 13. Phenocrysts of rhyolites of the upper unit. (a) and (b) show plagioclase phenocrysts in plain light and under crossed polars respectively. Sample 15647, from the Yeera Bluff reference section. The subhedral form, rather simple twinning, and tendency for aggregation (glomeroporphyritic texture) are typical. (c), (d) and (e) show extensively resorbed  $\beta$ -quartz phenocrysts. Sample numbers are 47214, 94713, and 15622 respectively, from Woongarra Gorge, Coondiner Creek, and Nallanaring Creek. Quartz phenocrysts ('eyes') tend to be larger than those of the lower unit (Fig.11), but share the property of retaining optical continuity of the whole crystal despite extensive resorption

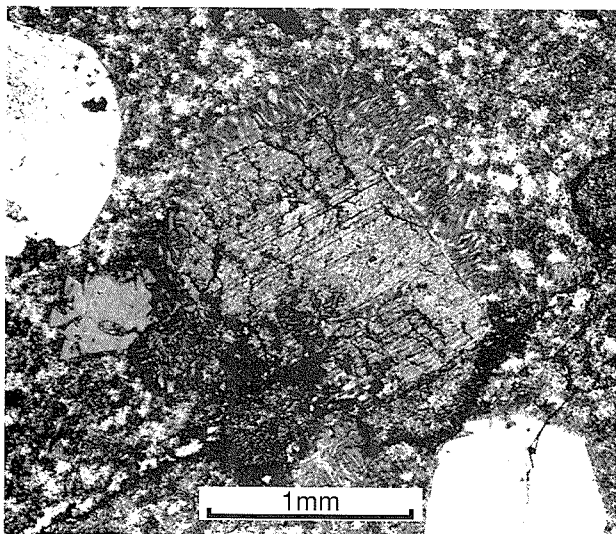


Figure 14. Granophyric corona on plagioclase phenocryst in rhyolite of the upper unit. Sample 15674, from the Duck Creek reference section. The corona is about 0.3 mm thick, and consists of a micrographic intergrowth of quartz and K-feldspar. The typically fine-grained ('snowflake') extinction pattern of the matrix of the upper unit is well displayed (compare Fig.15 (b)). Parts of two quartz phenocrysts appear at top left and lower right

the internal brecciated levels at Woongarra Gorge, there is no sign of possible internal divisions or discontinuities.

With the exception of some rocks from the mainly marginal zones of internal brecciation or flow banding, described below, phenocrysts are evenly distributed. They are predominantly quartz, and have a remarkably uniform upper size limit of about 4 mm in all thin sections examined, although most are between 1 and 3 mm across (Figs 13 and 15). It is estimated that the phenocrysts are separated by an average distance of 10 mm, and this, with an assumed average phenocryst diameter of 2.5 mm, suggests that quartz phenocrysts form about 6% of the total volume of the rock. Euhedral, stumpy, bipyramidal  $\beta$ -quartz forms are not uncommon, but some degree of marginal resorption is usual, and the larger crystals, in particular, tend to be extensively corroded and embayed (Fig. 13). Feldspar phenocrysts are much less common than quartz, and seem to be more abundant nearer the margins of the unit. They may be subhedral to euhedral, in which case they are commonly of albite-oligoclase and show simple or broadly lamellar twinning. However, they are commonly polycrystalline within a vaguely subhedral envelope. Aggregation into glomeroporphyritic clusters is common (Fig. 13), but not universal (Fig. 15). A granophyric overgrowth, or corona, has been noted around one plagioclase phenocryst in a sample from the

Duck Creek reference section (Fig. 14); the example is unique in the numerous thin sections examined in the course of the reported study. Patches of microcrystalline chlorite presumably represent degraded ferromagnesian phenocrysts within the original magma, but provide no morphological clues to their original identity. They are even less common than plagioclase phenocrysts.

In thin section (Fig. 15), the matrix of rocks of the upper unit appears to have a finely mottled texture caused by a uniform, poorly defined, incomplete meshwork made up of dark lines of microcrystalline chlorite, in which the cells of the mesh are about 0.1 mm across. Under high magnification each cell is seen to consist of a number of vaguely defined, interlocking subareas of generally consistent extinction; this, again, is the 'snowflake' texture of Snyder (1962), already noted in the lower unit, but here the average diameter of the individual 'snowflakes' is about 0.1 mm, contrasting with the average of about 0.5 mm in the lower unit. In detail, the extinction is always irregular, presumably reflecting the complex structure of quartz-feldspar intergrowths that cannot be resolved with an optical microscope. Within this confused texture, small (0.02 mm long), interlocking, elongate areas of coherent extinction have the appearance of feldspar laths, but cannot be positively identified.

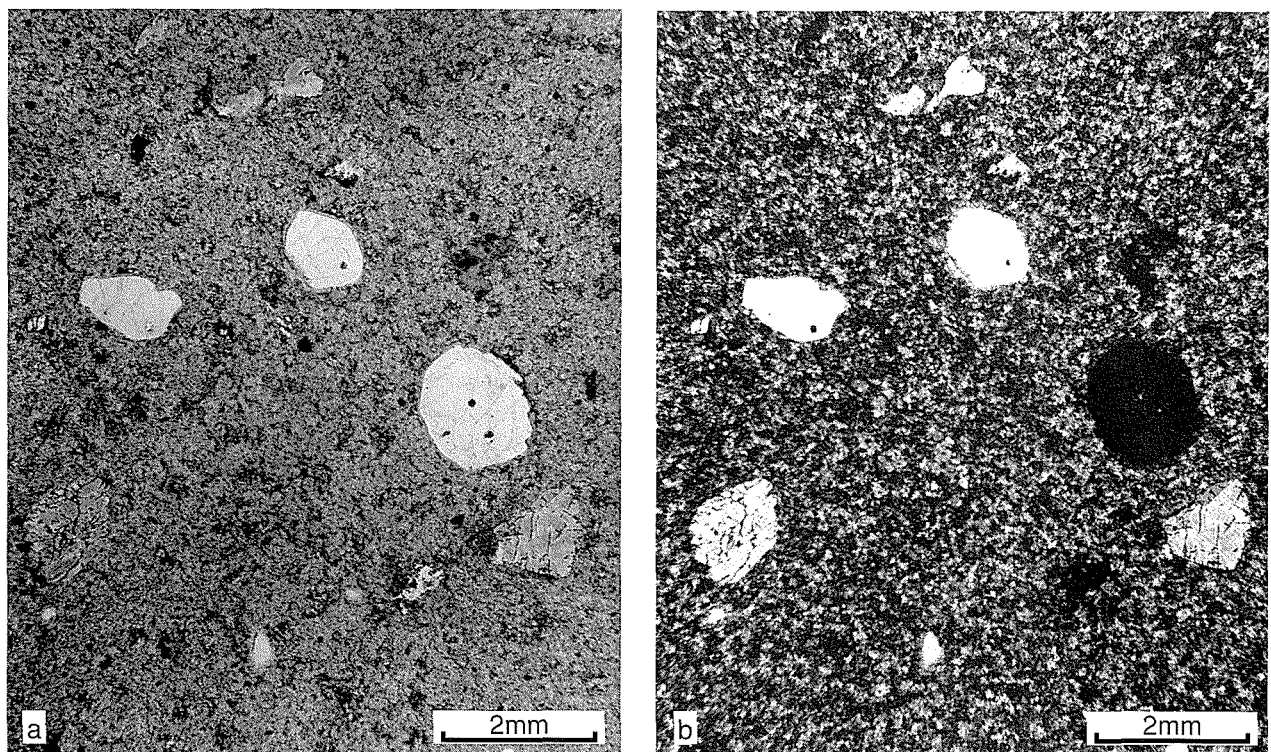


Figure 15. Typical thin-section appearance of rhyolite of the upper unit, under plain light (a) and crossed polars (b). Sample 47205, from Woongarra Gorge. (a) shows the common size, shape and distribution of phenocrysts; the  $\beta$ -quartz phenocrysts vary from subhedral (centre) through rounded (right) to a form rendered anhedral by corrosion (left), while plagioclases (lower left and right) are subhedral. (b) shows finely mottled ('snowflake') extinction pattern of the matrix, with patches of common extinction about 0.1 mm across. Compare this with the coarser extinction pattern of the lower unit (Figs 7 and 8)

In clean field exposures, autobrecciation is commonly present in both upper and lower marginal parts of the upper unit, and more rarely in intermediate levels. This is described as autobrecciation to emphasize that many of the constituent angular metre- and decimetre-scale blocks are commonly not far displaced from their matching neighbours, leaving a general impression of breakup in situ. Generally, the broken pieces appear darker on clean, weathered surfaces than the lighter interstitial infill, although both consist essentially of porphyritic rock closely resembling the main mass of the unit. In freshly broken rock such brecciation is not discernible on the smooth, black fracture surfaces. In thin section these autobrecciated rocks display similar, smaller, dark, broken pieces reflecting the style of the macroscopic shattering. The darker fragments, viewed under plain light, commonly show well-developed perlitic cracking defined by clear lines, edged with microcrystalline chlorite, transecting the transparent matrix. Irregular blotches of chlorite occur centrally within the cores of the concentrically cracked material, and are often associated with patches of finely granular sphene. Under crossed polars the transparent material of the perlitically cracked areas appears as a fine-grained (~0.1 mm) irregular intergrowth of quartz and feldspar, the latter usually with crudely fanned extinction. The extinction of individual grains of this mosaic sometimes transects, but is generally delimited by, the lines of the cracks. Small ( $\leq 0.5$  mm), perfectly circular patches of quartz mosaic, with or without chlorite, may be interpreted as infilled spherical bubbles (amygdales). In some samples, autobrecciated fragments contain such patches, which are elongate and parallel, with differing orientations in adjacent clasts (Fig. 16).

Medium-scale, swirling, flow-banded structures are present, more rarely than autobrecciation, both close to the upper margin and within the central part of the unit (Fig. 17). As in the case of autobrecciation, these are clearest on slightly weathered surfaces in the field, and are expressed as dark and light variations of essentially similar porphyritic rhyolite (Fig. 18).

## The rocks about the upper contact

### Problems of definition

The distribution of peperites about the upper contact raises problems with the exact stratigraphic definition of the top of the Woongarra Rhyolite. From Figure 21 and accompanying later text, it is clear that in some of the reference sections, for example at Nallanaring Creek, a separate sill of peperite lies above the upper contact of rhyolitic rock against sedimentary rocks, in this case BIF. In other sections, such as Kalgan Creek West (Figs 21 and 27–29), such sills are demonstrably lenticular; whereas in others again, for example the type section at Woongarra Gorge, there are no such sills. While it may at first seem that a simple solution to this would be to define the top of the Woongarra Rhyolite as the top contact of the uppermost lavalike rhyolite with sedimentary rock, this presents problems.

In the first place, there is locally, such as in the Kalgan Creek South section (Figs 21 and 26), an upwards transition at the top of the upper unit from solid lavalike rhyolite, through autobrecciated rhyolite, into peperite. In such cases the top of the Woongarra Rhyolite would need to be defined, if it were to be precise, at the contact between this peperite and the BIF overlying it. But similar peperite occurs within this BIF here at higher levels; and it is shown under the heading **Geochemistry** that peperites from about the upper contact, whether they come from the top of the upper unit or from sills with no demonstrable physical connection with it, all have the same major- and trace-element compositions as the rhyolites. Thus the peperites are an integral and consanguineous component of the Woongarra Rhyolite, and any stratigraphic definition should ideally include them all. A formally defined top of the Woongarra Rhyolite that separated integral peperites of the upper unit from those in sills above would be artificial.

Until the question of stratigraphic discordance at the upper margin, already raised above and discussed in more detail later, is definitively resolved, the related problem of precise stratigraphic definition of the top of the Woongarra Rhyolite cannot be settled. In this Report it is provisionally defined by reference to a type section at Woongarra Gorge. Wherever possible in all other reference sections, the factual stratigraphic detail of the upper contact is shown (Fig. 21) and an indication given of the point used as the top of the upper unit (Fig. 20), without implication of precise stratigraphic equivalence. Avoiding the problem of precise correlation in this way does not affect any judgements based on gross stratigraphy, since the uncertainties involved in formal definition of the upper contact are relatively minor.

### Peperite

Peperite generally occurs either at the top of the main body of the upper unit, or in sills above it (Fig. 21); such sills are discontinuous both at a regional (Fig. 21) and a local scale (Fig. 27). All of the rocks grouped under the term peperite (see under the heading **Nomenclature**) share the common characteristic that they are clearly clastic rocks, made up of fragmentary material, at least some of which is of direct igneous origin. However, the individual clasts show wide variation in their size, derivation, degree of deformation and modification, and in the degree to which they are welded together; in effect, the immense compositional and textural variety of these rocks is one of their main features.

The material that forms the sill in the Nallanaring Creek section, which is about 10 m thick (Fig. 21), may be taken as typical of peperites with a high sedimentary component. A sample (15640) of the tough, magnetic, heavy (SG = 3.27) rock from this sill was described in detail by Trendall (1972). In hand specimen, brick-red fragments of microbanded chert, clearly derived from the adjacent BIF, are scattered unevenly within the dark-grey matrix. Most are between 1 and 3 cm across, and vary in shape from angular to rounded and from flat to equant; some have streaked-out 'tails', which are parallel to the preferred orientation of smaller discoidal fragments

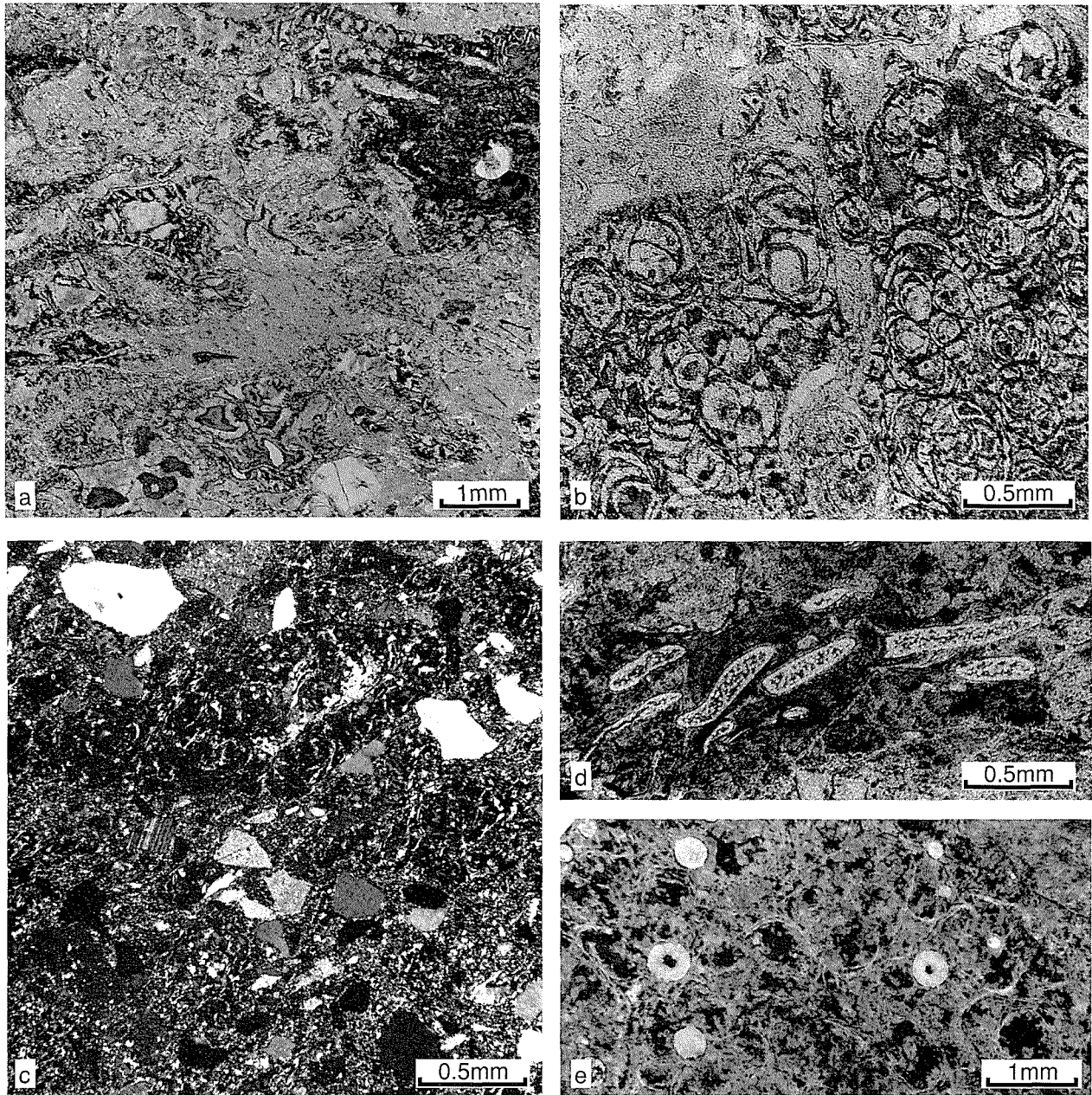


Figure 16. Brecciated material from rocks of the upper unit. (a) Sample 30504, from the northern extremity of the Turee Creek Syncline. The rock consists of an irregular quartz-feldspar mosaic, within which lie recognizable quartz phenocrysts (e.g. lower edge, just right of centre) and dark chloritic patches which define the outlines of broken and compressed fragments of glass. (b) Sample 42174, from Woongarra Gorge. Angular glass fragments with perlitic cracking defined by microcrystalline chlorite lie in a fine-grained quartz-feldspar matrix. (c) shows another field of view from the same thin section as (b), at the same scale but under crossed polars. The outlines of small perlitic fragments are discernible as darker patches; the angular fragmentation of quartz and feldspar phenocrysts is apparent. (d) Sample 47201, from Woongarra Gorge. Bubbles within a glass fragment are flattened and filled by quartz and chlorite. (e) Sample 15647, from the Yeera Bluff reference section. Small spherical quartz-filled bubbles within a perlitically cracked fragment

vaguely defined by slight colour variations within the matrix. Elongations on broken faces vary between about 2:1 and 20:1. The cleavage faces of dark-green, equant feldspars, 2–4 mm across, are also discernible in hand specimen.

Part of the same thin section illustrated by Trendall (1972) appears in Figure 19a. Pale, highly elongate

fragments of compressed chert derived from the adjacent BIF commonly have fiamme-like terminations, and lie in a dark microcrystalline matrix of quartz, stilpnomelane, magnetite, hematite, and carbonate. The largest such fragment in Figure 19a is more than 15 mm long. In the surrounding matrix successively smaller, subparallel fragments show up as paler patches within the general matrix of microcrystalline quartz, heavily impregnated



Figure 17. Plastic flowage fold in rhyolite of the upper unit in the Wyloo Dome reference section. The laminar structure delineating the fold is not discernible in the fresh rock, either in hand specimen or in thin section, and the minor compositional variations defining it are only detectable when etched by weathering. The photograph is of a subhorizontal surface, with north to the right. The axis of the fold is near vertical and the axial plane is thus close to east–west and vertical. In gross stratigraphic orientation the WR in this reference section has an east–west strike and a northerly dip of about 45°. The fold axis is thus oblique to the stratigraphic boundaries of the upper unit

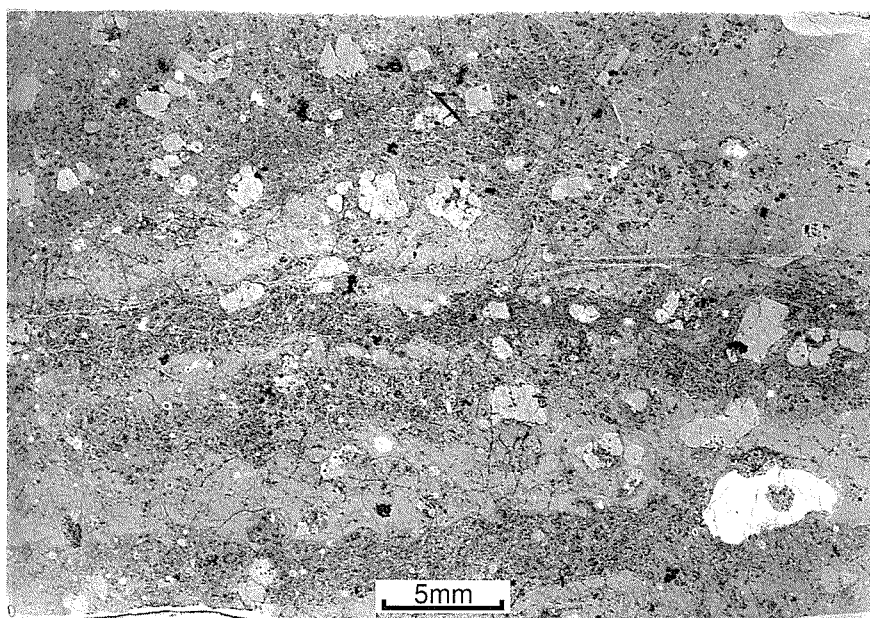


Figure 18. Flow banding in rhyolite of the upper unit; macrophotograph of large thin section. Sample 15647, from the Yeera Bluff reference section. Light and dark banding in this slightly brecciated rhyolite appears irregularly swirled in field exposure

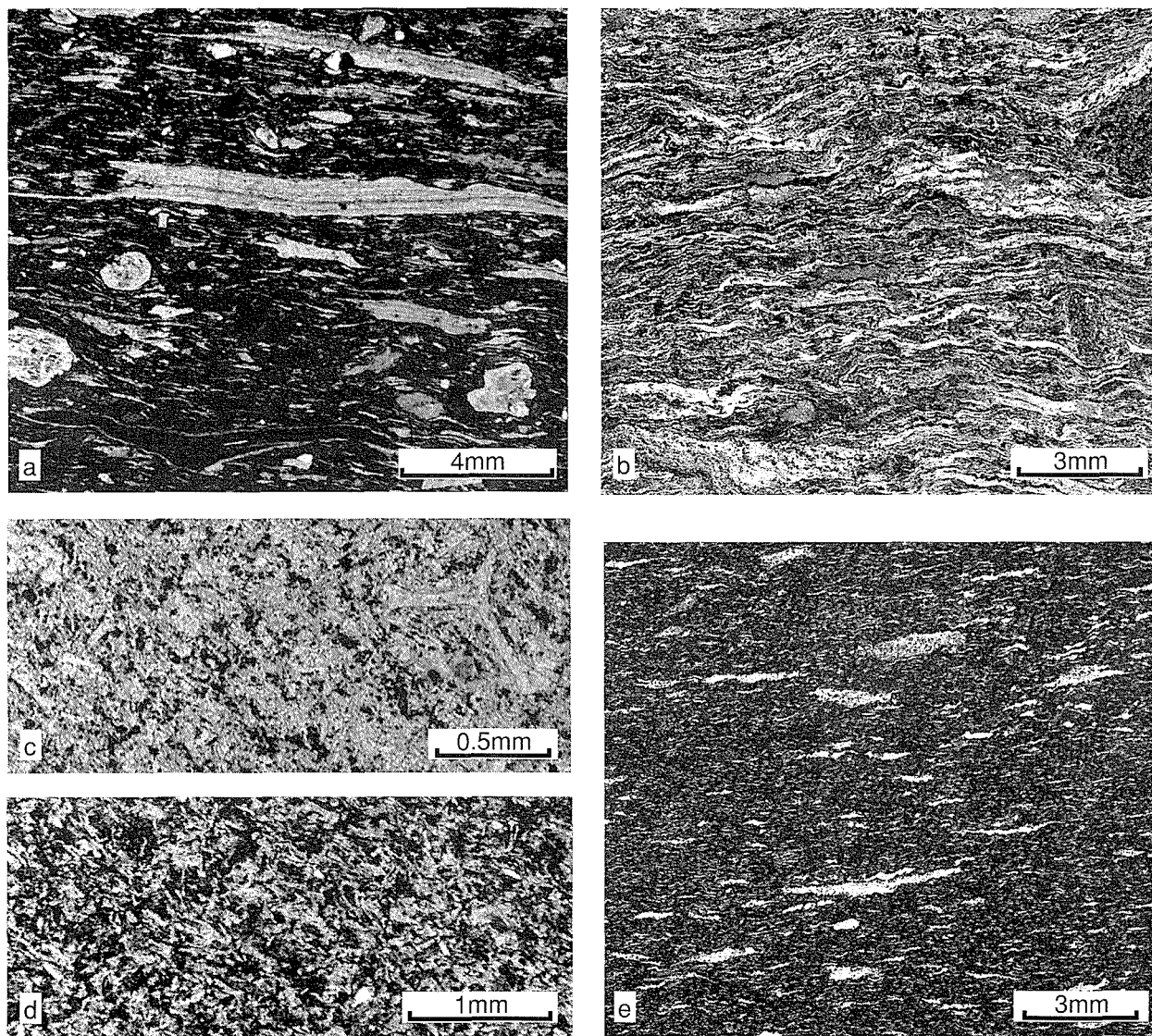


Figure 19. Photomicrographs and macrophotos of thin sections of peperites associated with the upper contact. (a) Sample 15640, from Nallanaring Creek. This rock was also illustrated by Trendall (1972), and was shown to have a chemical composition approximating to a mixture of rhyolite and BIF in a 2:3 ratio. In this view, thin plates of compressed microbanded chert have fiamme-like terminations, while undeformed feldspar phenocrysts identical to those of the upper unit are clearly visible near the left and right edges of the lower part of the picture. This rock comes from a 10 m-thick sill above the top of the Woongarra Rhyolite (Fig. 21). (b) Sample 30517, from the Kalgan Creek reference section (Fig. 21). This highly compressed peperite has a general framework of microcrystalline silica, and the darker colour of the matrix by which the light fragments are outlined is due to fine hematite 'dust' and minor fine-grained euhedral magnetite. There is no conclusive evidence that any of the fragments are of volcanic derivation, although some have internal streaks suggesting flattened bubbles within compacted pumice. Two large, equant fragments close to the right-hand edge appear to be of shale. (c) Sample 94710, from Kalgan Creek West. Barely discernible, somewhat compacted, interlocking shards are the main component of this fine-grained quartz-feldspar-chlorite rock from an injected sill above the top of the Woongarra Rhyolite. See also Figures 21, 27 and 28 for location of this rock, of which a chemical analysis appears in Table 1. A good example of an undeformed bubble-wall shard appears in the upper right-hand part of the photo. (d) Sample 30503 from the northern part of the Turee Creek Syncline (not a reference section). Compositional variations within a fine-grained mosaic of quartz, feldspar and chlorite define a random mesh of replaced shards mainly about 0.1 mm long, together with other comminuted and replaced volcaniclastic debris of similar grain size. (e) Sample 30519, from the Kalgan Creek reference section. This rock has undergone substantial secondary silicification, but shows the texture well. The pale elongate patches consist of a microcrystalline (<0.01 mm) mosaic of quartz, complicated by minor chalcedony and colourless chlorite. A similar mosaic continues through the darker areas, which also contain abundant fine-grained martite octahedra and poorly crystalline goethite. The fragments clearly have near-circular outlines on bedding surfaces of this rock

with a dust of hematite and magnetite. Plagioclase phenocrysts derived from the rhyolite component of the rock are also visible in Figure 19a. As discussed under the heading **Geochemistry**, the chemical composition of this rock is approximated by a mix of 60% BIF and 40% rhyolite.

Another peperite, from one of a number of thin sills within BIF at the top of the Kalgan Creek reference section, is shown in Figure 19b. In this rock the compaction is extreme, and there is no obvious evidence that any of the material is of igneous derivation. By contrast, the rocks that are illustrated in Figure 19c,d lie at the other extreme of the range in both clast type and grain size. Both consist of a microcrystalline quartz–feldspar–chlorite mosaic within which irregularities in chlorite distribution mark the outlines of silicic shards, including bubble-wall types. The similarity of the two rocks shown in this figure illustrates the identical appearance of shard-rich peperite from a sill within BIF above the upper unit (Fig. 19c) and peperite from the uppermost part of the upper unit itself (Fig. 19d). It is a matter of speculation whether such shards, now unrecognizable, may originally have formed a component of the highly compressed rocks of Figure 19a,b. Figure 19e shows a similar rock to those illustrated in Figure 19a,b, but from the top of the upper unit; it is included to re-emphasize the point that the textural and compositional ranges of peperites from the top of the upper unit and from the sills above it are identical.

All the peperites illustrated in Figure 19 are fine grained, but many peperites contain scattered larger clasts. These are commonly of banded chert, comparable with that of the enclosing BIFs. Such irregular lumps have been noted up to a metre across: clasts as big as this are rare, but pieces between 10 and 20 cm in diameter are not uncommon, especially in areas where peperites are well exposed, such as the Kalgan Creek South section. These larger clasts are commonly equant, but where they are elongate their greatest diameter lies along the direction of flattening of the finer material.

One occurrence of unusual peperite is present at the base of the upper unit in the Duck Creek reference section, and is described under that heading.

## The immediately overlying strata

Notwithstanding the difficulty in precisely defining the top of the upper unit, discussed above, Figures 20 and 21, which summarize information from the following descriptions of the type and reference sections, show that there is substantial regional variation in the nature of the immediately overlying sedimentary rocks. The top of the Woongarra Rhyolite is variously overlain by shale, which may either be relatively thick (Woongarra Gorge) or thin (Wyloo Dome), or by BIF, which may consist of a thin band succeeded by shale (Yeera Bluff) or may be relatively continuous upwards. There are also differences in the nature of the overlying BIF, which are noted in the descriptions of the individual sections below, and where the significance of these lithological variations is also discussed.

## The type and reference sections

### Woongarra Gorge

This section was specified by MacLeod et al. (1963) as the type section of the 'Woongarra Dacite', but was not described in detail. A sketch map and stratigraphic column were later given by Trendall (1976; Figs 21 and 22). The description here essentially reproduces Trendall's earlier description, in order to fulfil the requirements (Staines, 1985) for its formal establishment as the type section of the redefined Woongarra Rhyolite. All other sections described below are reference sections.

#### *Location and access*

Woongarra Gorge lies about 70 km west-southwest of the township of Tom Price (Fig. 1). Access is by way of an unmaintained track running for 13 km northwest from an unmarked turning off the sealed Nanutarra–Wittenoom road, about 18 km west of the Paraburdoo turn-off.

#### *Map sheet*

Topographic 1:100 000 sheet — ROCKLEA (2352); geological 1:250 000 sheet MOUNT BRUCE (SF50-11).

#### *AMG references*

Woongarra Rhyolite: top — 504694; base — 510699.

#### *Topography and exposure*

The gorge is an incised part of the course of the Beasley River about 3 km long, where the river flows west-southwest and provides generally good exposures of the upper units of the Hamersley Group. The Woongarra Rhyolite is well exposed along the lower (downstream) part of the gorge, at and upstream from the permanent Woongarra Pool (Fig. 3), below which the river valley opens onto a broad alluvial plain underlain by the Kungarra Formation of the Turee Creek Group. The best exposures are generally those immediately adjacent to the river bed.

#### *Structure and stratigraphy*

The Hamersley Group here forms the northern limb of the Hardey Syncline; the strike is close to 120°, and the south-southwesterly dip varies from about 70° at the top of the Woongarra Rhyolite section to about 60° at the base. A summary stratigraphic section appears in Figure 20, which essentially reproduces that of Trendall (1976). The base can be most closely identified away from the river to the southeast, but there is an exposure gap of about 2 m between the strongly weathered lowermost rhyolite and a thin shale of the underlying Weeli Wolli Formation which immediately overlies the top of a dolerite sill. There is a further exposure gap, estimated at about 30 m, between this poorly defined basal section and the lowermost rhyolite of the lower unit in the good exposures in low

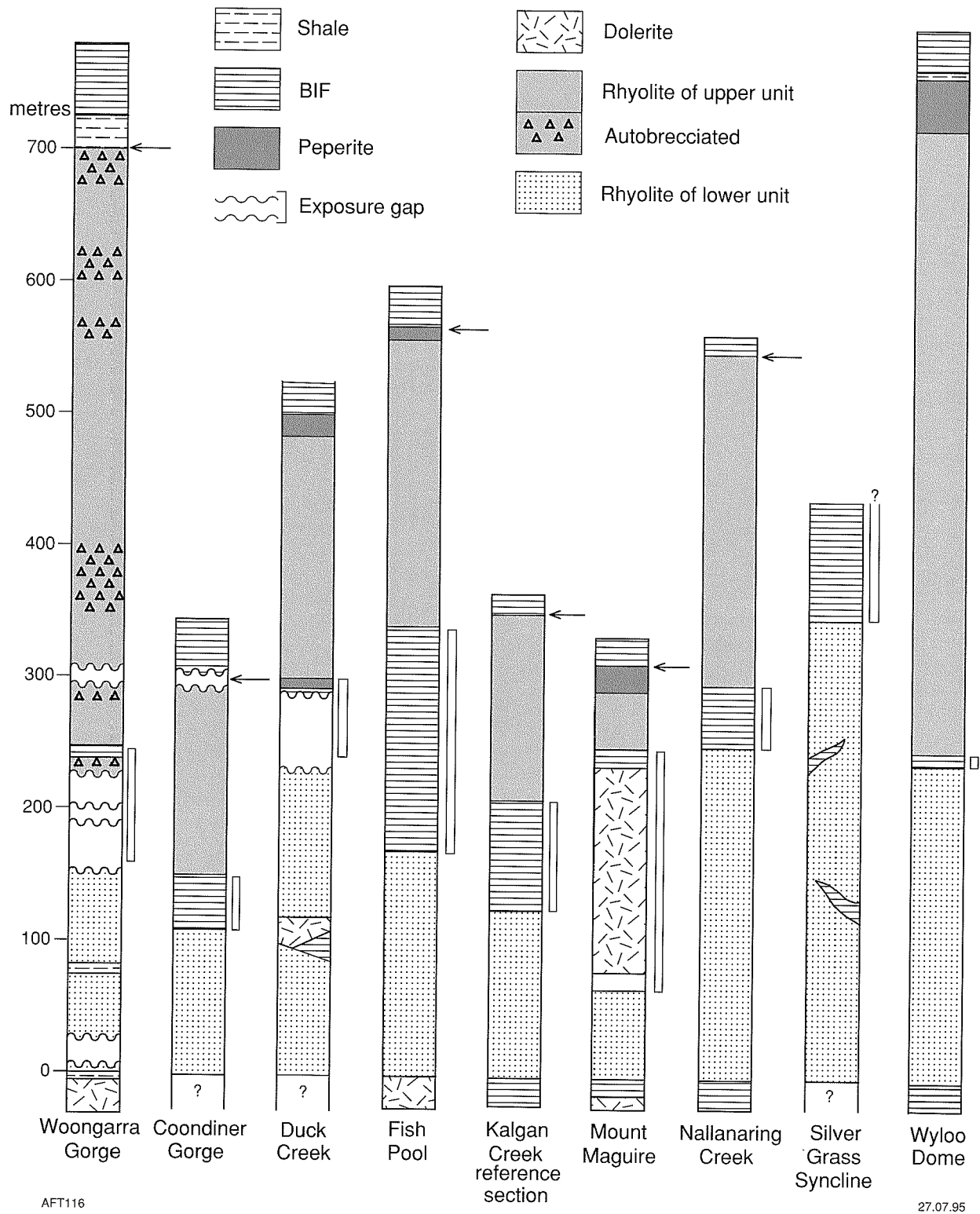
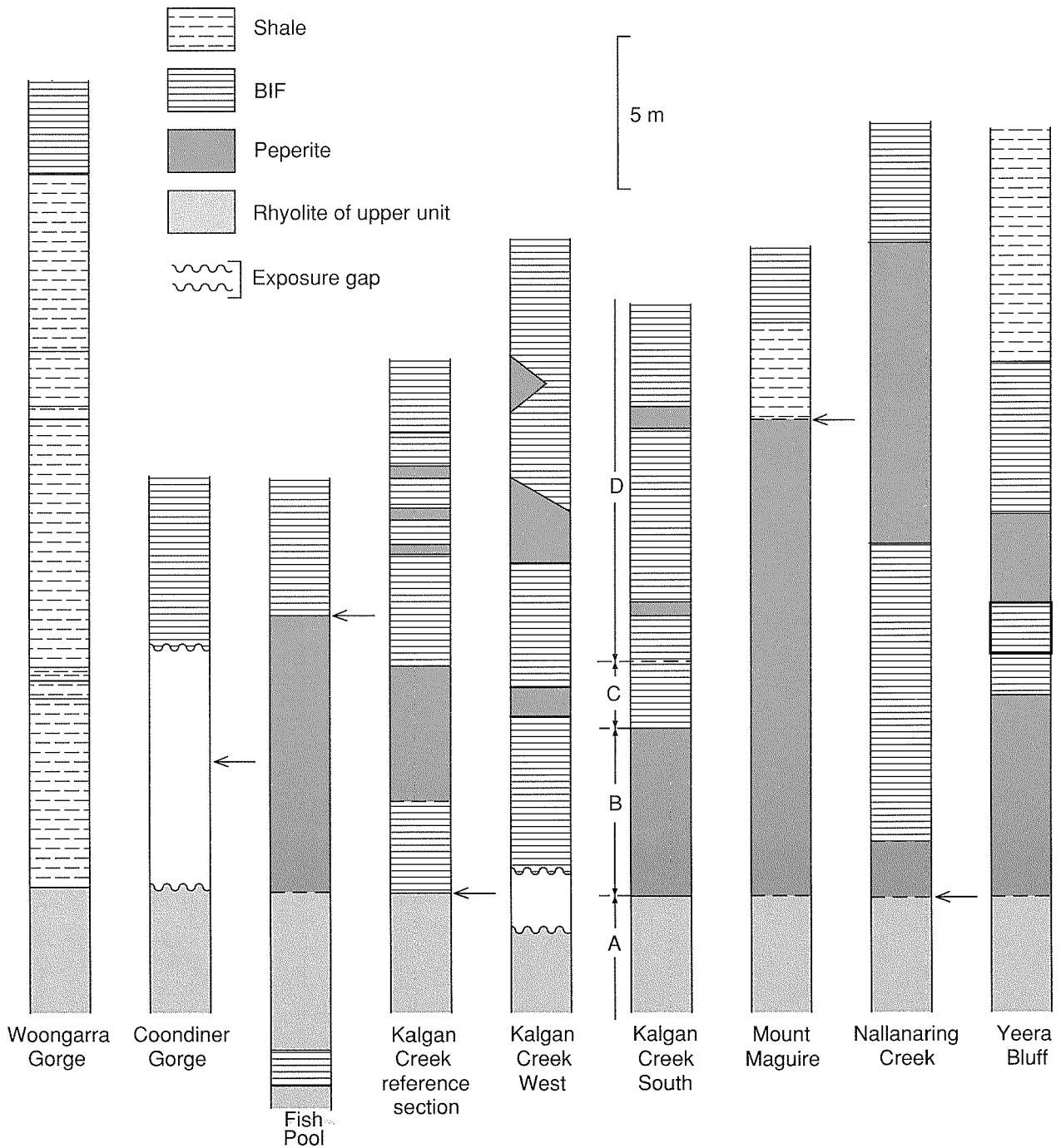


Figure 20. Comparative stratigraphic sections of the Woongarra Rhyolite in selected locations. The type section is on the left-hand end, with reference sections across the page in alphabetical order. Where the detail of the upper contact of a column is also given in Figure 21, an arrow appears on the right hand side of the column, corresponding to an identically placed arrow in the appropriate column of Figure 21. Exposure gaps are indicated only where these are specifically noted in the accompanying text; they are not shown where exposure is generally poor. The rectangular bar to the right of each column shows the extent of the median raft complex; the main lithology is shown where there is a mixture of rock types. Peperite above the top of the upper unit is not shown where a detailed column of the upper contact is also shown in Figure 21. Uncertainty concerning the immediately underlying rock is shown by question marks in three of the columns



AFT117

27.07.95

Figure 21. Comparative sections of the upper contact of the Woongarra Rhyolite in selected locations. The type section on the left-hand end, with reference and other sections across the page in alphabetical order. Arrows at the right hand side of some columns indicate correlation with the equivalent columns of Figure 20. Exposure gaps are marked only where they are specifically referred to in accompanying text. The column for Kalgan Creek West summarizes the stratigraphic situation shown in detail in Figures 26–28. The lettered arrows on the Kalgan Creek South column refer to the informal zones used solely for convenience of description in the text. Solid lines show sharply defined contacts; pecked lines show uncertain or gradational contacts

cliffs on the northwest side of the river. The lower unit here consists, atypically, of two parts. The lower part, of which a thickness of about 45 m is exposed, consists of very uniform massive grey-green, rough-textured rhyolite, with a well-developed joint set parallel to the stratigraphic dip. Some clean joint surfaces are patterned by faintly defined cracks representing incipient autobrecciation. A set of anastomosing, subparallel planes, marked by paler rhyolite, is also locally present, and is similar to those noted at the Silver Grass Syncline and Coondiner Gorge sections. This lower part is separated from an upper part of about the same thickness by a screen of fine-grained green, laminated shale about 5 m thick ('tuff' of Trendall, 1976), dipping conformably with the stratigraphic orientation. The upper part of the lower unit is about 50 m thick, and consists of rhyolite generally similar to that of the lower part of the rhyolite, but differing in showing more patchy variation in texture and colour. There is irregular variation within it from dark-grey, smooth-fracturing rhyolite to strongly mottled varieties; tightly compressed flowage folds occur near the top.

Above the lower unit there is an exposure gap (Fig. 20) corresponding to the median raft complex, which probably consists largely of shale and dolerite, before continuous exposure of the upper unit commences in the higher cliffs on the southeast side of the river. There are excellent exposures along the base of these cliffs, where autobrecciation is well developed. The upper unit rhyolite is typically porphyritic (Fig. 15), with both clear quartz and pale feldspar phenocrysts evenly distributed within a fine-grained, dark grey matrix with a conchoidal fracture. In contrast to the rhyolite of the lower unit, there is no main joint set oriented parallel to the stratigraphic dip. The uppermost part of the upper unit is strongly autobrecciated (Fig. 16b,c,d) and is overlain by about 26 m of dark-grey to green, variably laminated shale with a few thick mesobands of white, widely microbanded chert (Fig. 22). Clearly defined thin (1–3mm) white bands in the upper part appear to be direct ash-fall tuffs. Above this shale (Figs 3 and 21) the base of a unit of dark-grey to black massive BIF is sharply defined. This BIF is representative of that accepted (e.g. Trendall, 1975, 1976, 1983) as confined to the Boolgeeda Iron Formation. A stratigraphically delimited zone of early soft-sediment deformation, less than a metre thick, lies about 3 m below the base of the BIF. The contact between shale and the underlying brecciated top of the upper unit (Fig. 23) is sharply defined; some shearing along the contact is probably related to the accommodation of strain resulting from formation of the Hardey Syncline.

### Summary of thicknesses

Total 700 m. Lower unit 160 m; median raft complex 90 m; upper unit 450 m.

### Features of special interest

Sharp top margin lacking peperite. Lower unit has two slightly different units with a separating raft of shale. Autobrecciation (with perlitic quenching) is exceptionally abundant in the upper unit. Second thickest section recorded, mainly due to contribution of the upper unit.



**Figure 22.** The upper contact of the upper unit at Woongarra Pool; the position of this photograph is indicated on Figure 3. About half a hammer length to the right of the hammer a pale chert mesoband about 70 mm thick is in situ, and dips steeply south-southwest (upper left to lower right); immediately above, it is concealed by fallen blocks, but above these again it runs in situ up to the arrow as an undisturbed band. The shales to both left (beneath) and right (above) of the chert band dip concordantly with it, and the latter extend to the right-hand edge of the photograph. The blunt (left-hand) end of the hammer head rests on the top of pale, autobrecciated, and silicified rhyolite of the upper unit, and this boundary extends upwards parallel to the bedding of the overlying shale. Massive autobrecciated rhyolite extends to the left-hand edge of the photograph. The upper contact of the Woongarra Rhyolite at this locality is unusual in the absence of a marginal peperite layer (see Figs 21 and 26). The hammer is 33 cm long

## Coondiner Gorge

### Location and access

Coondiner Falls is about 33 km from Newman township on a bearing of about 340°. Access is via the same 4WD track leading to the Kalgan Creek area (shown on the 1:100 000 topographic sheet); this track was almost impassible in 1987 at a point just east of Kalgan Pool (AMG 762330), but it is also accessible from the main Newman – Port Hedland road to the west.



**Figure 23.** Vertical cliffs, about 80 m high, cut in massive rhyolite of the upper unit on the west bank of Coondiner Creek immediately north of Coondiner Falls, which are just outside the left-hand edge of the picture; AMG (2851) 644443, vehicle (Toyota Landcruiser) is circled for scale. The view is westward, across the deep gorge of the north-draining creek. The photograph shows well the unstratified, massive character of the unit. The line of low cliffs in the background marks the near-horizontal outcrop of the (heavily lateritized) overlying BIF. Compare Figure 3

#### Map sheet

Topographic 1:100 000 sheet — NEWMAN (2851); geological 1:250 000 sheet — NEWMAN (SF50-16).

#### AMG references

Coondiner Falls — 644444; base of Woongarra Rhyolite going north — 647451; northern reappearance of base — 647470; northerly dipping top — 652478.

#### Topography and exposure

Coondiner Creek flows northward into the Fortescue River valley from the northern part of the Hamersley Range near its eastern end. The name Coondiner Gorge is applied to the deeply incised section of the creek north of Coondiner

Falls. Although exposure around the falls is spectacular (Fig. 23) the Tertiary Hamersley Surface, into which the creek is incised, is here deeply lateritized. Fresh exposures downstream from the falls are virtually confined to the immediate vicinity of the creek bed, and significant sections of this are concealed by boulder debris from the steep slopes of the gorge.

#### Structure and stratigraphy

Coondiner Gorge cuts through the crest and northern limb of a gently west-plunging anticline. At the top of the falls, which is just below the top of the upper unit, there is a southerly dip of a few degrees (Fig. 23). Upstream, about 300 m to the south, the overlying BIF is exposed along the east bank of the creek, with substantial variation in dip due to parasitic folding; the contact itself is not exposed. The BIF locally breaks into the thin (~10 mm) 'flagstones' typical of surface exposures of the striped facies of the Weeli Wollli Formation. Downstream, the Woongarra Rhyolite is best exposed on the northern, north-dipping, limb of the anticline, the core of which provides unusually good exposures of the intrusive margins of dolerite sills within the Weeli Wollli Formation; some of these exhibit vesicular pillowed dolerite. The stratigraphic summary in Figure 20 is derived from that northern-limb section, in which the dip varies between about 25° and 30°. Thicknesses shown there, and noted below, are not reliable, due to the generally poor exposure. However, the two-fold division of rhyolites is clearly expressed, with the median raft complex consisting largely of BIF, marginally contaminated with extensively disrupted dolerite (Fig. 12d). Rhyolite of the lower unit is greenish grey, and exceptionally massive, coarse and homogeneous in field appearance; locally anastomosing subparallel planes of bleached rock, similar to those at Woongarra Gorge, are present.

#### Summary of thicknesses

Total 300 m. Lower unit 110 m; median raft complex 40 m; upper unit 150 m.

#### Features of special interest

BIF of Weeli Wollli Formation type ('striped facies') above the upper contact. Spectacular cliffs of upper unit at Coondiner Falls.

## Duck Creek

#### Location and access

The Duck Creek reference section lies about 3 km north-northeast of Duck Creek Homestead, along a tributary creek draining southwards into Duck Creek. Access to Duck Creek is by way of an unsealed road turning eastwards off the main Nanutarra–Wittenoom road at Mount Stuart. The tributary creek along which the section runs crosses this road about a kilometre west of the homestead, just east of the station airstrip, and is negotiable by 4WD vehicle.

### Map sheets

Topographic 1:100 000 sheet — FARQUHAR (2253);  
geological 1:250 000 sheet — WYLOO (SF50-10).

### AMG references

Top of Woongarra Rhyolite crosses creek bed at about 575125; base at about 582133.

### Topography and exposure

Although the unnamed tributary creek along which the section lies is incised about 100 m into the heavily lateritized Tertiary Hamersley Surface, fresh exposures are generally confined to the immediate vicinity of the creek bed, and are discontinuous.

### Structure and stratigraphy

The Woongarra Rhyolite forms the southerly dipping limb of an easterly plunging anticline; measured dips vary between 20° and 40°, and the average strike close to 90°. A summary stratigraphic section of the Woongarra Rhyolite in this reference section is shown in Figure 20; thicknesses shown there, and noted below, are estimates from dip and outcrop width. The lower margin is concealed. Rhyolite of the lower unit closely resembles that of the type section; in cliffs in a constricted part of the creek both sheet jointing oriented parallel to the stratigraphic dip and a joint set normal to it, resembling columnar jointing, are well developed. Rhyolite, typical of the lower unit (massive, green, rough-fracturing, non-porphyrific, with coarse micropoikilitic texture), occurs above and below well-exposed BIF, on the western slopes of the valley, and dolerite, exposed in the creek bed. Both the BIF and the dolerite are interpreted as components of a raft within the lower unit.

Farther downstream, at about AMG 580127, there are excellent exposures in low rubbly cliffs in the east bank of the creek of unusually 'bedded' clastic rocks, illustrated in Figure 24. The stratification has an average southerly dip of 35°, and the strike is close to 75°. There is a moderately well-developed cleavage associated with the anticline, of which the whole Woongarra Rhyolite outcrop forms part, and this has a northerly dip of about 80° with a strike close to 90°. The immediate impression given by these rocks is that they closely resemble turbiditic sediments. The coarser parts of the beds, which are centimetres to tens of centimetres thick, are made up of dark-green, closely packed, subangular fragments; and these coarse parts commonly grade within each bed into fine-grained, dark slaty rock in which individual fragments cannot be resolved with the naked eye. Many of these fine-grained rocks are finely laminated, and one example was observed in which the dark, fine-grained part of a bed projected as a flame structure into the coarse edge of the adjacent bed. However, the grading is mostly less regular than that of typical turbidites, and may reverse several times within a bed, resulting in irregularly gradational alternations of coarse and fine material. Close examination reveals that the impression of regular bedding given by these rocks is misleading. It can be seen from Figure 24

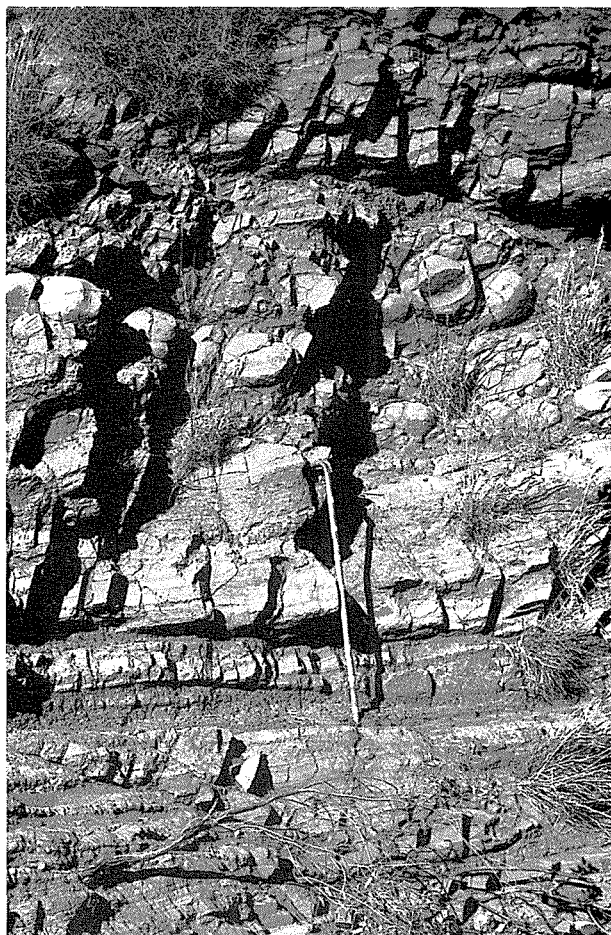
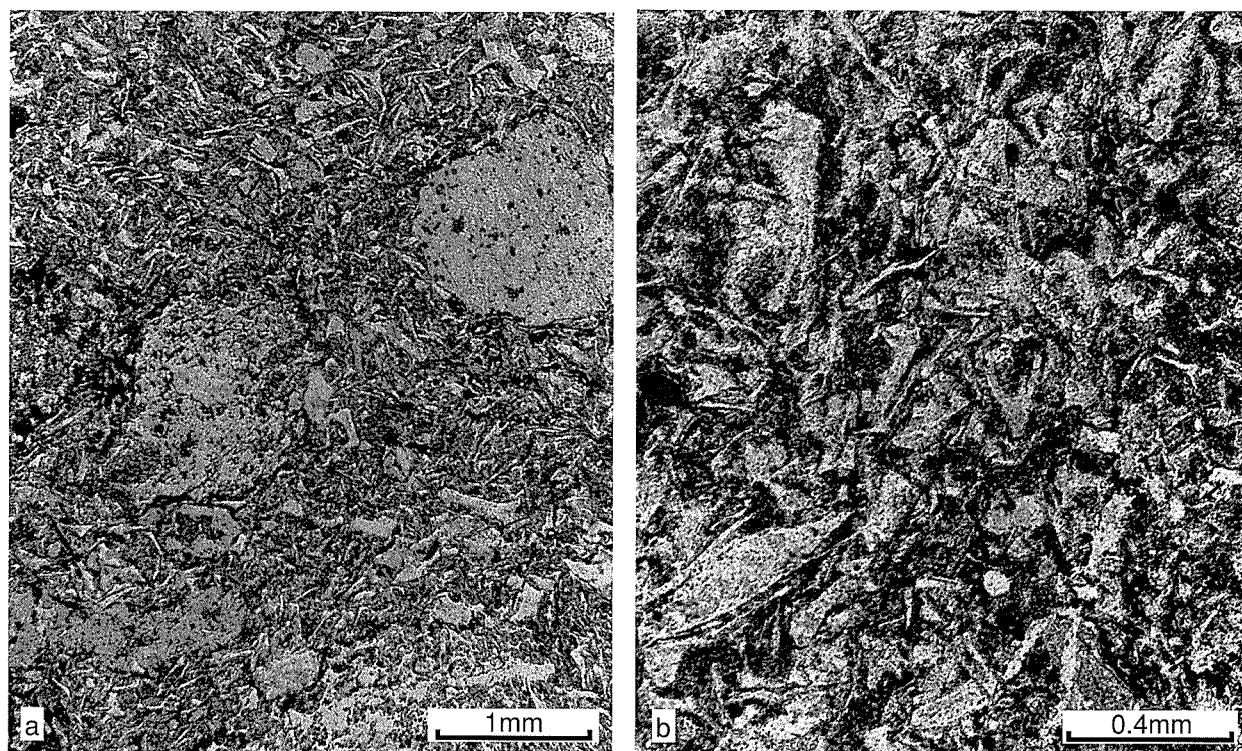


Figure 24. Banded peperite at the top of the median raft complex in the Duck Creek reference section. Looking south-southeast (down dip) at exposure in bank of south-draining creek at AMG (2851) 580127. Coarse (1 cm) to fine (aphanitic) clastic material resembles turbiditic sediments. See Figure 25 for photomicrographs of this material. The white marks on the shaft of the stick are at 10 cm intervals

that many beds are lithologically variable along their length, and that there are oblique discontinuities, both within and between beds, of a type atypical of turbiditic sediments. In thin sections of these rocks the constituent material, insofar as it is identifiable at all, appears to be entirely of volcanic origin. The individual dark clasts consist of aggregates of finely crystalline chlorite, while the aphanitic matrix which binds them, and which forms the finer grained parts of each bed, consists of a microcrystalline quartz–feldspar–chlorite aggregate in which the textural relationships of these minerals delineate a close-packed mass of shards (Fig. 25a,b). In accordance with earlier discussion of nomenclature these rocks are included under the blanket name 'peperite', notwithstanding the apparent absence of a sedimentary component. These banded peperites are exposed for a total stratigraphic thickness of 8 m, and overlie BIF. Their upper contact is not clearly exposed. Porphyritic grey rhyolite of the upper unit, closely



**Figure 25.** Thin-section photographs of the 'stratified' tuffs of the Duck Creek reference section. (a) Sample 94748. The matrix of the rock consists of close-packed, randomly arranged, 'shards' mostly about 0.5 mm long. These consist of a mosaic of K-feldspar and quartz, average grain diameter about 0.05 mm; the former is either clear or slightly clouded with hematite dust. Their outlines are defined by a pervasive microcrystalline (<0.01 mm) quartz-chlorite aggregate, which has a speckled grey colour in the figure. The >1 mm areas of different texture (e.g. upper right, centre left) are broken fragments of fine-grained quartz-feldspar-chlorite mosaic. (b) Sample 15673. A very similar rock to 94748, at a higher magnification that shows the random 'shard' structure more closely; the fragments in this rock also include angular broken quartz and feldspar crystals

resembling that at the type section, is exposed not far above, both in the creek bed and the rubbly sides of the valley. The top contact of the Woongarra Rhyolite is not well exposed in this section, but lateritized exposures near the crest of the ridge on the east side of the creek reveal about 15 m of peperite lying between the uppermost rhyolite and overlying BIF. The top section is not sufficiently well exposed for inclusion on Figure 21.

#### *Summary of thicknesses*

Total 500 m. Lower unit 240 m; median raft complex 60 m; upper unit 200 m.

#### *Features of special interest*

Of particular interest because of the unusually 'bedded' peperite at the base of the upper unit. A major raft consisting mainly of BIF lies roughly centrally within the lower unit.

## **Fish Pool**

#### *Location and access*

This reference section has a bearing of about 340°, parallel to, and about 1.5 km west of, Turee Creek where it cuts

through the Hamersley Group in the northwestern limb of the Turee Creek Syncline. The section is about 75 km south-southeast of Tom Price township, and lies about 2 km north-northwest of Fish Pool (on Turee Creek), after which it is named. Access is by an unmaintained 4WD track that turns off the main Paraburdoo-Tom Price road; southward from Fish Pool the track follows the line of Turee Creek.

#### *Map sheet*

Topographic 1:100 000 sheet — SNOWY MOUNT (2551); geological 1:250 000 sheet — TUREE CREEK (SF50-15).

#### *AMG references*

Upper contact at 088393 and the base at 084341.

#### *Topography and exposure*

The Woongarra Rhyolite here forms a well-defined set of parallel strike ridges similar to those of the Kalgan Creek reference section (Fig. 2). The Boolgeeda Iron Formation forms a ridge on the south side of the outcrop which is succeeded northwards by a ridge of the median raft complex. The next strike valley north is formed by the

lower unit and a dolerite sill of the Weel Wolli Formation, and this is followed by a strike ridge of BIF of that unit.

### Structure and stratigraphy

The parallel ridges strike about 70°, and dip about 45° south-southeastward towards the axis of the Turee Creek Syncline. They present a continuous stratigraphic section which is summarized in Figures 20 and 21. The lower contact is not well exposed, but the lowest exposed rhyolite of the lower unit is separated from dolerite of the Weeli Wolli Formation by an exposure gap of only a few metres. The median raft complex, which consists mainly of BIF with minor shale and dolerite, shows exceptional irregularity; much of the BIF is tightly folded and contorted. The overlying grey porphyritic rhyolite of the upper unit is very similar to that of the type section. At the top a band of fine-grained peperite, about 10 m thick and of porcelanous appearance, immediately underlies the lowest BIF of the overlying Boolgeeda Iron Formation. The peperite is here weathered white, and appears to pass gradationally downwards into the uppermost autobrecciated rhyolite; a thin section from unweathered rock in the same stratigraphic position in the northernmost part of the syncline, about 25 km along strike to the east-northeast, shows that this peperite consists of a thoroughly welded mesh of small shards (Fig. 19d), closely resembling the material from lenses above the top of the upper unit at the Kalgan Creek West location (Fig. 19c). BIF, which appears to lie within rhyolite of the upper unit along the line of this reference section (Fig. 21), is not continuous along strike, and may be an isolated raft or the result of landslip unrelated to real stratigraphy.

### Summary of thicknesses

Total 560 m. Lower unit 170 m; median raft complex 170 m; upper unit 220 m.

### Features of special interest

The Fish Pool section is very typical of Woongarra Rhyolite exposure over much of the Hamersley Range, and shows no exceptional or unusual features.

## Kalgan Creek area

Kalgan Creek (Fig. 1) is a tributary of the Fortescue River flowing east and draining the central part of the Ophthalmia Range, where the Woongarra Rhyolite is well exposed in a series of both tight and open folds. The Woongarra Rhyolite was examined in three separate places in the Kalgan Creek area. One of these was traversed completely from top to bottom, as well as examined for some kilometres along strike, and is designated the Kalgan Creek reference section. At the two other places, here called Kalgan Creek West and Kalgan Creek South, only the upper contact was examined closely.

### Location and access

The Kalgan Creek reference section lies north of Kalgan Creek about 16 km due east of its confluence with the

Fortescue River. This locality is about 20 km from the centre of Newman township on a bearing of 10°. Kalgan Creek West is about 9 km from the reference section on a bearing of about 260°, and Kalgan Creek South, about 2.5 km from the reference section on a bearing of 190° (Fig. 2). The Kalgan Creek area is readily accessible via a 4WD track which closely follows the south bank of the creek, and turns west off the main Newman–Roy Hill road about 25 km north of the Roy Hill road turning off the Great Northern Highway.

### Map sheet

Topographic 1:100 000 sheet — NEWMAN (2851); geological 1:250 000 sheet — NEWMAN (SF50-16).

### AMG references

The southern end of the reference section (the structural and stratigraphic top of the Woongarra Rhyolite) is at 832338 and the northern end at 833343. The Kalgan Creek West location is centred at 750307 and the Kalgan Creek South location is centred at 828319.

### Topography and exposure

The flat and smoothly lateritized Tertiary Hamersley Surface in this area had a generally concordant elevation of between 600 and 650 m above sea level before its rejuvenation and dissection. The present drainage pattern of Kalgan Creek has been incised about 50–60 m below this surface, and is partly strike controlled and partly superimposed; as a consequence the present topography has a complex pattern of flat-topped ridges (Figs 26 and 27) separated by steep-sided valleys in which exposure is generally good. At the reference section, and commonly elsewhere in the area, the Woongarra Rhyolite forms a set of parallel strike ridges clearly visible on the airphotos (Fig. 2).

### Structure and stratigraphy

At the Kalgan Creek reference section the Woongarra Rhyolite has a strike of 100° and a general southerly dip close to 45° (Fig. 2); a southwesterly trending fault cutting across the section is not believed to affect the stratigraphic section on either side. A summary stratigraphic section of the Woongarra Rhyolite in the area of the main Kalgan Creek reference section is shown in Figure 20 and details of the upper contact at all three locations appear in Figure 21. The three main divisions of the Woongarra Rhyolite — the massive green rough-fracturing rhyolite of the lower unit, the BIF-rich median raft complex, and the grey porphyritic rhyolite of the upper unit — are stratigraphically consistent and easily recognizable throughout the Kalgan Creek area. The description here concentrates on features of the upper contact which are present in all three sections, but are particularly well exposed at the Kalgan Creek West and Kalgan Creek South locations.

At Kalgan Creek South the upper contact is described by reference to four zones, lettered A–D upwards, which

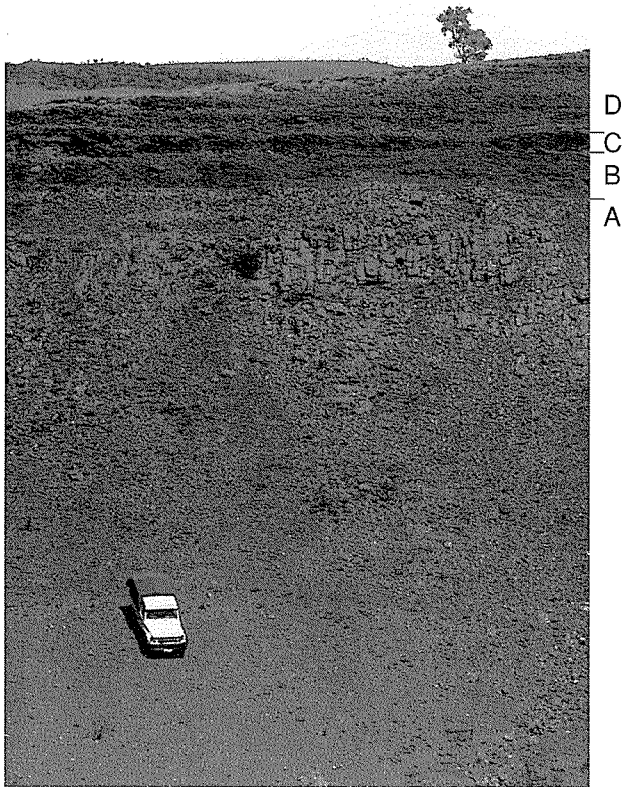


**Figure 26.** The upper contact of the Woongarra Rhyolite at the Kalgan Creek South locality (see Fig. 2). The view looks southward from a ridge crest of the Woongarra Rhyolite at AMG (2851) 824320, across a valley draining eastwards (right to left). Towards the top of the north-facing slope across the valley a clearly defined boundary between the massive pale rhyolite (A) of the upper unit (compare Figs 3 and 23) and the overlying darker peperite (B), associated with the upper contact, is visible. Above the peperite a darker band of massive BIF (C) is succeeded upwards by rather thin-bedded BIF (D) with two further thin bands of fine-grained peperite. There is a uniform southerly dip of about 40° (i.e. away from the observer). The stratigraphy of this exposure of the upper contact, including zones A, B, C and D, is shown in Figure 21

are clearly visible in outcrop (Fig. 26) and are marked both on that figure and on Figure 21; they have no status other than descriptive convenience. Zone A essentially consists of the massive top of the grey porphyritic rhyolite of the upper unit. However, the uppermost part of this pale-weathering zone shows an increasing amount of autobrecciation, as well as associated fragmental textures. Some thin sections from the top of this zone have textures resembling those of Figure 16a, which shows a rock from the northern Turee Creek Syncline; these uppermost rocks show no sign of compression or flattening of fragments. The contact between zones A and B is quite sharply defined. The

slightly greater degree of weathering in zone B (lighter grey in Fig. 26) makes precise identification of its components difficult, but it is estimated to consist of peperite with approximately equal proportions of sedimentary (shale and BIF) and rhyolitic debris. Figure 19b,e, from an equivalent level of the nearby (Fig. 2) reference section, is representative of the finer parts of the peperite, which shows intense flattening of all medium-sized clasts. Elsewhere within the zone such material acts as a matrix within which larger clasts of more resistant rocks, up to a metre long and consisting mainly of chert or BIF, have resisted both compaction and fragmentation, to form a chaotic and unsorted melange. Zone B is about 5.5 m wide. Zone C, which appears as a dark band in Figure 26, is a continuous band of thinly mesobanded BIF, about 2 m thick. The BIF above it (zone D), which appears paler in Figure 26, has a more shaly appearance, and has within it thin discontinuous lenses of fine, pale, flinty peperite. The highest such band seen was about 0.8 m thick, with its base about 10 m above the top of the peperite of zone B.

These peperite lenses within zone D are very similar to the thicker examples developed at the Kalgan Creek West locality, illustrated in Figure 27. In that section the uppermost part of the upper unit is poorly exposed, and no obviously mixed peperites equivalent to zone C of Kalgan Creek South were noted, although their possible presence is not precluded. But the BIF overlying the Woongarra Rhyolite is very well exposed there in small north-facing cliffs near the top of a ridge, and lenticular sheets of fine-grained, flinty pale-weathering peperite are well exposed within it. The lenses range up to 3 m in thickness, and have sharply defined planar boundaries against the adjacent BIF (Figs 28 and 29). The material within them consists of a thoroughly welded aggregate of rhyolitic shards, including bubble-wall forms (Fig. 19C).

#### *Summary of thicknesses*

(Based on the Kalgan Creek reference section) Total 350 m. Lower unit 125 m; median raft complex 85 m; upper unit 140 m.

#### *Features of special interest*

The laterally variable lenses of peperite within BIF above the top of the Woongarra Rhyolite at the Kalgan Creek West locality (Figs 27–29) are of particular interest. Peperites of the upper contact are also well displayed at Kalgan Creek South (Fig. 26) and at the southern end of the reference section.

## **Mount Maguire**

### *Location and access*

Mount Maguire (Fig. 1) is 17 km southeast of Paraburdoo township and lies at the western end of a conspicuous straight ridge about 10 km long on a bearing of about 120°. The reference section runs on a bearing close to 210°.

### Map sheets

Topographic 1:100 000 sheet — PARABURDOO (2451); geological 1:250 000 sheet — TUREE CREEK (SF50-15).

### AMG references

Stratigraphic top at 766180 and the base at 769184.

### Topography and exposure

This reference section is situated on the steep, northward-facing, rather broken slopes of the ridge that has Mount Maguire at its western end.

### Structure and stratigraphy

The strike of the Woongarra Rhyolite in the northern face of the ridge is about 300°, and there is an average south-southwesterly dip of about 65°. The ridge is cut by numerous faults (Thorne et al., 1991), and the choice of a reference section was made within a small fault-bounded block where the risk of tectonic modification of stratigraphy was minimized. A stratigraphic summary of the Woongarra Rhyolite in the Mount Maguire reference section appears in Figures 20 and 21. The underlying exposures of Weeli Wolli Formation in the lower slopes of the ridge reveal a complex alternation of BIF with thin dolerite sills. The massive green rhyolite of the lower unit conforms closely to the general description already given. The median raft complex in this section is unusually thick, and the dark-green, fine-grained dolerite which forms the bulk of its thickness is easily mistaken for an acid volcanic rock in the field; thin sections are needed for confident identification. The rhyolite of the upper unit is also lithologically typical, but the unit is thin, and quite poorly exposed on the spinifex-covered slopes of the ridge. Below the upper contact against BIF there are about 19 m of fine-grained, white-weathered porcelanous rock of uniform appearance. Thin-section examination reveals that the uppermost 3 m of this is probably a shale, and that the lower 16 m is a fine-grained peperite consisting mainly of welded shard debris. The two rock types are not clearly distinguishable in the field.

### Summary of thicknesses

Total 315 m. Lower unit 70 m; median raft complex 180 m; upper unit 65 m.

### Features of special interest

The median raft complex is exceptionally thick, and consists largely of dolerite.

## Nallanaring Creek

It is not possible to designate a complete reference section in this area with confidence, since the abundant north-trending strike faults make exact stratigraphic interpretation impossible without detailed mapping. The main

location described here is a point on Nallanaring Creek where the top contact of the Woongarra Rhyolite is well exposed; however, a complete section, of dubious reliability, is also given (Fig. 20) because of the location of the section near the northwestern outcrop limit of the Woongarra Rhyolite.

### Location and access

Nallanaring Creek drains northwards into the Fortescue River, and joins that major river about 45 km upstream from its mouth. The location can be reached by an unmaintained track leaving the south side of the North West Coastal Highway about 1.5 km southwest of the Fortescue River crossing (Bilanoo). The track crosses the (ill-defined) Nallanaring Creek after about 10 km; the creek bed is negotiable with care by 4WD vehicle.

### Map sheet

Topographic 1:100 000 sheet — FORTESCUE (2155); geological 1:250 000 sheet — YARRALOOOLA (SF50-6).

### AMG references

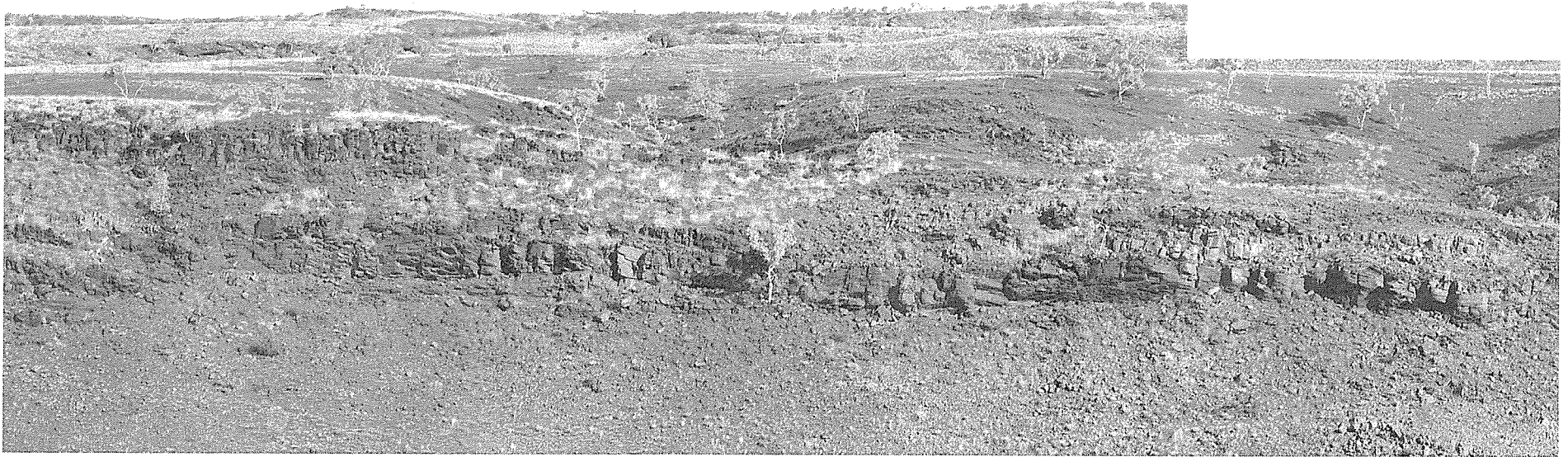
The upper contact in cliffs on the west side of Nallanaring Creek is at 134283; the probable base in a tributary creek joining from the east is at 154282.

### Topography and exposure

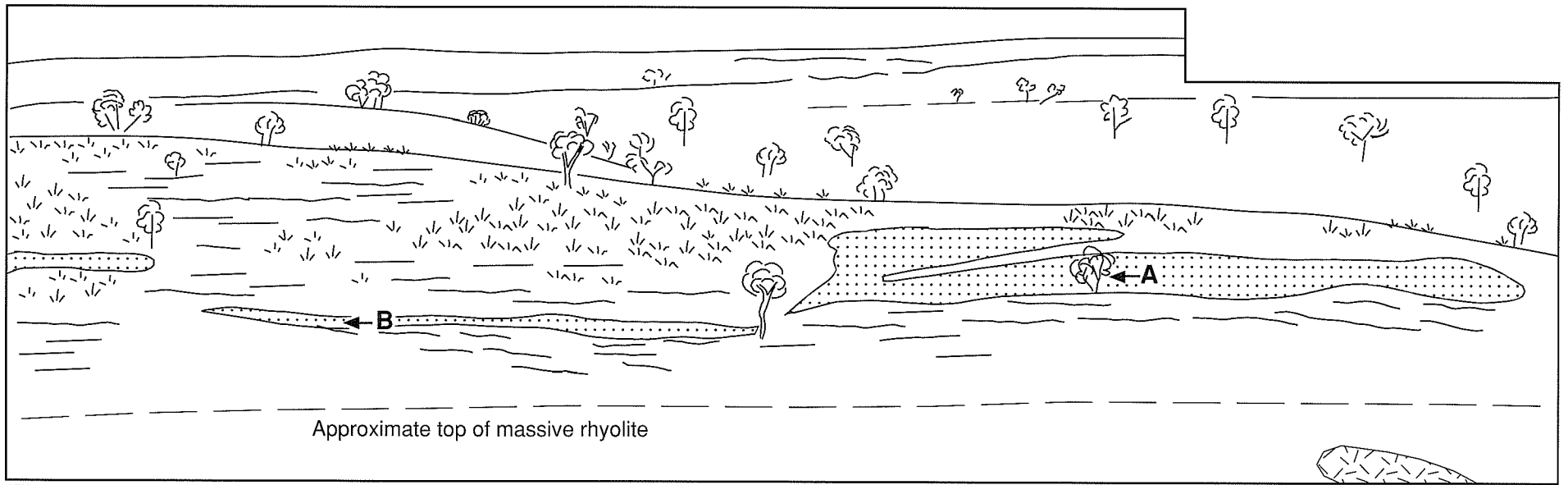
The Tertiary Hamersley Surface in this area forms a smooth and deeply lateritized plateau with an elevation of about 150 m above sea level. Nallanaring Creek and its tributaries are incised into this surface to a depth of about 60 m, so that the only clean exposures are along the creek beds and adjacent steep hillslopes where these are not concealed by screes.

### Structure and stratigraphy

The upper part of the Hamersley Group in the area has a general easterly dip of 20–40°, with a strike close to north. The pervasive north-striking faults make thickness estimates unreliable (Fig. 20). Lower and upper units are distinguishable, with a rather thin central BIF raft. A summary stratigraphic section of the upper contact, where it is well exposed in the west bank of Nallanaring Creek at the location specified above, is shown in Figure 21. The thicknesses of the individual units vary along strike, and those shown are averages. Massive, grey, porphyritic rhyolite typical of the upper unit is cleanly exposed in the edge of the creek bed; complexly swirled flow banding is common. It is overlain by a 2 m band of peperite consisting mainly of coarsely brecciated BIF, and this is succeeded upwards by about 10 m of BIF which has undergone substantial deformation, mainly expressed as discordances in the banding. Above this is a sharply defined 10 m-thick sill of black, magnetic peperite which was illustrated and described in detail by Trendall (1972). A summary of that description has already been repeated above, and part of a thin section of a typical sample appears in Figure 19a. BIF with a



32



AFT122

2.03.95

minor proportion of grey shale continues upslope to the lateritized top of the slope.

### Summary of thicknesses

Total 550 m. Lower unit 250 m; median raft complex 50 m; upper unit 250 m.

### Features of special interest

Excellent exposures of a peperite sill above the top of the upper unit rhyolite, and the first location from which these rocks were described. Trendall (1972) provided a detailed description of a single peperite sample ('an unusual eutaxitic rock') from this location.

## Silver Grass Syncline

### Location and access

The location of the Silver Grass Syncline is shown in Figure 1. The area is reached by a track leaving the Hamersley Iron Pty Ltd company railway maintenance road (a private road) westwards at a point close to AMG (2453) 660640; the turning is just south of 'Camp Anderson'. The unmaintained track continues for some 40 km in a westerly direction, gradually climbing, via Caliwinga Creek, onto a high (~500–550 m above sea level) undulating plateau which is drained by the headwaters of the Robe River. The tracks on the plateau are neither maintained nor accurately marked on any map. Although the plateau surface is easily negotiable by 4WD vehicle the absence of strong topographic features makes location on airphotos difficult, and a hand-held GPS unit is useful.

### Map sheet

The selected reference section lies on the MILLSTREAM (2354) topographic 1:100 000 sheet and the PYRAMID (SF50-7) geological 1:250 000 sheet. The outcrop area of Woongarra Rhyolite in the Silver Grass Syncline is roughly centred on the corners of four 1:250 000 geological sheets: PYRAMID (SF50-7), YARRALOOOLA (SF50-6), WYLOO (SF50-10), and MOUNT BRUCE (SF50-11).

### AMG references

A reference section was selected along a north–south line from 070680 to 070730.

### Topography and exposure

The plateau in this area is a component of the Tertiary Hamersley Surface of MacLeod (1966, p. 13), and is here deeply altered, and locally mantled by either silcrete or laterite. Exposure is therefore generally poor, but some components of the selected section are outstandingly well exposed.

### Structure and stratigraphy

The line selected as a reference section traverses the gently south-dipping northern limb of the Silver Grass Syncline. The southern point specified lies on strongly lateritized BIF, with a southerly dip of about 5°, and the northern end is on rubbly green rhyolite of the lower unit. The lower contact, against the Weeli Wolli Formation, was not examined but is believed not to be clearly exposed. While the Woongarra Rhyolite undoubtedly has a general southerly dip along the line of section, the poor exposure precludes precise measurement, so that the thickness of rhyolitic rock present is very uncertain, and dependent on the assumed average dip. The massive green rhyolite of the lower unit is very well exposed along the northern part of the defined line, and shows the typical false granularity and pseudostratification (Fig. 6). Low hills midway along the defined line consist of strongly weathered BIF, and are irregularly folded. Lateritization makes the relationship with the rhyolite difficult to interpret. Observations of the lower BIF contact with rhyolite in these hills were the basis for Kriewaldt and Ryan's (1967, p. 20) description of 'fragments of iron formation lying in the acid rock and short tongues of acid rock cutting the iron formation'.

Towards the southern end of the section the better exposed rhyolite is grey and porphyritic, and this is finally overlain by the lateritized cherty BIF which forms the highest preserved stratigraphic unit along the axis of the syncline. No good exposures of the contact were found. While this southern rhyolite resembles that of the upper unit in the field, its appearance in thin section is strongly akin to that of the lower unit. Specifically, it has well-developed quartz paramorphs after tridymite and coarse-grained micropoikilitic texture; neither feature is present

Figure 27. (facing page) Wide-angle photograph and explanatory sketch of the upper contact of the Woongarra Rhyolite at Kalgan Creek West location (see also Fig. 21). The positions and directions of view of Figures 28 and 29 are marked by the letters A and B and the adjacent arrows. The view looks southwards from a ridge crest of the Woongarra Rhyolite at AMG (2851) 752318, across a valley draining westwards (left to right). The nearest ridge is a scarp face in which the upper part of the upper volcanic member and the base of the overlying Boolgeeda Iron Formation dip southwards, away from the observer, at an average dip of about 15°; the flat crests of the more distant ridges are heavily lateritized, and are strike ridges related to tight folding of the upper part of the Hamersley Group. The top of the Woongarra Rhyolite is largely concealed by scree, but its approximate position can be fixed closely from the boulders, and a patch of rhyolite in situ is shown near the lower right-hand corner; it is marked along strike by a slight step in the hillslope. Discontinuous lenses of peperite (stippled) are intercalated within the lower BIF of the Boolgeeda Iron Formation (bedding indicated where exposed). The boundaries between BIF and peperite are sharply defined (Fig. 29) and the lens thicknesses vary markedly (compare Figs 28 and 29). The photograph covers a strike length of about 80 m, and the height between the top of the nearest ridge and the top of the scree below varies between about 5 and 20 m

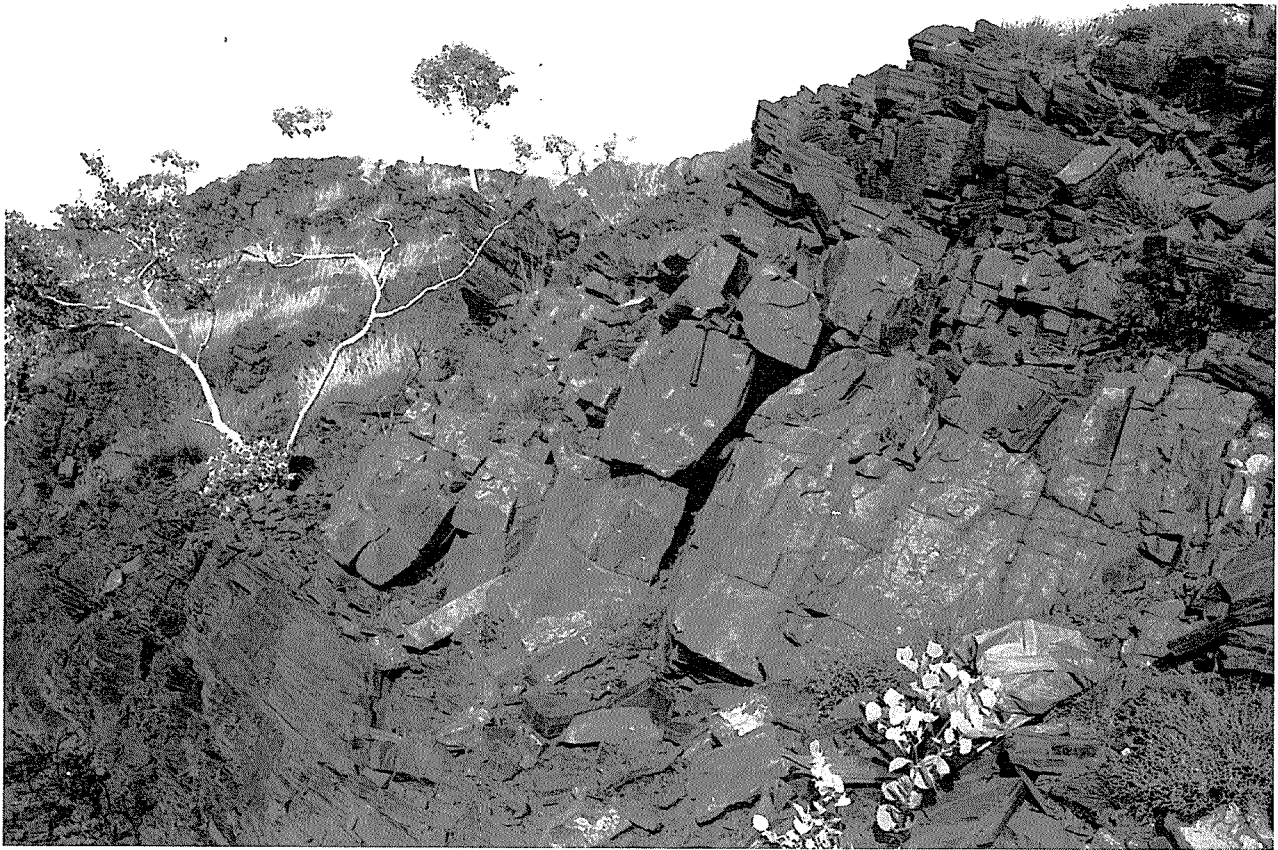


Figure 28. Peperite lens, about 2.3 m thick, dipping gently south at the locality of Figure 27; this view looks easterly along the face of the ridge, at the point marked 'A' on that figure. The pale, blocky field appearance of the peperite contrasts with that of the darker laminated BIF above and below. Both the upper and lower contacts are planar and sharply defined, similar to those better displayed in Figure 29, which shows a similar but thinner lens. A microphotograph of the rock from this lens appears in Figure 19(c), and a chemical analysis in Table 1 (sample 94710). The hammer is 33 cm long

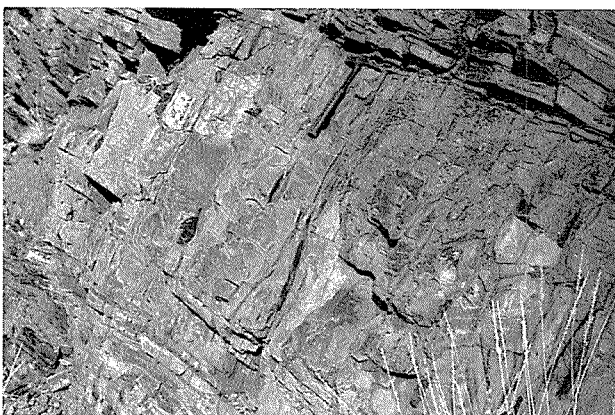


Figure 29. Peperite lens, about one metre thick, dipping gently south at the locality of Figure 27; this view looks easterly along the face of the ridge, at the point marked 'B' on that figure. Compare Figure 28. The sharply defined upper contact of the lens, just above the head of the hammer is well shown in this photograph. The hammer is 33 cm long

elsewhere in rhyolite of the upper unit, but both are typical of lower unit rhyolites in other sections. The whole of the reference section is therefore interpreted here as belonging to the lower unit, and the BIFs midway along the section are interpreted as rafts within it. An alternative interpretation would be that the grey porphyritic rhyolite is indeed part of the upper unit, which here had a different cooling history; and corollaries of this alternative would be that the BIF along the axis of the syncline is the Boolgeeda Iron Formation, and that the BIF hills midway along the selected reference section are components of the median raft complex. The summary stratigraphic section of the Woongarra Rhyolite in the Silver Grass Syncline area in Figure 20 is based on the first, preferred, interpretation. However, because there is an element of uncertainty in this interpretation, the resultant thickness estimate of the lower unit is not used in Table 1.

#### *Summary of thicknesses*

(Based on preferred interpretation) Total unknown. Lower unit 350 m; median raft complex >95 m; upper unit unknown.

### Features of special interest

The most significant feature of the reference section described is the doubt that remains as to whether the stratigraphically highest BIF exposed along the axis of the syncline is the Boolgeeda Iron Formation or a component of the median raft complex. Large outcrop areas of Woongarra Rhyolite, particularly in the northwestern part of the syncline, were not visited during this study, and from inspection of airphotos probably contain excellent exposures.

## Wyloo Dome

### Location and access

The Wyloo Dome reference section lies in the northeastern sector of the ovoid dome, and is about 15 km from Metawandy, a location on the main Nanutarra–Wittenoom road. A 4WD track turns north off the Nanutarra–Wittenoom road at Metawandy, and runs generally north-northwest via Billeroo Bore and through a conspicuous gap in the range along the north of the dome. The northern end of the gully along which the section runs can be reached by 4WD vehicle by turning eastwards off this track at any convenient point north of the gap.

### Map sheet

Topographic 1:100 000 sheet — WYLOO (2152); geological 1:250 000 sheet WYLOO (SF50-10).

### AMG references

Stratigraphic top — 368047; stratigraphic base — 369042.

### Topography and exposure

The section follows the line of a small gully draining northwards off a broad, flat-topped east–west ridge of the Hamersley Group. From the top of the Woongarra Rhyolite southwards the depth of incision of the gully below the general ridge-top level steadily decreases. Exposure in the bed and bouldery slopes of the gully is generally good, but not continuous.

### Structure and stratigraphy

The Hamersley Group in this part of the Wyloo Dome has a strike close to 90° and an average northerly dip of about 45°. If this dip is applied to the rhyolitic rocks of the Woongarra Rhyolite, in which no stratigraphic orientation is available for measurement, the total thickness of the unit is greater than any other reference section (Fig. 20). The lower contact, against BIF dipping evenly north at 45°, can be located to within 2 m in the rubbly slopes of the gully, but it is not cleanly exposed. The rhyolite of the lower unit is similar to that of the type section; at least one minor (1–2 m) raft of contorted BIF is present. The median raft complex is represented by a relatively thin band of red cherty BIF which is strongly brecciated and contorted. Above it the grey porphyritic rhyolite of the upper unit has abundant autobrecciation, and also commonly has a

sheared appearance, but with no consistent orientation. A plastic flowage fold from within this unit is illustrated in Figure 17. Although the upper contact is well exposed in cliffs on the east side of the gully, deep weathering at this point makes rock identification difficult. However, the uppermost 40 m of the upper unit appear to consist of peperite, in which the sedimentary component consists largely of chert; the largest clast noted was 2 m long and 0.5 m wide, but most are much smaller, and they are chaotically distributed within the rhyolitic base. At the top of the peperite about 3–5 m of cherty shale separate it from massive BIF.

### Summary of thicknesses

Total 750 m. Lower unit 240 m; median raft complex 10 m; upper unit 500 m.

### Features of special interest

This is the thickest of the reference sections, with the thinnest and least conspicuous median raft complex.

## Yeera Bluff

### Location and access

Yeera Bluff is the name given to prominent steep slopes, about 60 m high on the northern side of the Robe River, immediately downstream (west) of Deepdale Homestead. Access is by 4WD vehicle down the Robe River from Deepdale Homestead, which is close to the main (sealed) road linking the township of Pannawonica to the North West Coastal Highway.

### Map sheet

Topographic 1:100 000 sheet — PANNAWONICA (2154); geological 1:250 000 sheet YARRALoola (SF50-6).

### AMG references

Location on north side of river — 122953; south side of river — 118946.

### Topography and exposure

The major Robe River transects the northwesterly termination of the Hamersley Range at this location, and provides excellent exposures of the upper contact of the Woongarra Rhyolite, especially on the north side of the river.

### Structure and stratigraphy

At the specified location on the north side of the river the top of the Woongarra Rhyolite and the overlying sediments dip north at between 10° and 15°. A summary stratigraphic section appears in Figure 21. Rather rubbly exposures of the topmost rhyolite of the upper unit occupy the lowest 15 m of the slope; the immediate appearance of the

rhyolite is fresh and massive, but close inspection shows extensive irregular autobrecciation, and thin sections of many samples (Fig. 16c) show smaller scale brecciation, often with angular, quenched, perlitically cracked clasts, and small amygdales. Irregularly swirled flow banding is also locally present (Fig. 18). Such rhyolite is overlain by about 7 m of peperite. This has abundant fragments of green microbanded chert, mainly only 1–3 cm long but occasionally reaching about 10 cm. They are elongate at least 4:1 along the bedding direction of the overlying BIFs and lie in a matrix consisting of smaller sedimentary clasts and rhyolitic debris, recognizable as such only in thin section. The contact between peperite and the overlying BIF (Fig. 21) is sharply defined. The BIF is cherty, and not deformed or folded; some of the thick, coarsely microbanded, red mesobands within it strongly resemble those typically found in parts of the Weeli Wolli Formation. The BIF is followed upwards by a sill of peperite similar to that immediately overlying the rhyolite, but finer grained and with a less conspicuous sedimentary component. The clasts from within most of its thickness are strongly flattened, but a thin section of a thin glassy selvage at the top consists of a welded and silicified aggregate of fine-grained shards which are relatively little flattened. A 5 m band of BIF above this sill is followed upwards by at least 30 m of uniform green shale, reminiscent of that overlying the upper unit in the type section at Woongarra Gorge, before the appearance of BIF of Boolgeeda Iron Formation type near the top of the slope.

Massive rhyolite of the upper unit, the peperite band at the top of the unit, and the overlying BIF are also well exposed in clean exposures on the south bank of the river.

#### *Summary of thicknesses*

No thickness data available as only the top section is exposed.

#### *Features of special interest*

Excellent exposures of the upper contact, especially on the north side of the Robe River.

## Geochemistry

### Data available

Very little chemical analysis has been carried out on rocks of the Woongarra Rhyolite. The available data are listed below in chronological order of analysis.

- Four samples used for Rb–Sr geochronology by Leggo et al. (1965), who reported chemical Rb and Sr in addition to isotopic ratios.
- Forty-six samples used for further Rb–Sr geochronology. Analyses by P. A. Arriens, at the Research School of Earth Sciences of the Australian National University, included chemical Rb and Sr, as well as isotopic analysis. Splits of the same samples were

also analysed for K and Na by the Western Australian Government Chemical Laboratories (GCL) (now Chemistry Centre of Western Australia (CCWA)).

- Three analyses carried out by the GCL, and reported by Trendall and de Laeter (1972).
- Two analyses carried out by the GCL, and reported by Trendall (1972).
- Twenty analyses carried out by the CCWA, on representative rocks selected for the purposes of this publication.

The resultant data from all the listed work have been compiled onto a diskfile (WOONGARR.GDA) designed for use in conjunction with a comprehensive IBM PC-based geochemical data analysis system, known as GDA (Sheraton and Simons, 1988). The GDA software package was designed, and is distributed, by the Australian geological Survey Organisation in Canberra.

A feature of GDA is its requirement for the definition of groups for plotting purposes. Although the criteria for group definition may be varied at will, it is convenient for presentation here to split the data within WOONGARR.GDA into the following groups.

Group 1 — Major-oxide and (in part) trace-element analyses of upper unit samples from various locations [n = 10].

*Notes:* This group includes seven (15622, 15647, 30523, 94711, 94713, 94726, 94744) of the 20 samples analysed for the purposes of this study, one (15624) of the analyses reported by Trendall (1972), and two (R207, R627) of the analyses reported by Trendall and de Laeter (1972).

Group 2 — Major-oxide and (in part) trace-element analyses of lower unit samples from various locations [n = 11].

*Notes:* This group includes ten (15644, 15688, 15694, 30513, 30544, 94715, 94729, 94734, 94737, 94749) of the samples analysed for the purposes of this study and one (R89) of the analyses reported by Trendall and de Laeter (1972).

Group 3 — Major-oxide and (in part) trace-element analyses of peperites from various locations [n = 4].

*Notes:* This group includes three (15639, 15649, 94710) of the samples analysed for the purposes of this study and one (15640) of the analyses reported by Trendall (1972).

Group 4 — Partial analyses (Rb, Sr, K, Na) of upper unit samples from Woongarra Gorge, used for Rb–Sr geochronology [n = 25]

*Notes:* Sample numbers 47201A–F, 47202–47220.

Group 5 — Partial analyses (Rb, Sr, K, Na) of samples from the upper part of the lower unit at Woongarra Gorge, used for Rb–Sr geochronology [n = 10].

*Notes:* Sample numbers 47233–47242.

Table 2. Chemical composition of selected samples from the Woongarra Rhyolite

Column number	1	2	3	4	5	6	7	8	9	10
Sample group	<i>Rhyolites of the upper unit</i>									
Sample number	15622	15624	15647	30523	94711	94713	94726	94744	R207	R627
Locality	Nallanaring Creek	Nallanaring Creek	Yeera Bluff	Kalgan Creek	Kalgan Creek	Coondiner Gorge	Kalgan Creek	Duck Creek	Woongarra Gorge	Kalgan Creek
AMG (Zone 50)	136284	136284	117947	820340	744321	644443	825317	576124	106696	822341
Bibliographic ref.		Trendall, 1972							Trendall and de Laeter, 1972	
SiO <sub>2</sub>	68.80	73.98	70.60	73.40	74.40	69.80	78.10	76.80	75.40	75.20
TiO <sub>2</sub>	0.54	0.50	0.50	0.53	0.30	0.53	0.43	0.34	0.33	0.27
Al <sub>2</sub> O <sub>3</sub>	13.10	11.28	12.30	12.10	9.92	11.60	9.29	11.80	10.60	9.54
Fe <sub>2</sub> O <sub>3</sub>	1.15	0.73	1.29	0.61	1.26	1.23	0.91	0.70	0.66	0.87
FeO	3.68	2.42	3.98	1.71	3.84	4.86	1.86	1.74	2.93	3.17
MnO	<0.05	0.02	0.10	<0.05	0.05	0.05	<0.05	<0.05	0.10	0.03
MgO	1.21	0.60	1.22	0.76	1.76	2.26	0.77	0.46	0.64	1.17
CaO	0.11	0.51	0.86	0.10	<0.05	0.10	0.08	<0.05	0.44	0.24
Na <sub>2</sub> O	0.54	0.43	3.88	0.42	0.10	0.18	0.12	4.83	0.81	0.71
K <sub>2</sub> O	9.13	8.02	3.22	9.08	5.98	6.91	7.00	2.67	6.19	6.28
P <sub>2</sub> O <sub>5</sub>	0.10	0.09	0.09	0.10	<0.05	0.09	0.09	<0.05	0.03	0.23
H <sub>2</sub> O+	—	1.07	—	—	—	—	—	—	1.46	1.82
H <sub>2</sub> O-	—	0.15	—	—	—	—	—	—	0.11	0.10
CO <sub>2</sub>	—	0.24	—	—	—	—	—	—	—	—
LOI	1.30	—	2.20	1.08	1.78	2.17	1.24	0.84	—	—
Rest	0.26	0.16	0.24	0.28	0.25	0.23	0.21	0.26	0.00	0.00
Total (%)	99.92	100.20	100.48	100.17	99.64	100.01	100.10	100.44	99.70	99.63
<b>Trace elements in parts per million</b>										
Ba	670	630	429	1 048	555	730	564	386	—	—
C	400	—	210	200	200	—	—	200	—	—
Ce	98	—	117	71	75	73	96	133	—	—
Co	—	17	—	—	—	—	—	—	—	—
Cr	5	18	5	6	<4	6	6	<4	—	—
Cu	<4	59	5	<4	<4	<4	7	14	—	—
Ga	17	—	20	11	20	17	8	16	—	—
La	52	—	57	36	39	40	53	64	—	—
Li	6	—	<6	6	20	12	6	<6	—	—
Nb	14	—	17	15	20	16	11	18	—	—
Ni	<3	15	<3	<3	<3	3	<3	<3	—	—
Pb	15	160	42	31	5	10	59	49	—	—
Rb	177	—	95	207	130	158	169	65	—	—
S	300	—	500	300	400	400	400	500	—	—
Sc	13	—	12	12	5	13	10	7	—	—
Sn	4	—	6	4	6	4	4	7	—	—
Sr	10	10	21	13	9	7	11	29	—	—
Th	21	—	22	20	18	20	15	26	—	—
U	6	—	7	5	7	6	4	7	—	—
V	6	<10	6	8	5	12	5	6	—	—
Y	43	—	54	43	98	52	40	56	—	—
Zn	74	75	139	65	94	87	121	288	—	—
Zr	321	340	347	312	420	326	230	412	—	—

Group 6 — Partial analyses (Rb, Sr, K, Na) of samples from the lower part of the lower unit at Woongarra Gorge, used for Rb–Sr geochronology [n = 8].

Notes: Sample 47221–47227, 47229.

Group 7 — Partial analyses (Rb, Sr) of upper unit samples reported by Leggo et al. (1965) from various locations [n = 2].

Notes: Sample numbers are R258 and R259.

Group 8 — Partial analyses (Rb, Sr) of lower unit samples reported by Leggo et al. (1965) from various locations [n = 2].

Notes: Sample numbers are R255 and R656.

## Principal features

### General character and homogeneity of composition

Table 2 displays the analytical data for rhyolites of the upper unit (Group 1, columns 1–10) and lower unit (Group 2, columns 11–21). In Figure 30, these analyses are shown on an XY plot of silica against total alkalis, recommended by the Subcommission on the Systematics of Igneous Rocks of the International Union of Geological Sciences for the standardization of volcanic rock nomenclature (Le Maitre et al., 1989). Apart from one sample from the upper unit, which falls marginally within the trachydacite field, and another from the lower unit marginally within the dacite field, all samples fall within the recommended nomenclatural field for rhyolite,

Table 2. (continued)

Column number	11	12	13	14	15	16	17	18	19	20	21
Sample group	Rhyolites of the lower unit										
Sample number	15644	15688	15694	30513	30544	94715	94729	94734	94737	94749	R89
Locality	Nallanaring Creek	Mount Maguire	Fish Pool	Kalgan Creek	Kalgan Creek	Coondiner Gorge	Silver Grass	Silver Grass	Woongarra Gorge	Duck Creek	Boolgeeda Creek
AMG (Zone 50)	147286	773177	083398	814317	725287	625476	093664	015649	109698	582130	125063
Bibliographic ref.											Trendall and de Laeter, 1972
SiO <sub>2</sub>	70.90	72.50	74.80	72.60	70.80	69.60	70.30	73.90	76.30	71.00	74.30
TiO <sub>2</sub>	0.53	0.51	0.32	0.29	0.71	0.53	0.53	0.32	0.51	0.34	0.29
Al <sub>2</sub> O <sub>3</sub>	11.60	10.80	10.80	11.40	11.40	11.40	12.00	11.20	10.80	12.20	10.80
Fe <sub>2</sub> O <sub>3</sub>	1.50	1.23	1.17	1.06	1.35	1.93	1.79	0.94	0.63	0.89	0.69
FeO	4.35	3.85	2.97	3.21	4.63	4.47	3.67	3.29	1.42	3.07	3.10
MnO	<0.05	<0.05	0.05	<0.05	0.05	0.05	<0.05	<0.05	<0.05	<0.05	—
MgO	1.89	1.89	1.19	2.00	2.77	1.82	1.35	1.48	0.80	2.33	1.10
CaO	0.12	0.12	0.07	<0.05	0.15	0.11	0.62	<0.05	0.14	<0.05	—
Na <sub>2</sub> O	1.30	0.22	1.01	1.00	2.45	0.12	2.84	2.05	0.85	0.10	0.31
K <sub>2</sub> O	5.90	6.60	6.18	6.63	3.32	7.35	4.68	4.95	7.41	8.15	7.50
P <sub>2</sub> O <sub>5</sub>	0.10	0.11	0.05	<0.05	0.12	0.10	0.10	0.05	0.11	0.05	—
H <sub>2</sub> O+	—	—	—	—	—	—	—	—	—	—	1.65
H <sub>2</sub> O-	—	—	—	—	—	—	—	—	—	—	0.09
CO <sub>2</sub>	—	—	—	—	—	—	—	—	—	—	—
LOI	1.80	1.85	1.54	1.72	2.29	2.05	1.72	1.59	0.98	1.93	—
Rest	0.23	0.27	0.24	0.21	0.20	0.21	0.28	0.20	0.22	0.24	0.00
<b>Total (%)</b>	<b>100.22</b>	<b>99.95</b>	<b>100.39</b>	<b>100.12</b>	<b>100.24</b>	<b>99.74</b>	<b>99.88</b>	<b>99.97</b>	<b>100.17</b>	<b>100.30</b>	<b>99.83</b>
<b>Trace elements in parts per million</b>											
Ba	554	817	484	502	302	643	765	604	631	376	—
C	300	300	300	—	100	—	300	200	200	300	—
Ce	54	56	82	144	82	82	113	152	67	139	—
Co	—	—	—	—	—	—	—	—	—	—	—
Cr	4	<4	<4	<4	<4	5	5	<4	<4	<4	—
Cu	<4	14	<4	<4	29	8	9	<4	<4	<4	—
Ga	18	19	18	18	22	17	20	19	13	11	—
La	27	30	41	78	36	44	61	78	32	78	—
Li	6	14	14	<6	16	11	13	11	<6	19	—
Nb	16	19	18	17	25	14	16	21	17	21	—
Ni	3	<3	<3	<3	<3	3	3	<3	<3	<3	—
Pb	5	14	15	<4	7	8	30	9	10	<4	—
Rb	121	131	139	128	71	175	144	126	118	140	—
S	400	400	400	300	300	300	300	400	300	300	—
Sc	13	8	5	6	11	12	13	6	9	7	—
Sn	<4	<4	5	5	16	4	<4	9	<4	<4	—
Sr	9	7	7	12	16	7	39	7	21	5	—
Th	22	17	19	17	19	20	22	20	17	19	—
U	6	5	5	4	5	6	6	5	5	6	—
V	12	10	4	5	31	6	10	5	13	5	—
Y	43	60	66	88	93	51	48	94	67	113	—
Zn	50	68	68	53	83	82	135	49	22	33	—
Zr	336	381	432	394	400	317	352	461	370	469	—

geochemically validating the revised name Woongarra Rhyolite used in this report.

In an AFM diagram (Fig. 31a) all rhyolites follow a 'calc-alkaline' trend, but on the Jensen plot (Fig. 31b) the analyses straddle the dividing line between tholeiitic and calc-alkaline rocks. On that diagram their rather low alumina content causes them to drift into the andesite and (one sample) basalt fields. However, their silica content clearly makes these names inappropriate.

Apart from the rather low alumina content, and unusually high MgO/CaO ratios, the compositions shown in Table 2 may be matched with published analyses of

rhyolites from many other areas. In this report, petrogenetic aspects of the Woongarra Rhyolite are not discussed; however, in Figures 32 and 33 selected major oxides and trace elements are plotted against silica. Collectively, these plots show that there are no significant compositional differences between the upper and lower units. This conclusion is emphasized by Figure 34, which shows close comparability of trace-element spidergrams for the upper and lower units. Columns 26 and 27 of Table 2 show average compositions of the upper and lower units, and clearly indicate their very close chemical similarity.

Subtle differences between the upper and lower units are noted below.

Table 2. (continued)

Column number	22	23	24	25	26	27
Sample group	Peperites				Upper unit	Lower unit
Sample number	15639	15640	15649	94710	Mean of columns 1-10	Mean of columns 11-21
Locality	Nallanaring Creek	Nallanaring Creek	Yeera Bluff	Kalgan Creek		
AMG (Zone 50)	134283	134283	121953	750316		
Bibliographic ref.		Trendall, 1972				
SiO <sub>2</sub>	46.50	56.95	67.50	79.20	73.65	72.45
TiO <sub>2</sub>	0.25	0.24	0.33	0.21	0.43	0.44
Al <sub>2</sub> O <sub>3</sub>	6.83	6.85	12.70	9.36	11.15	11.31
Fe <sub>2</sub> O <sub>3</sub>	26.90	15.71	1.70	0.55	0.94	1.20
FeO	7.82	9.47	4.72	1.33	3.02	3.46
MnO	0.17	0.07	0.05	<0.05	0.05	0.03
MgO	1.70	2.20	1.90	0.82	1.09	1.69
CaO	1.88	1.17	0.22	<0.05	0.25	0.14
Na <sub>2</sub> O	2.61	2.30	1.30	0.09	1.20	1.11
K <sub>2</sub> O	2.22	2.17	7.52	7.18	6.45	6.24
P <sub>2</sub> O <sub>5</sub>	0.29	0.17	0.05	<0.05	0.09	0.08
H <sub>2</sub> O+	—	1.20	—	—	1.45	1.65
H <sub>2</sub> O-	—	0.25	—	—	0.12	0.09
CO <sub>2</sub>	—	1.26	—	—	0.24	—
LOI	2.42	—	1.72	1.01	1.52	1.75
Rest	0.74	0.09	0.35	0.24	0.26	0.24
<b>Total (%)</b>	<b>100.33</b>	<b>100.10</b>	<b>100.06</b>	<b>99.99</b>	<b>101.89</b>	<b>101.89</b>
<b>Trace elements in parts per million</b>						
Ba	303	210	651	868	626.50	567.80
C	1 100	—	800	—	242.00	225.00
Ce	51	—	149	113	94.71	97.10
Co	—	15	—	—	17	—
Cr	13	20	5	<4	6.25	2.80
Cu	6	27	<4	<4	11.63	7.20
Ga	11	—	17	10	15.57	17.50
La	20	—	78	65	48.71	50.50
Li	<6	—	9	<6	8	11
Nb	<7	—	18	13	15.86	18.40
Ni	8	19	<3	<3	3.38	1.95
Pb	13	120	49	103	46.38	10.20
Rb	85	—	299	184	143.00	129.30
S	5 300	—	400	300	400.00	300.00
Sc	5	—	6	4	10.29	9.00
Sn	4	—	8	4	5.00	4.90
Sr	70	60	23	6	13.75	13.00
Th	10	—	30	22	20.29	19.20
U	3	—	9	5	6.00	5.30
V	21	<10	<3	3	6.63	10.10
Y	29	—	50	44	55.14	72.30
Zn	33	110	74	40	117.88	64.30
Zr	139	160	432	298	338.50	391.20

## Peperite composition

The analyses of four peperites shown in Table 2 (Group 3, columns 22–25) are also included on Figures 30 and 31. Only two of these analyses, those with almost no sedimentary content, appear on most of the plots of Figure 32. However, the range of the silica (X) coordinate is extended in Figure 32h, so that all four peperite analyses are included.

The peperite analyses confirm (Trendall, 1972) that the compositions of those with a significant sedimentary (BIF) component can be closely modelled by appropriate mixtures of rhyolite and BIF end-members. The additional analyses provided here also indicate that

the rhyolite end-member of the peperites is chemically indistinguishable from rhyolites of the upper and lower units, either in major-oxide (Fig. 32) or trace-element (Fig. 34) composition.

## Chemical effect of autobrecciation

The analytical data of Groups 4–6 (not tabulated here) are displayed in Figure 35. Comparison of Figure 35 components c,d,e, and f indicate that autobrecciation in the upper unit (Fig. 20) is correlated with variations in the alkali contents, perhaps suggesting that development of this feature was related to differences in permeability by fluids.

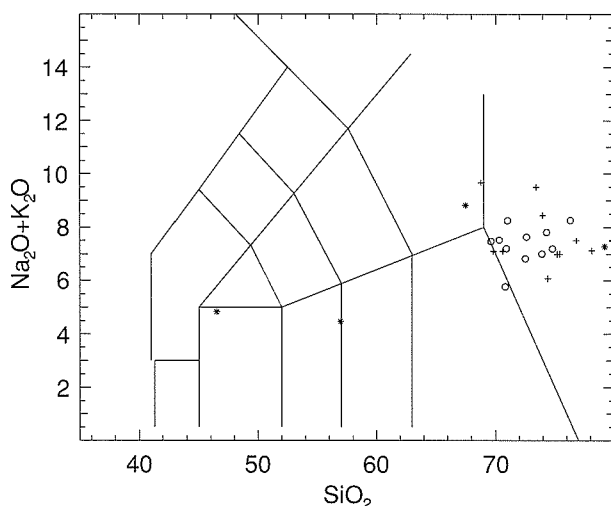
## Differences between the upper and lower units at Woongarra Gorge

Figure 35 also shows subtle chemical differences both between the upper and lower units (e.g. Fig. 35b) and between the upper and lower parts of the lower unit (e.g. Fig. 35f). All such differences are relatively trivial compared with the general uniformity shown in other figures. There is some suggestion in the rather poor coherence between such components as Rb and  $K_2O$  (Fig. 36), and more particularly between Sr and  $Na_2O$  (Fig. 37), that such elements have been mobile after emplacement, and that the compositional differences between the upper and lower units are not, or not entirely, primary.

## Discussion

### Salient features to be explained

Any hypothesis for the emplacement of the Woongarra Rhyolite must account for its lavalike lithology, its dimensions and shape, the existence of upper and lower units with different characteristics, the presence and nature of the median raft complex, the nature of the lower and upper contacts, and the chemical composition.



#### Key to symbols (Figs 30 - 37)

- + Upper Unit (UU)
- o Lower Unit (LU)
- \* Peperites
- \* Rb - Sr (UU)
- ◇ Rb - Sr (LU1)
- Rb - Sr (LU2)
- △ Leggo et al (LU)
- ▽ Leggo et al (UU)

AFT123

08/03/95

Figure 30. Silica/total alkalis plot for groups 1, 2 and 3

## Lavalike lithology

The term 'lavalike' has so far been used without definition, other than that it is a name applied to felsic rocks that have the lithologies of lavas; the lithological features which characterize lavas, particularly those that distinguish them from ash flows, now require closer examination.

In reporting a field conference convened specifically to establish whether extensive rhyolite sheets in Idaho were lavas or ash flows Ekren et al. (1984, p. 2) noted three main criteria used by the experienced group to characterize rocks emplaced as coherent viscous lavas:

- ubiquitous flow layering;
- occurrence of flow breccia at the base;
- lack of pyroclastic textures.

Ekren et al. (1984) provided extensive discussion of these criteria, particularly in relation to subtleties in distinguishing between lava flows, welded ash flows, and very hot ash flows which coalesced and flowed as 'secondarily melted' liquids before coming to rest. In this report, similar criteria are followed.

While flow layering is a common feature of rhyolitic lavas it is by no means always present, and the inner parts of rhyolitic flows may also be homogeneous, and 'stony' (Cas and Wright, 1987). In respect of this first criterion the term lavalike, as applied to the Woongarra Rhyolite, therefore means that, with the exception of the margins, the rocks are massive and either even grained or (if porphyritic) that the phenocrysts are evenly distributed throughout the matrix. If flow banding is present it is of the type usual in rhyolitic lavas (e.g. Cas and Wright, 1987, p. 81-85). That is, it is vaguely defined, continuous banding in which petrographic and compositional differences between adjacent bands are subtle (Fig. 18); commonly, it is irregularly swirled and inclined at high angles to the lower and upper surfaces of the flow.

Although the base of the Woongarra Rhyolite has only been examined in one locality (Fig. 4) in many other places an exposure gap of only a few metres separates the lowest exposures of the lower unit from the underlying BIF. Basal flow breccia of the kind referred to by Ekren et al. (1984) has nowhere been seen.

A lack of pyroclastic textures in lavalike rocks means that no internal components have textures in which fragments of different materials, either of different lava types or of other rocks, are discernible on any scale or in any textural relationship. In particular, the extreme flattening of such fragments typical of welded ash flows, parallel with each other and to the upper and lower bounding surfaces, is not present. Phenocrysts in porphyritic rocks are euhedral or subhedral, according to the degree of resorption; they do not have the angular shapes typical of mechanical breaking.

Bonnichsen and Kauffman (1987) and Henry et al. (1988, table 1) have also discussed the features distinguishing lavas and ash flows. The lithological differentiation criteria of Bonnichsen and Kauffman (1987), which are based on study of rhyolitic rocks of the Snake River Plain, essentially match those of Ekren et al. (1984), but they

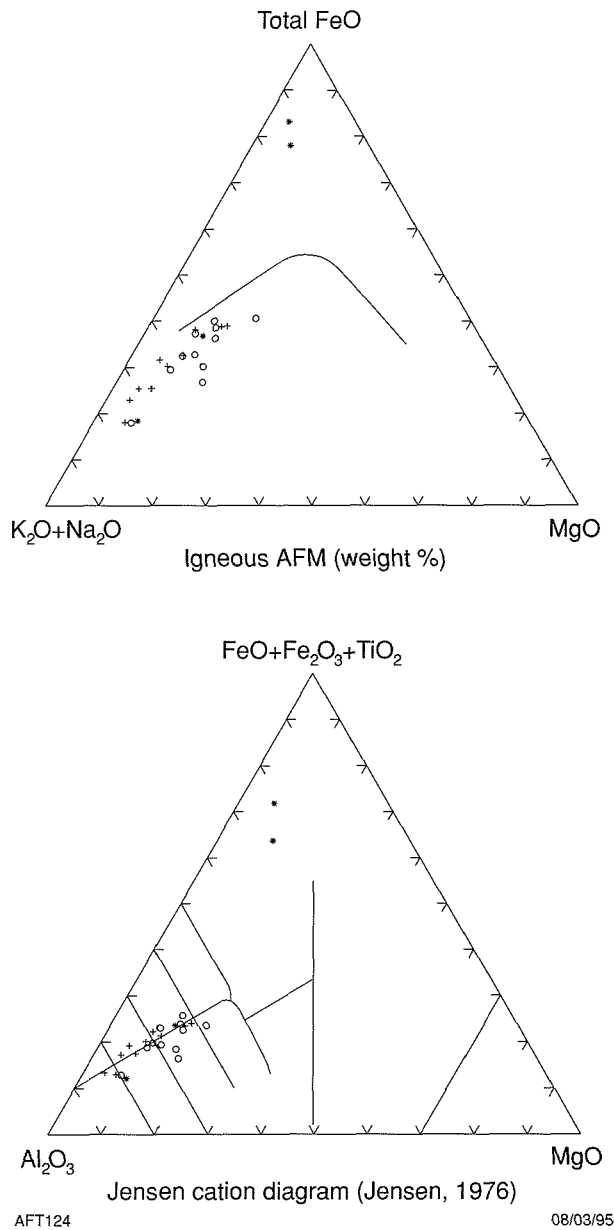


Figure 31. Jensen (1976) and AFM diagrams for groups 1, 2 and 3 (see Fig. 30 for key to symbols)

focused also on such features as shrinkage fractures and cooling-related joints, the lateral terminations of the rock body, and its associated rocks.

In summary, description of the rocks of the Woongarra Rhyolite as lavalike amounts to a statement that, apart from equivocal marginal facies, their lithologies are entirely consistent with cooling and crystallization in situ from a liquid magma.

### Shape and dimensions: area, thickness, volume

Apart from the slight stratigraphic discordance of the upper contact, discussed under the heading **The upper contact**,

the Woongarra Rhyolite is a concordant tabular sheet within the stratigraphic succession of the Hamersley Group; neither of the two rhyolitic units of which it consists is known to be missing in any section of the group. The greatest linear dimension of the outcrop area (Fig. 1) is almost exactly 500 km, from the vicinity of the Nallanaring Creek reference section east-southeast to the easternmost exposures about 70 km east of the Kalgan Creek reference section. It covers an area of about 37 500 km<sup>2</sup>.

From the thickness estimates set out earlier for the reference sections, summarized in Figure 20, separate estimates for the upper and lower units have been made of their maximum, minimum, and average thicknesses; these are shown in Table 1. Both units have the same present outcrop area, and the resultant volume estimates are also listed. These volumes are of course minimum volumes, since the Woongarra Rhyolite must be assumed to have extended significantly outside the present limits of its outcrop area. From the thicknesses given, and the distribution of the Woongarra Rhyolite in outcrop (Fig. 1), the aspect ratios of the upper and lower units are about 1:900 and 1:1300\* respectively.

### The upper and lower units

Any genetic hypothesis for the Woongarra Rhyolite needs to take into account the constant association of these two lithologically distinct units over the entire outcrop area, with the same characteristics and mutual relationship.

### The median raft complex

The median raft complex marks the division between the lithologically distinct upper and lower units of the Woongarra Rhyolite throughout its outcrop area. Hypotheses for the emplacement of the Woongarra Rhyolite need to account for the mixed rock types within the raft complex, the common occurrence of very irregular deformation and the presence of pervasive chaotic shattering at a range of scales, as well as the regional variations in thickness.

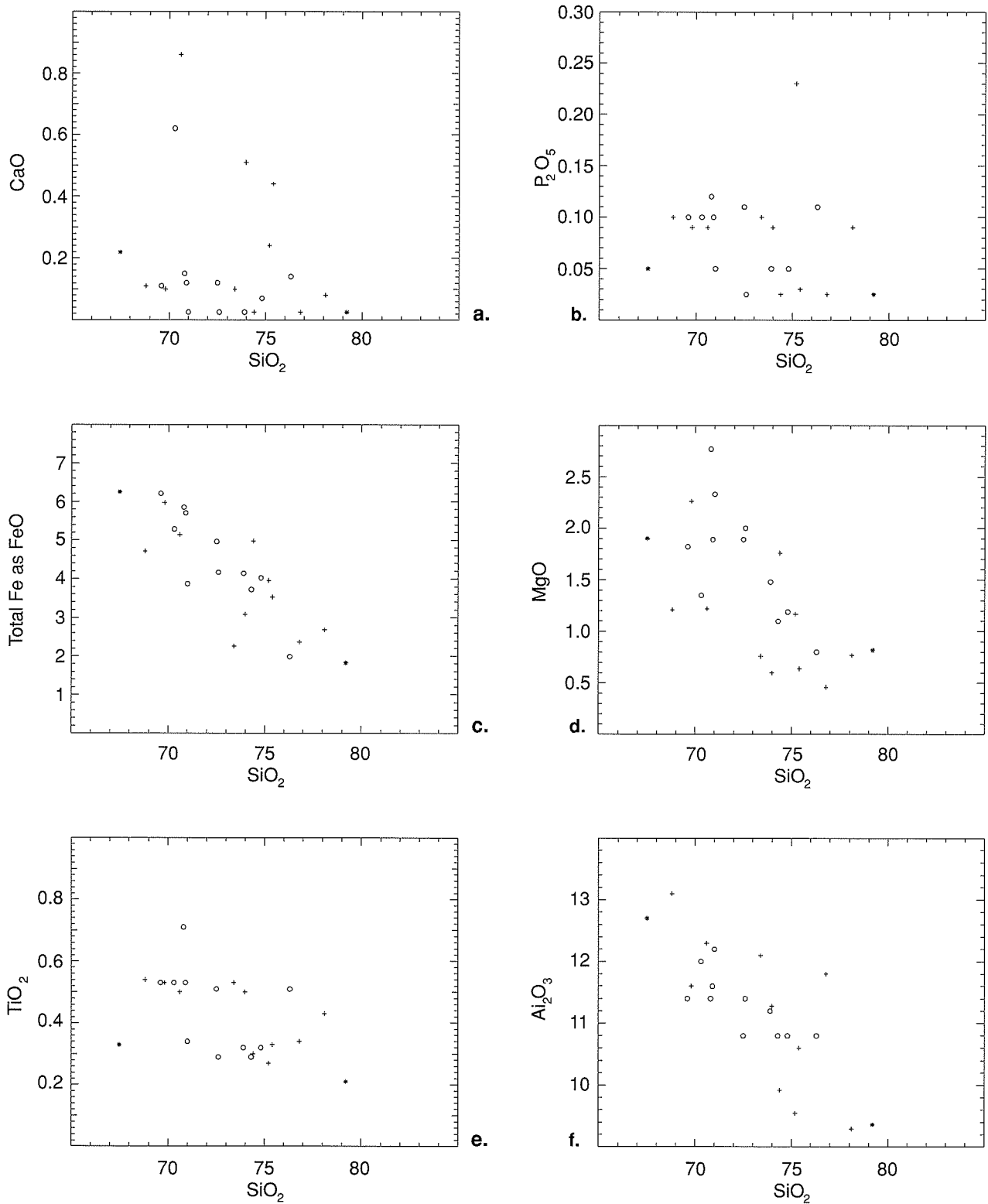
### The lower contact

In the only well-exposed section of the lower contact seen during this study, the lowermost rhyolite, which is slightly chilled, is in sharp, stratigraphically conformable contact with lithified BIF.

### The upper contact

Features of the upper contact that need to be integrated into a fully persuasive hypothesis for emplacement are

\* The aspect ratios specified are those of Cas and Wright (1987, p. 63) rather than those of Walker (1973, appendix I). Both figures are rounded.



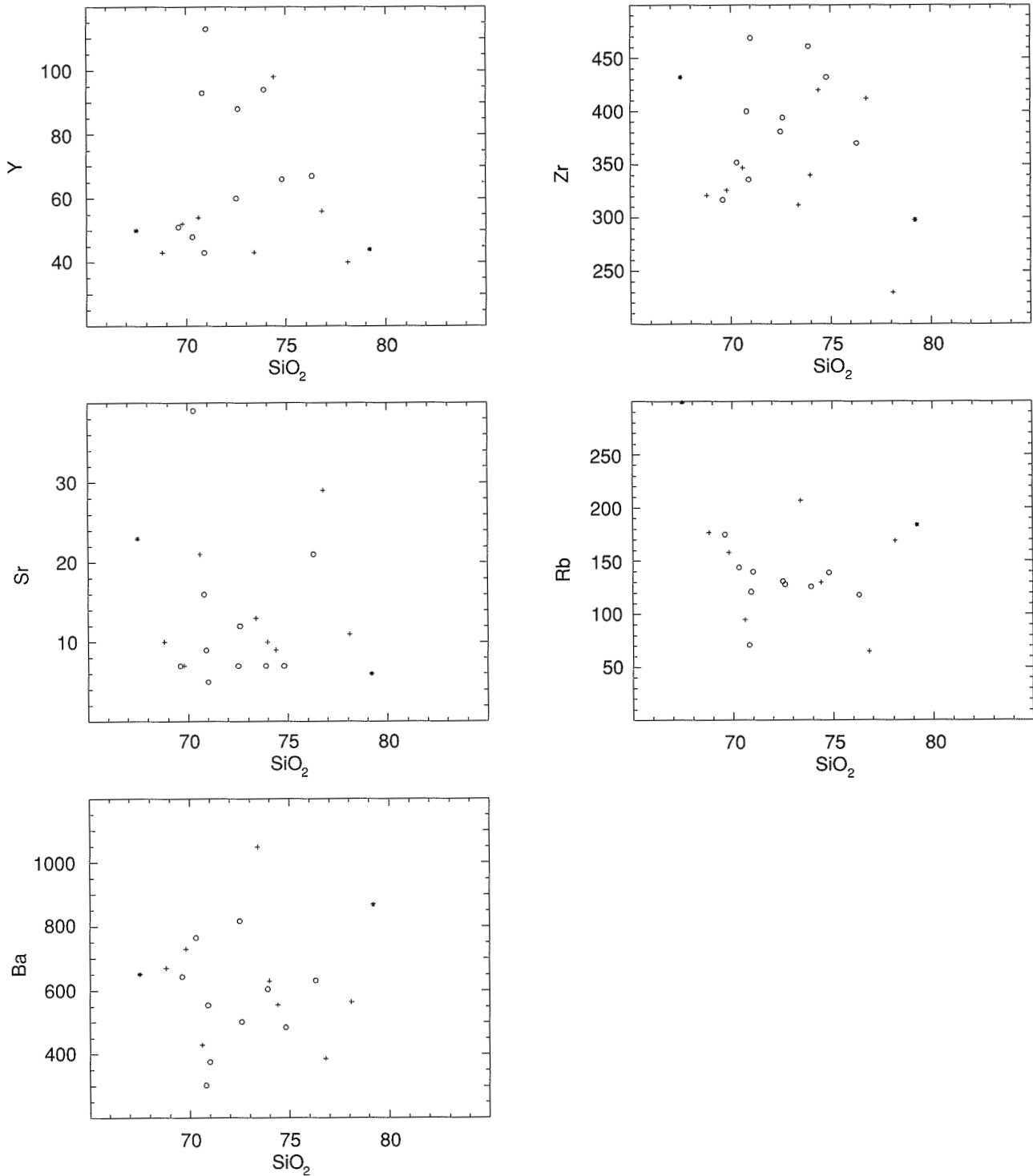
AFT125

08/03/95

Figure 32. Harker plots of major oxides for groups 1, 2 and 3 (see Fig. 30 for key to symbols)

the common presence of a peperite layer between the overlying strata and the top of the rhyolite, the existence of a clearly defined junction between this peperite and the commonly autobrecciated uppermost part of the rhyolite, and the presence of peperite sills

and lenses with a varying admixture of lava and comminuted country rock in the immediately overlying rocks. Additional details requiring explanation are the abundance of shards in the peperite, attesting to violent vesiculation, and the fact that the fragments in the



AFT126

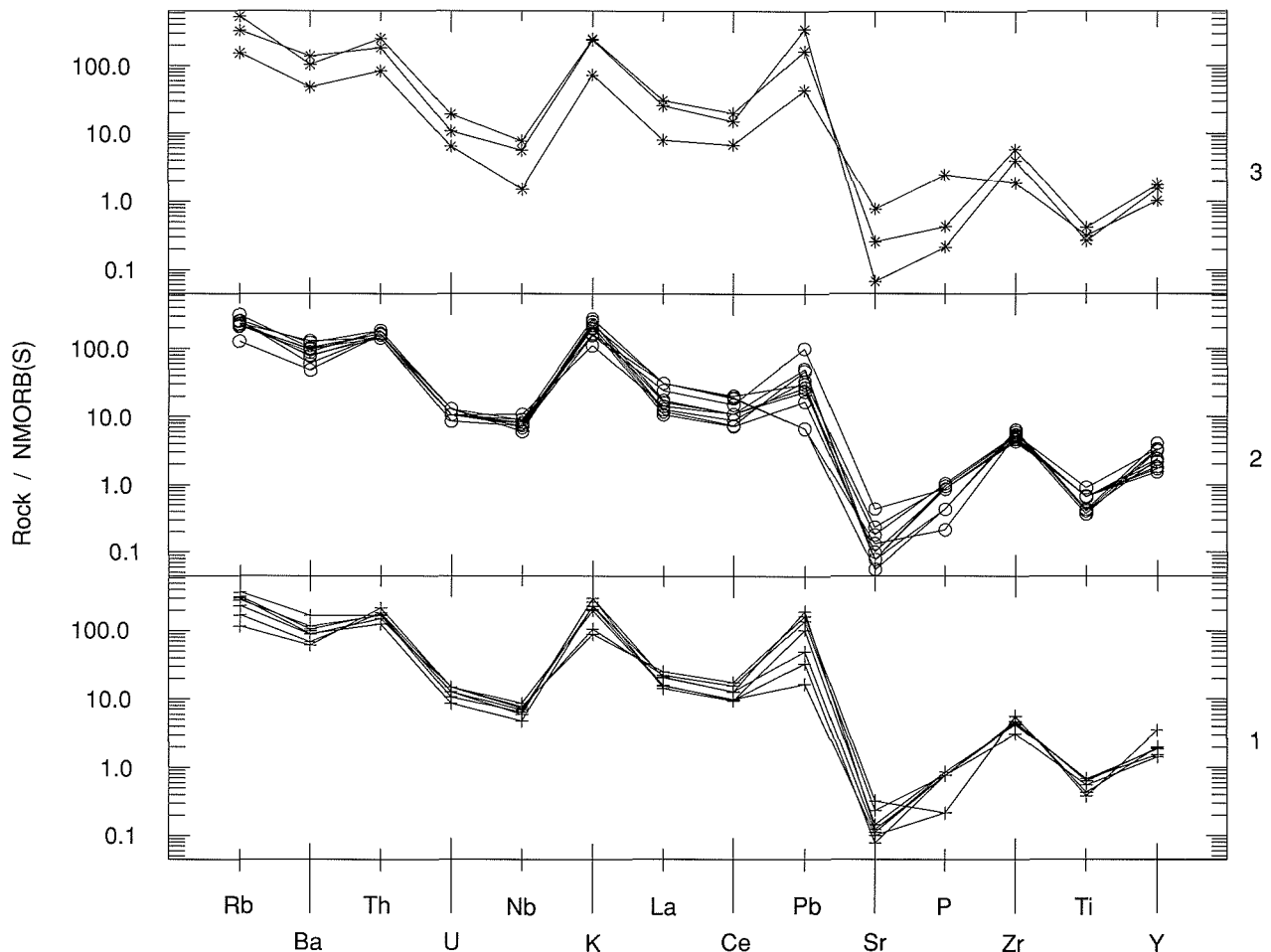
08/03/95

Figure 33. Harker plots of selected minor elements for groups 1, 2 and 3 (see Fig. 30 for key to symbols)

eutaxitic peperite have equant rather than elongate shapes in plan.

An explanation is also needed for the significant local differences in the nature of the immediately overlying sedimentary rocks (Fig. 21, and preceding descriptions of typical sections). Two contrasting explanations are possible

for these differences. The first is that they are the result of regional facies variations in the sediments laid down over the extrusive volcanic rocks of the Woongarra Rhyolite; the second is that the rocks of the Woongarra Rhyolite are intrusive, and that differences in the overlying rocks are related to stratigraphic discordance within a regionally invariant stratigraphic sequence.



AFT129

08/03/95

Figure 34. Spidergrams for groups 1, 2 and 3, showing comparative trace element patterns. All analyses are normalized to the MORB values of Sun and McDonough (1989). Tie lines spanning several elements omitted for clarity. (see Fig. 30 for key to symbols)

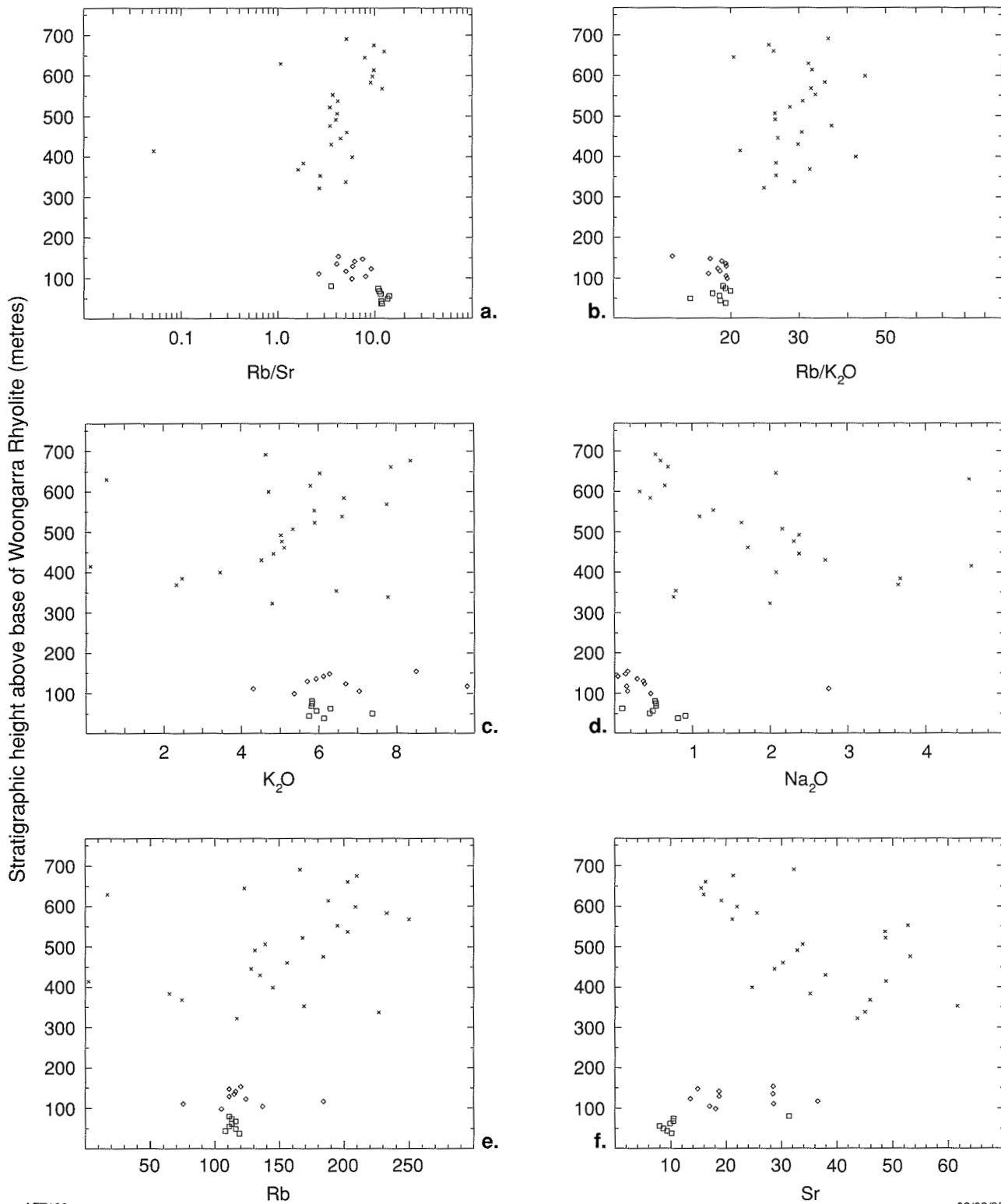
A problem in evaluating these possibilities is that all published work on the Hamersley Group has assumed, either implicitly or explicitly, that the Woongarra Rhyolite is a valid stratigraphic marker separating the older Weeli Wollli Formation below from the younger Boolgeeda Iron Formation above. This assumption cannot be made in the present discussion, whose purpose is an objective evaluation of all possible emplacement mechanisms, including intrusion.

Thus Trendall's claim (1975, 1976, 1983) that each of the major BIF units of the Hamersley Group (Fig. 1) has distinctive lithological features must be viewed with caution insofar as differentiation between the Boolgeeda Iron Formation and Weeli Wollli Formation is concerned; but it will nevertheless be useful to review the evidence for purely lithological distinction between these two formations.

From Trendall's (1983) table 3-IV, distinctive features of the Boolgeeda Iron Formation include the presence of dark-grey to black, fine-grained iron-formation lacking both mesobands and microbands; features typical of the Weeli Wollli Formation include the local presence

of 'striped facies' rocks and alternations of red and white mesobands. Shale is noted as present in both formations. The term striped facies was introduced by Trendall and Blockley (1970, p. 90) for continuously microbanded, non-mesobanded, fissile, red iron-formation which typically splits into thin sheets in weathered exposures; a more detailed description of the cyclicity which defines the 'stripes' has been given by Trendall (1973). Trendall and Blockley (1970) also provided a more detailed lithological description of the Boolgeeda Iron Formation.

Davy (1992) has recently made a detailed chemical and mineralogical study of the Weeli Wollli Formation. Working on drillcore from a single location, he found it 'difficult to relate the physical appearance of the Weeli Wollli Formation in this core to the description of the formation given in Trendall and Blockley (1970, p. 90-91)'. Davy (1992) applied the name iron-formation to all of the rocks that he described, on the ground that all had more than 15% total iron. He nevertheless pointed out that 'much of the iron-formation has a shaly appearance', and showed that the lower parts of the core, where such material was more abundant, had a



AFT130

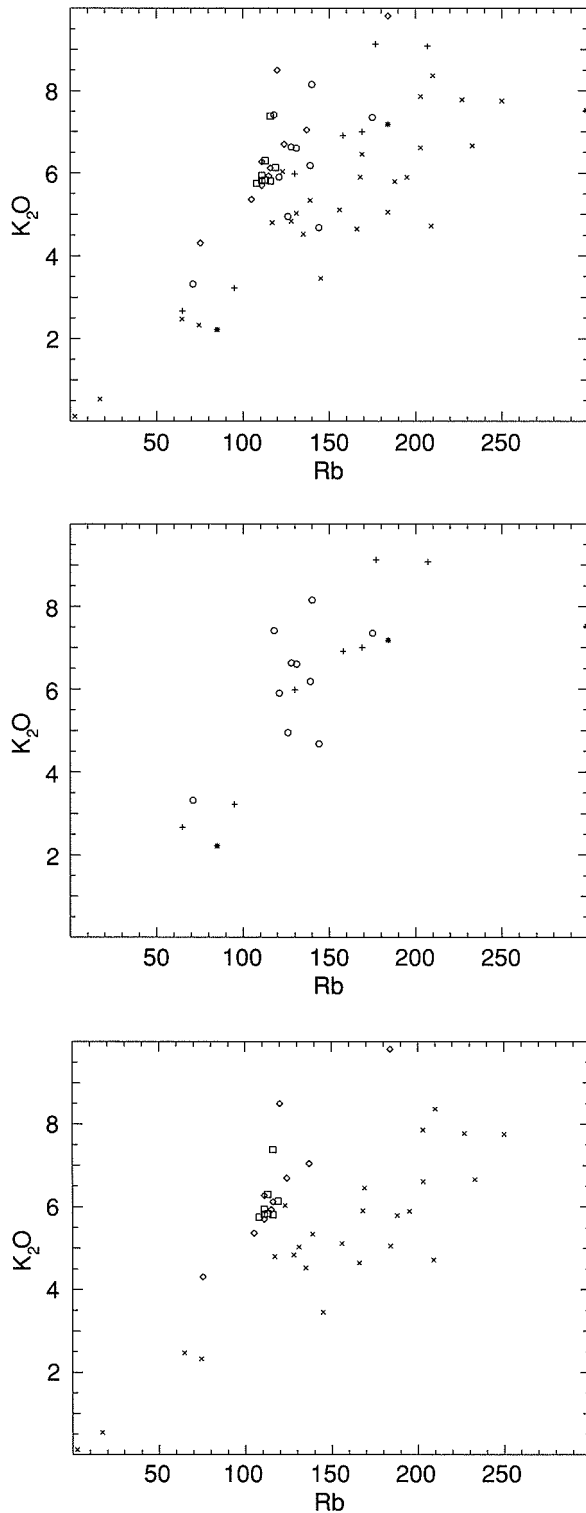
08/03/95

Figure 35. Graphs of various components against stratigraphic height for Woongarra Gorge section (see Fig. 30 for key to symbols)

generally lower iron content, and significantly higher  $Al_2O_3$ ,  $K_2O$  and  $MgO$  than 'oxide-facies' banded iron-formation higher in the core. This shaly iron-formation, in which Davy found a significant clastic, probably volcanoclastic, component, is equivalent to rocks which

would be loosely called 'shale' in the field, and which are so named in this Report.

In summary, there are no lithological grounds for allocating any rock describable as shale from field



AFT128

08/03/95

**Figure 36. Graphs of Rb/K<sub>2</sub>O for all samples (see Fig. 30 for key to symbols)**

appearance to either the Boolgeeda Iron Formation or Weeli Wolli Formation. However, from available information striped facies BIFs are typical of, although not abundant within, the Weeli Wolli Formation, and massive, dark-grey, homogeneous iron-formation lacking

both mesobanding and microbanding is only present within the Boolgeeda Iron Formation (Fig. 3). Although both formations may contain relatively thick, red, microbanded chert mesobands they are more abundant in the Weeli Wolli Formation.

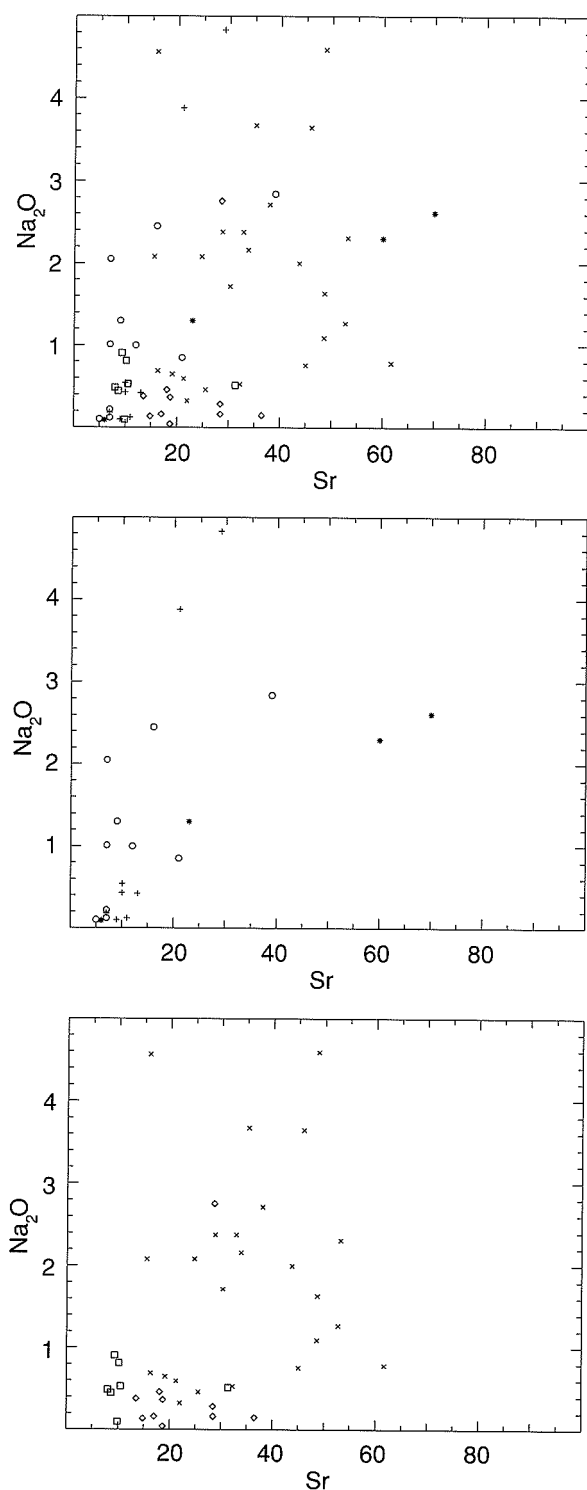
Regardless of the present validity of those criteria in terms of stratigraphic nomenclature, both the local presence of either BIF or shale immediately overlying the Woongarra Rhyolite, and the local presence of striped facies BIF above the Woongarra Rhyolite (Coondiner Gorge), contrasting with its demonstrable absence elsewhere (Woongarra Gorge), still show that either stratigraphic discordance or significant facies variations must be present. The second hypothesis is not an immediately attractive one in view of the spectacular lateral stratigraphic continuity, on a wide range of scales, that has been clearly demonstrated elsewhere in Hamersley Group iron-formations (Trendall and Blockley, 1970; Ewers and Morris, 1981). But because no evidence is available to discredit it, stratigraphic discordance of the Woongarra Rhyolite cannot be claimed as more than a probability on the evidence presented in this Report; it is accorded that status in the following discussion.

### Chemical composition

The bulk chemical composition of the Woongarra Rhyolite is not unusual, and is similar to that of major rhyolite effusions elsewhere; in terms of magma petrogenesis it is not likely that its origin requires any special local explanation. Two chemical features, however, need to be accounted for in terms of the emplacement mechanism: these are the close chemical similarity of the lithologically distinct lower and upper units, and the chemical similarity of the peperite bodies associated with the upper contact to both the lower and upper units. This chemical similarity indicates that the peperites are a closely related component of the Woongarra Rhyolite, rather than fortuitously juxtaposed rocks.

### Relationship to sills of the Weeli Wolli Formation

In descriptions of the type and reference sections already given, it was noted that in several locations the Woongarra Rhyolite is closely underlain by dolerite; dolerite also commonly forms a component of the median raft complex. Figure 20 illustrates these points. In both cases the dolerites are accepted as sills, which are a regionally consistent component of the Weeli Wolli Formation. In later discussion these sills are accepted as earlier than the Woongarra Rhyolite. Their petrogenetic relationship to the Woongarra Rhyolite, and their comparative emplacement dynamics, are problems of considerable relevance for a full understanding of the Woongarra Rhyolite. However, in view of the length and detail of the following discussion these questions are not touched on further in this Report.



AFT127

08/03/95

Figure 37. Graphs of Sr/Na<sub>2</sub>O for all samples (see Fig. 30 for key to symbols)

## Emplacement

### Alternative hypotheses

All early accounts of the Woongarra Rhyolite described the rocks as lavas, and an extrusive origin was assumed. MacLeod (1966, p. 54) was nevertheless puzzled by the

wide lateral extent of lavas whose composition would imply high viscosity, and he concluded that this could be attributed to submarine volcanism. Trendall and Blockley (1970, p.285) also accepted this, and suggested a source immediately west of the present outcrop area of the Hamersley Group. Trendall (1975, p. 134; 1976, p. 22–23) first raised the possibility of an intrusive origin. Although the second of those papers referred to evidence published earlier (Trendall, 1972), that evidence was not directly linked in 1972 to a preferred origin for the main body of the Woongarra Rhyolite. Horwitz (1978) stated that the Woongarra Rhyolite could be subdivided into a lower acid volcanic part (here the lower unit) and an intrusive porphyry sill (here the upper unit) forming the top half; however, the evidence on which these judgements were based was not specified. Although Trendall (e.g. 1983, 1990) repeated his suggestions of intrusion on later occasions these appealed only to unpublished evidence. In this Report the relative merits and demerits of possible modes of emplacement are approached from first principles, and reviewed without further reference to earlier discussion.

Individually, both the upper unit and the lower unit are stratigraphically discrete, laterally extensive, lithologically homogeneous rhyolite sheets. In these general respects they have no differences sufficiently distinctive to suggest that their origins are different, and it is therefore initially supposed here that they have the same emplacement mechanism. The main possibilities are then:

1. The Woongarra Rhyolite was extrusive
  - 1.1 Emplacement was subaerial
    - 1.1.1 Emplacement was as lava
    - 1.1.2 Emplacement was as ash flow
  - 1.2 Emplacement was subaqueous
    - 1.2.1 Emplacement was as lava
      - 1.2.1.1 Eruption was subaerial
      - 1.2.1.2 Eruption was subaqueous
    - 1.2.2 Emplacement was as ash flow
      - 1.2.2.1 Eruption was subaerial
      - 1.2.2.2 Eruption was subaqueous
2. The Woongarra Rhyolite was intrusive

Each of these possibilities is examined in turn below.

### Evaluation of the hypotheses

Both hypotheses involving subaerial emplacement (1.1.1 and 1.1.2) require that before this took place the undoubtedly subaqueous depositional surface of the underlying Weeli Wolli Formation BIF was exposed at the surface. Judgement of the credibility of such an event needs an appreciation of the depositional environment of BIF within the Hamersley Basin.

Trendall and Blockley (1970) set out the evidence available from the BIFs of the Hamersley Group for their depositional environment and subsequent diagenetic development; their work focused principally on the Dales Gorge Member of the Brockman Iron Formation. They envisaged derivation of the BIF by lithification of a continuous sequence of thin annual layers (microbands) of chemical precipitate, each microband possessing

an iron-rich and a silica-rich (iron-poor) component, reflecting the response of basin-water chemistry to changing seasonal conditions during a single year. They suggested that the primary depositional thickness of each microband was 0.5 mm, and that the two main chemical constituents of the BIF, iron and silica, were precipitated as components of a hydrous colloidal gel with a bulk density of 1.1 g/cm<sup>3</sup> and an approximate bulk composition (wt%): SiO<sub>2</sub> 8; Fe<sub>2</sub>O<sub>3</sub> 4; FeO 2; CO<sub>2</sub> 1; H<sub>2</sub>O 85. They proposed further that various long-term climatic cycles, astronomically controlled, resulted in corresponding subtle variations in primary composition, and that those variations led in turn to varying diagenetic responses of the microbands during compaction. The processes which they envisaged to have taken place in association with compaction included expulsion of the water contained in the primary precipitate, re-solution and redistribution of silica between groups of microbands to form the coarser banding (mesobanding) for which the BIF is named, and development of the present BIF mineral composition (principally magnetite and finely crystalline quartz). All these resulted in a bulk density increase from the 1.1 g/cm<sup>3</sup> of the primary precipitate to about 3.2 g/cm<sup>3</sup> in the finally lithified BIF.

For the depository in which this depositional process took place Trendall and Blockley (1970) suggested a barred basin with an area of about 100 000 km<sup>2</sup>, with margins lying some unknown distance outside the present outcrop area of the Hamersley Group and a connection to the open ocean to the northwest. They emphasized the extreme stability of conditions in the basin during the time of BIF deposition, which resulted in continuity of mesobands, and even microbands less than a millimetre thick, across its entire area. Trendall and Blockley (1970) noted various arguments for water depth in the basin, and concluded that it was probably between 50 and 250 m during BIF deposition.

Since the publication of Trendall and Blockley's (1970) basin and depositional models other workers have provided important, and equally valid, alternative interpretations for some aspects of Hamersley Group geology. Thus Morris and Horwitz (1983) introduced the possibility of Hamersley Group deposition on a submarine plateau comparable in size and geometry to the Bahamas Platform, so that the present absence of any preserved shoreline of the Hamersley Basin is due to the fact that no shoreline in the strict sense ever existed: the limits of the area of Hamersley Group deposition were instead abrupt slopes descending to deep oceanic water. And in respect to Trendall and Blockley's (1970) model of diagenetic mesoband development Morris (1993) also proposed an alternative theory for the development of mesobanding, in which periods of storm-generated turbulence effectively led to the development of mesobanding in the primary precipitates.

No subsequent work, however, has challenged the points of Trendall and Blockley's (1970) depositional model which have important relevance for Woongarra Rhyolite emplacement. These are:

- the uniformity of depositional conditions throughout the area of the depository;

- continuous, or near-continuous, chemical precipitation of finely particulate iron- and silica-rich colloidal material for substantial periods of time;
- diagenetic conversion of the initially light, cohesive sediment to dense, well-banded, lithified BIF.

Two parameters of the depository that are also important for interpretation of Woongarra Rhyolite emplacement are still not well constrained: the water depth, and the depth below the water/sediment interface at which BIF lithification was completed. In respect to water depth it is noted here that Trendall and Blockley's (1970) arguments were mainly concerned with constraints on the minimum depth, and that none of their arguments precluded a much greater depth than 250 m; their model would work equally well with a depth greater than 1 km. Morris and Horwitz (1983) did not provide a quantitative estimate of water depth in their depositional model, other than to describe it (p. 294) as 'relatively deep'. Neither Trendall and Blockley (1970) nor any later authors have committed themselves to a quantitative statement concerning the likely depth at which lithification was effectively complete. If an analogy with the diagenesis of argillaceous sediments is valid, then it will be less than 500 m, the base of the 'shallow-burial' zone of Muller (1967).

Neither Trendall and Blockley (1970), who set out arguments against it, nor any later authors have suggested a closed basin for the depository of the Hamersley Group. It follows, from the basin models summarized above, that subaerial extrusion of the Woongarra Rhyolite (hypotheses 1.1.1 and 1.1.2) could not have occurred following quiet evaporative desiccation of the basin, but would have necessitated either tectonic (epeirogenic) uplift of the entire depositional surface or a large and abrupt drop in global sea level. The latter possibility would require a coincidental drop of sea level immediately before the eruption of the Woongarra Rhyolite, and can surely be discounted. Tectonic uplift of the entire basin floor without accompanying tilt, warping, or local irregularity of any kind is hardly more credible. The concordance at a regional scale of the overlying Boolgeeda Iron Formation would necessitate subsequent resubmersion of the uplifted basin floor for BIF deposition to continue as before on the surface of the lava. However, none of the upper contacts of the reference sections examined and described here reveals any suggestion of the relationships between rhyolite and BIF that might be expected if the latter were deposited on the resubmerged irregular surface of a subaerial lava flow. If the BIF of the median raft complex is to be explained then a double emergence and resubmergence of the basin floor must presumably be supposed; a contrived alternative might be that the lower unit was an invasive flow (e.g. Schmincke, 1967) which supported a surface skin of BIF and other rocks excavated from the exposed basin floor, but this scarcely seems credible when the densities of silicic magma (~2.2 g/cm<sup>3</sup> — Walker, 1989) and BIF (~3.2 g/cm<sup>3</sup>) are compared. The overlying sills and lenses of peperite are also hard, if not impossible, to accommodate in such a model.

But even if credence can be given to the tectonic gymnastics required for either a single or double uplift and

depression, further difficulties remain with hypotheses involving subaerial emplacement (1.1.1 and 1.1.2). Hypothesis 1.1.1, emplacement as a subaerial flow, is considered first. The emplacement of a subaerial flow, or flows, with the shape and dimensions of the Woongarra Rhyolite is contrary both to all that is known concerning the physical principles governing the shapes of lava flows, and to the empirical evidence derived from the recorded dimensions of silicic lavas.

All erupted lavas move more slowly than do ash flows; the 5–15 km/hour (~1.4–4.2 m/s) suggested for Columbia River basalts by Shaw and Swanson (1970) is probably above average for major flows away from vents of high central volcanoes, where Williams and McBirney (1979) recorded speeds of 64 km/hour (~18 m/s) from Hawaii. This means that their motion is directly controlled by gravity, and that the shapes of single flow units are in turn importantly controlled by the geometry of the surface over which they flow. Almost all lava flows start from a source with a small area and move immediately downslope as a narrow flow whose width increases, or may become lobate, with increasing distance from the source. Few single lava flows of any composition are extensively tabular, and cannot be so unless the surface over which they are erupted is perfectly horizontal. Even in the classical continental flood basalt provinces such as the Deccan, and Columbia River, it is only those flows erupted over smooth surfaces created by a succession of earlier flows that approach a tabular shape; a good example of extensive irregularity and ponding in a flow of the Columbia River Basalt Group is described by Martin (1989).

The dimensions of the 'exceptionally large' (Guest and Sanchez, 1969) Chao dacitic flow of northern Chile was regarded by those authors as sufficiently remarkable to justify detailed documentation; the main flow has an estimated volume of 24 km<sup>3</sup> and a width of about 5 km, and it flowed for about 10 km from its source vent. The first paper to provide a systematic compilation of the dimensions of silicic (and other) flows was that of Walker (1973). The data collected by Walker showed median flow lengths of 1.1 and 1.2 km respectively for groups of 176 rhyolite flows and 147 andesite and dacite flows. Only one flow, an andesite, had a volume greater than 10 km<sup>3</sup>. The largest area covered by a rhyolite flow was less than 20 km<sup>2</sup>, and the longest rhyolite flow noted by Walker was the Star Mountain rhyolite, described by Gibbon (1969), as extending 35 km from its source. In later papers Hausback (1987) described the 8.6 km<sup>3</sup> Providencia rhyodacite flow of Mexico as 'a siliceous lava that flowed an unusually long distance from its source' (23 km). Henry et al. (1988, table 2) have since listed the lateral extent of the Star Mountain Formation as 70 km, although they note that it is a composite unit. Bonnicksen and Kauffman (1987, table 1) noted a minimum volume of 200 km<sup>3</sup> and a thickness of about 250 m for the Sheep Creek Rhyolite of southern Idaho. This flow extends over a distance of 42 km, and is one of many other extensive silicic flows in the area, another of which, the Dorsey Creek Rhyolite, extends for 40 km. Henry et al. (1990) also recorded a lateral extent of 55 km for the Bracks Rhyolite of Trans-Pecos Texas, although Henry et al. (1988) had earlier reserved

judgement on whether that unit was a lava or an ash-flow tuff.

The numerical modelling of Manley (1992) is consistent with these reports of rhyolitic flows more extensive and voluminous than those listed by Walker (1973), but the fact remains that subaerial silicic flows with even a tenth of the area of the Woongarra Rhyolite are unknown both in the geological record and on the modern Earth; and they are also highly improbable from what is known of the rheology of erupted silicic magmas. Quite apart from the tectonic problem of evenly raising and then lowering the entire basin, possibly twice, the emplacement of the Woongarra Rhyolite as subaerial lava is simply not credible. If subaerial emplacement is to be considered at all, then the only reasonable hypothesis is 1.1.2, deposition as an ash flow.

Velocities attained by ash flows are up to three orders of magnitude higher than those usually reached by lavas. The theoretical modelling of Sparks et al. (1978) indicated initial velocities of over 300 m/s, with large flows having velocities over 100 m/s after travelling 50 km from their sources; and modern ash flows have been observed to travel up to 20 km from their vents at speeds up to 60 m/s (Davies et al., 1978). The lateral blast ('stone wind') of the 1980 eruption of Mount St Helens (Kieffer, 1981) may have reached supersonic speed (>332 m/s). The consequent momentum of ash flows gives them both greater capability of even distribution over a large area, and the potential to achieve this regardless of topographic irregularity; these are two reasons why hypothesis 1.1.2 is inherently more credible than 1.1.1.

The primary argument against identification of the Woongarra Rhyolite as an ash-flow tuff, resulting either from multiple ash flows or a single ash flow, lies in the lavalike lithology of both the upper and lower units. The characteristics implicit in this term have already been noted above. Apart from the margins, the rocks are massive and either even grained or, if porphyritic, the phenocrysts are evenly distributed within the matrix (Fig. 15); quartz phenocrysts have the well-preserved, fragile resorption shapes typically present in lavas (Figs 11 and 13).

The second argument against an ash-flow origin is the converse one that the main features of ash-flow tuffs are all absent. These have been well summarized by Cas and Wright (1987, chapter 8) from the voluminous literature. The principal missing features are the vertical and horizontal compositional and textural zoning related respectively to stages of the eruptive process and to distance from the vent, and the characteristic variety of unwelded and welded clastic textures. Although the latter are present in associated marginal rocks (Fig. 19) they are not present in the main bodies of either the upper or lower unit.

If the upper and lower units of the Woongarra Rhyolite were emplaced as subaerial ash flows, then the one forming the upper unit would be larger than any other known example. The largest single ash-flow tuff listed by Cas and Wright (1987, table 8.1) is the Fish Canyon Tuff, in the San Juan volcanic field of southwestern Colorado,

for which Steven and Lipman (1976) estimated a volume greater than 3000 km<sup>3</sup>. However, in comparing this with the minimum of about 9000 km<sup>3</sup> of the upper unit of the Woongarra Rhyolite (Table 1) it should be noted that from Steven and Lipman's (1976) data a 1.4 km-thick deposit within the source caldera forms some 30% of that volume, and that only about 2000 km<sup>3</sup> of the Fish Canyon Tuff is present in the surrounding tabular ash-flow sheet. In terms of area covered and distance travelled from source the Fish Canyon Tuff extended over an area of about 15 000 km<sup>2</sup> with a greatest diameter of about 150 km. As the vent (La Garita caldera) lay centrally within this area the greatest distance travelled by the ash flow was less than 100 km. Cas and Wright (1987, table 8.2) listed the Morrinsville ignimbrite (New Zealand) as having travelled 225 km from source, but gave no other information on this unit. The greatest diameter of the present outcrop area of the Woongarra Rhyolite is over 500 km, so that if either the upper or lower unit was formed by an ash flow this would have had to travel at least 250 km.

In summary, although hypothesis 1.1.2 is more credible than hypothesis 1.1.1 it still involves the need for implausible tectonic oscillation of the basin floor. If it is supposed that many typical textural features of ash-flow tuffs have been obliterated by secondary melting, to give an uncharacteristic lavalike lithology to the bulk of the rocks, the hypothesis is hard to ignore. However, it offers no obvious explanation for stratigraphic discordance at the upper margin, nor the associated discontinuously overlying sills and lenses of peperite. And to account for the nature of the lower contact, all unconsolidated material would have to have been stripped from the exposed basin floor, down to a sharply defined stratigraphic level within the lithified BIF, before emplacement of the rhyolite of the lower unit.

The four hypotheses numbered 1.2.\*.\* will all be considered to imply extrusive emplacement in a relatively deep-water environment, rather than simply a subaqueous one; that is, that emplacement occurred without any change in the depth of water in the depository of the Hamersley Group, other than any decrease directly associated with the emplacement itself. This eliminates any requirement for tectonic emergence and resubmersion of the basin floor. Hypotheses 1.2.1.1 and 1.2.1.2 are addressed first.

Hypothesis 1.2.1.1 can be quickly dismissed, since it involves initiation of the emplacement event as a subaerial flow, which immediately raises most of the problems that were discussed in relation to hypothesis 1.1.1. Hypothesis 1.2.1.2, on the other hand, warrants serious consideration, and would be the more easily accepted if it could be proven that other subaqueous silicic lava flows had similar characteristics.

The only widely cited examples of extensive tabular subaqueous silicic flows are those of the Early Devonian Merrions Tuff, in the Hill End Trough of New South Wales. Cas (1978) proposed that the three lavalike porphyry members of the Merrions Tuff erupted and flowed subaqueously. Although they are of smaller volume, these mainly rhyodacitic porphyry sheets closely resemble the upper and lower units of the Woongarra Rhyolite in their stratigraphic concordance and lavalike

character, and it is necessary to consider the evidence for their extrusive origin critically before using them as a genetic model.

Cas (1978, p. 1710) considered four alternative modes of emplacement for the porphyries: post-sedimentation sills, synsedimentation sills, ash flows, and lava flows. He rejected the ash flow possibility essentially on the criterion of absence of pyroclastic textures, but also cited the presence of vesicles in support of this rejection. Emplacement as post-sedimentation sills was rejected partly on the absence of the 'internal zonation or variation in crystal abundance that might be expected in a sill several hundred metres thick', but principally because the thickness of the lowest (B1) porphyry member, is antithetic to that of overlying clastic members; Cas accepted this as evidence that the B1 porphyry influenced the pattern of later deposition, and that it must therefore be older, and a lava. However, in considering the possibility of a synsedimentation sill, he noted that the 'admixture of porphyritic clasts and sediment in the marginal breccias of the porphyries is not inconsistent with their being synsedimentation sills, nor is their vesicular character'.

Four points need to be made about Cas' (1978) identification of the tabular porphyries of the Merrions Tuff as lavas:

- that an antithetic thickness relationship of a concordant felsic sheet to overlying sediments is consistent with either extrusion or intrusion;
- that deep submarine eruption of lava would be unlikely to form an extensive tabular sheet;
- that the evident vesicularity of Merrions Tuff porphyries is not consistent with high-pressure suppression of volatile evasion;
- that the nature of the upper margin as described by Cas (1978) is consistent with intrusion.

These points are amplified in sequence below.

### **Antithetic thickness relationship**

There is no reason to suppose that shallow (synsedimentation) sill injection might not have been accompanied by an overlying 'blister' on the floor of the basin with a height about equal to the sill thickness. Such a blister would have had exactly the same influence over later sedimentation that a lava flow would have done. An antithetic thickness relationship thus provides no criterion for the extrusive or intrusive nature of the porphyry sheets of the Merrions Tuff.

### **Formation of a tabular lava flow by eruption in deep water**

The primary control of gravity over the shapes of lava flows has already been discussed. It follows that a fluid lava erupted in deep water can only flow further down slope, and will pond in the deepest part of the basin. There is no physical means by which it can spread out sideways,

or achieve a higher position than that of its source. Cas (1977, 1978) gave no quantitative estimates of either the water depth of the depository of the Merrions Tuff or of the eruption depth of the porphyries, but some guess at these is essential if the extrusion model is to be realistically assessed, since the requirements of the two depths are interdependent and antithetic: the deeper the vent, or vents, relative to the deepest part of the basin the less likely that the erupted lavas will be either tabular or extensive, while the shallower the vents the less likely that vesiculation is suppressed.

## Vesicularity

Cas (1978) appealed to Jones' (1969) demonstration that the vesicularity of subaqueously erupted basalts varies with water depth, as well as Moore's (1965) finding that tholeiitic pillow basalts emplaced below 500 m had higher H<sub>2</sub>O+ contents, to argue that the escape of volatiles from the Merrions Tuff porphyries was suppressed by the high water pressure at the depth of the eruption site, and that the evident mobility of the silicic magmas involved could be attributed to their resultant high volatile content. Cas (1978) nevertheless described the Merrions Tuff porphyries as consistently vesicular, the vesicularity locally reaching 10 to 15%, and it is thus clear that the exsolution of volatiles was not, in fact, suppressed. In spite of substantial theoretical work relating vesicularity to the solubility of volatiles in magmas, Fisher and Schmincke (1984, p. 55) commented that the formation of bubbles in magma is a complex process that must be analysed in terms of both chemical parameters (melt composition, and types, amounts, and partial pressures of several volatile species) and physical parameters (including temperature, viscosity, surface tension, and diffusivity). It is thus not possible from available data on the Merrions Tuff porphyry to estimate precisely the pressure prevailing when the vesicles were formed. However, it seems to be the general case that silicic lavas which vesiculate at all, do so explosively to form pumice, and that substantial water depths do not affect this general truth. Thus Gass et al. (1963) reported a raft of floating pumice blocks extending over an area of about 5000 km<sup>2</sup> of the Southern Ocean near the South Shetland Islands, evidently derived from a submarine eruption at an estimated maximum depth of 2 km. Since the Merrions Tuff porphyries retain their petrographic character throughout their thicknesses, including their vesicularity, the lack of explosive loss of volatiles may be better construed as evidence that the porphyries are sills, and that explosive vesiculation was controlled by an overlying capping of sedimentary rocks.

## The upper margin

Although interpretation on the basis of published illustrations is not an effective substitute for field observations, it is worth noting that Cas' (1978, fig. 3B) sketch of the upper margin of the B1 porphyry sheet bears a remarkable similarity to Kokelaar's (1982, fig. 2A) sketch of the upper margin of an andesite sill at Turnberry, in Scotland, as well as to figure 6F of Kokelaar et al. (1985), which shows the margin of an irregular rhyolite

intrusion into wet sediments on Ramsey Island, southwest Wales.

These four points are not clear proof that the porphyry sheets of the Merrions Tuff are not lavas. However, there is insufficient published evidence for the Merrions Tuff porphyritic sheets to stand as proof of the existence of subaqueous tabular silicic lava flows spreading over thousands of square kilometres. This is especially so in view of Cas' (1978, p. 1711) apparent acceptance that the porphyries 'may have been intrusive into the shallow levels of an unconsolidated sediment pile'.

No other subaqueously erupted silicic lavas described in the literature have the tabular form and great areal extent of the porphyry components of the Merrions Tuff. Thus the Archaean Rouyn-Noranda rhyolites described by De Rosen-Spence et al. (1980) have strike lengths only up to about 10 km, and are geometrically consistent with the high viscosities associated with subaerial silicic lavas. They do not have regionally tabular extent, and are not convincing analogues of the Woongarra Rhyolite. The subaqueous rhyolitic domes described by Pichler (1975) from the Ponza Islands of the Tyrrhenian Sea are even less extensive.

If the existence of extensive tabular subaqueous silicic lavas is doubtful, hypotheses 1.2.2.1 and 1.2.2.2, in both of which emplacement of the Woongarra Rhyolite was as deep-water, subaqueous ash flows, become attractive alternatives. As with the choice between the two alternative hypotheses involving subaqueous lavas, so in this case one of the alternatives is immediately dismissed, but here the subaqueous (1.2.2.2) rather than the subaerial eruption option (1.2.2.1) is not given serious consideration. In earlier discussion of the subaerial ash-flow hypothesis (1.1.2) it was made clear that the lavalike lithology of the main bulk of the Woongarra Rhyolite made any hypothesis involving ash-flow emplacement unacceptable unless it was supposed that the normal textural features of ash-flow tuffs had been destroyed by secondary melting. Although present knowledge of large-scale subaqueous silicic eruptions is minimal, it is not credible from physical considerations that such remelting is possible in their products. The column collapse mechanism (Sparks et al., 1978) which is responsible for the high velocities, rapid emplacement, and consequent heat retention of subaerial ash flows is so grossly retarded in subaqueous eruptions that the resultant deposits are likely to be entirely unwelded, and large-scale secondary melting can be discounted. Fiske and Matsuda (1964) provided a model for such events, and the resultant complex range of pyroclastic products has been thoroughly reviewed by both Fisher and Schmincke (1984) and Cas and Wright (1987).

However, hypothesis 1.2.2.1, in which the upper and lower units are each supposed to result from massive subaerial explosive silicic eruptions in the vicinity of the depository of the Hamersley Group, seems to account persuasively for the geometry and stratigraphy of the Woongarra Rhyolite. The hypothesis envisages the resultant ash flows, catastrophically large compared with all recorded eruptions, to have spread over the entire depositional area of the Hamersley Group, and to have been emplaced as a regional tabular sheet along the

sediment–water interface, their momentum carrying them first down into the deepest area of the basin and then up the sides remote from the eruption site.

The best-documented examples of rocks thought to be subaqueously emplaced, hot (welded) ash-flow tuffs, are those in the Ordovician of North Wales, various aspects of which have been described, and beautifully illustrated, by Francis and Howells (1973), Howells et al. (1973, 1979, 1985, 1986), Howells and Leveridge (1980), and Reedman et al. (1987); variations in nomenclature between some of these papers are clarified by figure 2 of Howells et al. (1986). Discussions by Orton (1987) and Branney (1986) provide interesting supplementary debate. In summary, a number of stratigraphic units within the Caradocian sedimentary succession of the Snowdonia area, which were long identified as rhyolitic lavas (Williams, 1927), have been shown to possess typical lithologies and textures of ash-flow tuffs. Reedman et al. (1987) described one such unit up to 90 m thick, the lower Pitts Head tuff, as deposited subaerially on a terrain sloping from south to north, where it crossed a shoreline; and they continued: 'There is no evidence of disruption of the flow at the shoreline, and the flow continued for at least 10 km into the sea, while retaining sufficient heat for most of the tuff to weld following emplacement.' Howells and Leveridge (1980, fig. 4) showed diagrammatic cross-sections of the depositional environment of the rhyolitic units of the slightly older Capel Curig Volcanic Formation, in which the 1st Member (the Garth Tuff of Francis and Howells, 1973) flowed from north to south after subaerial eruption, into and below the sea. Subaqueously welded tuffs have also been well described by Lowman and Bloxam (1981) from the Lower Palaeozoic Fishguard Volcanic Group of South Wales, and are also believed to occur within the Coniston Limestone Formation of the English Lake District (Millward and Lawrence, 1985).

These examples of subaqueously welded ash-flow tuffs have been sceptically received in the volcanological literature. Thus Williams and McBirney (1979, p. 171) referred to Francis and Howells' (1973) paper but concluded that 'Spreading of gas-charged pumice- and ash-flows over the sea floor seems unlikely'. Fisher and Schmincke (1984, p. 295) found it 'difficult to imagine the process by which hot pyroclastic flows penetrate the air–water interface without explosively mixing with the water and destroying the character of the pyroclastic flow', and regarded as 'controversial' the acceptance of the marine nature of the enclosing sediments as evidence of subaqueous emplacement. Cas and Wright (1987) devoted several pages to a detailed critique of the published evidence claimed to support the hypothesis of subaqueous welding for the Snowdonia examples. And a recent review by Stix (1991, Abstract) referred to 'The lack of welded subaqueous deposits in the geologic record...'. This widespread reluctance to accept the evidence presented by the authors cited above in relation to the Snowdonia ash-flow tuffs seems surprising in the light of the demonstration of Sparks et al. (1980b) that it is theoretically possible for ash flows to enter the sea, and to retain substantial heat and velocity as they spread over the sea floor; indeed, it is arguable that the development of a steam carapace is more favourable to heat retention

than subaerial exposure, and that increased pressure beneath water increases the chances of welding. In that context Cole and DeCelles (1991) recently described evidence, from the Miocene Tecuya Formation of California, that hot pyroclastic flows generated on land can continue to flow subaqueously as high-yield-strength laminar flows, although in that case there was sufficient quenching by entrained water to inhibit welding. And there is other persuasive evidence that subaqueous penetration of ash flows does occur (Sparks et al., 1980a). Fisher and Dimroth (1978) at least conceded that the possibility of 'subaqueous welding still cannot be completely ruled out'.

The Ordovician rhyolitic ash-flow tuffs of Snowdonia are important for comparison with the Woongarra Rhyolite not because of their similarity, but because of two important differences: in the first place they do not possess lavalike characters, and in the second they are two orders of magnitude smaller. Although the various descriptive accounts of the Snowdonian examples do not give systematic estimates of the volumes of the pyroclastic units, Howells and Leveridge (1980) estimated a volume of 23 km<sup>3</sup> for the 1st Member of the Capel Curig Volcanic Formation, and suggested that it travelled at least 35 km from its source area. If it is accepted that such an ash flow may penetrate the air–water interface without difficulty, and spread extensively over the sea floor with sufficient retained heat to weld, it seems reasonable to speculate whether an eruption at least 150 times larger in volume that travelled at least 250 km from its source may have retained enough heat for remelting, and possible acquisition of lavalike characteristics.

Such an emplacement hypothesis seems to have advantages in explaining the regional extent and geometry of each of the units of the Woongarra Rhyolite. However, neither hypothesis 1.2.2.2 nor any of the other hypotheses so far considered provides persuasive explanations either for the presence of peperite sills and lenses in the strata overlying the Woongarra Rhyolite, or for the slight stratigraphic discordance of the upper contact. In addition, none of these hypotheses seems to account satisfactorily for the nature of the median raft complex. The final hypothesis to be considered, that the Woongarra Rhyolite is an intrusive sill, or more accurately a double sill, seems to provide the best solution to all the features requiring explanation.

### Intrusion: a preferred model

The hypothesis to be described here is illustrated in the cartoon cross-sections of Figure 38. The following discussion of the proposed mechanism is mainly a commentary on those cross-sections, in which the numbers in parentheses correspond with the circled numbers in that figure.

Figure 38a represents the Hamersley Basin at about the end of deposition of the Hamersley Group. The diagrammatic cross section is drawn through the central part of the basin and, for the purposes of this discussion, has no direction or scale. A basement of granite–greenstone terrane (1) is the deepest crustal level shown. The granitoids, ornamented with crosses, are associated

with scattered greenstone synclinoria; both components have ages between about 3.5 and 2.9 Ga. The locally irregular basal unconformity of the Fortescue Group (2) is overlain by a sequence of mainly mafic lavas and associated sedimentary rocks up to 7 km thick (3); the Fortescue Group was deposited between about 2.76 and 2.68 Ga. Its lower formations are discontinuous, but the uppermost unit, the subaqueous Jeerinah Formation, was laid down in quiet conditions in a basin-wide sea. The Hamersley group (4) overlies the Fortescue Group conformably, and is represented here as being about 1.8 km thick. It consists largely of BIF, with subordinate carbonate and shale. However, at the time represented there is, as discussed earlier, an upper zone (stippled, and numbered 5) of diagenesis and compaction, within which the primary colloidal precipitate lithifies, dehydrates, and increases in density from about 1.1 to about 3.2 g/cm<sup>3</sup>. The depth of water in the basin (6) is not critical for the intrusive model, but is supposed to be between 1 and 2 km in the centre of the basin; all that the model requires is that the intrusion of the rhyolite was not associated with decrease of water depth of a magnitude which would radically change depositional conditions in the basin.

At the base of the whole section, at some unknown depth within the crust, a magma chamber (7) is shown. It is not possible to place quantitative constraints on either the depth or dimensions of this chamber, but some points relevant to these are discussed later.

In Figure 38b a columnar diapir of silicic magma (8) has risen from the magma chamber and penetrated the granite-greenstone terrane, the Fortescue Group, and most of the thickness of the Hamersley Group, and has then spread out in a 'T' shape to begin emplacement of a basin-wide sill now represented by the upper unit. In later discussion it will be supposed that the top of the 'T' was an ellipse with a 5:1 elongation in plan, reflecting the elongate shape of the outcrop area. As the sill was injected, a raised 'blister' (9) on the floor of the basin formed above it, with a height equal to the sill thickness. Elevation of (land) surfaces of this magnitude, as a result of magma injection, have been described by Minakami (1950).

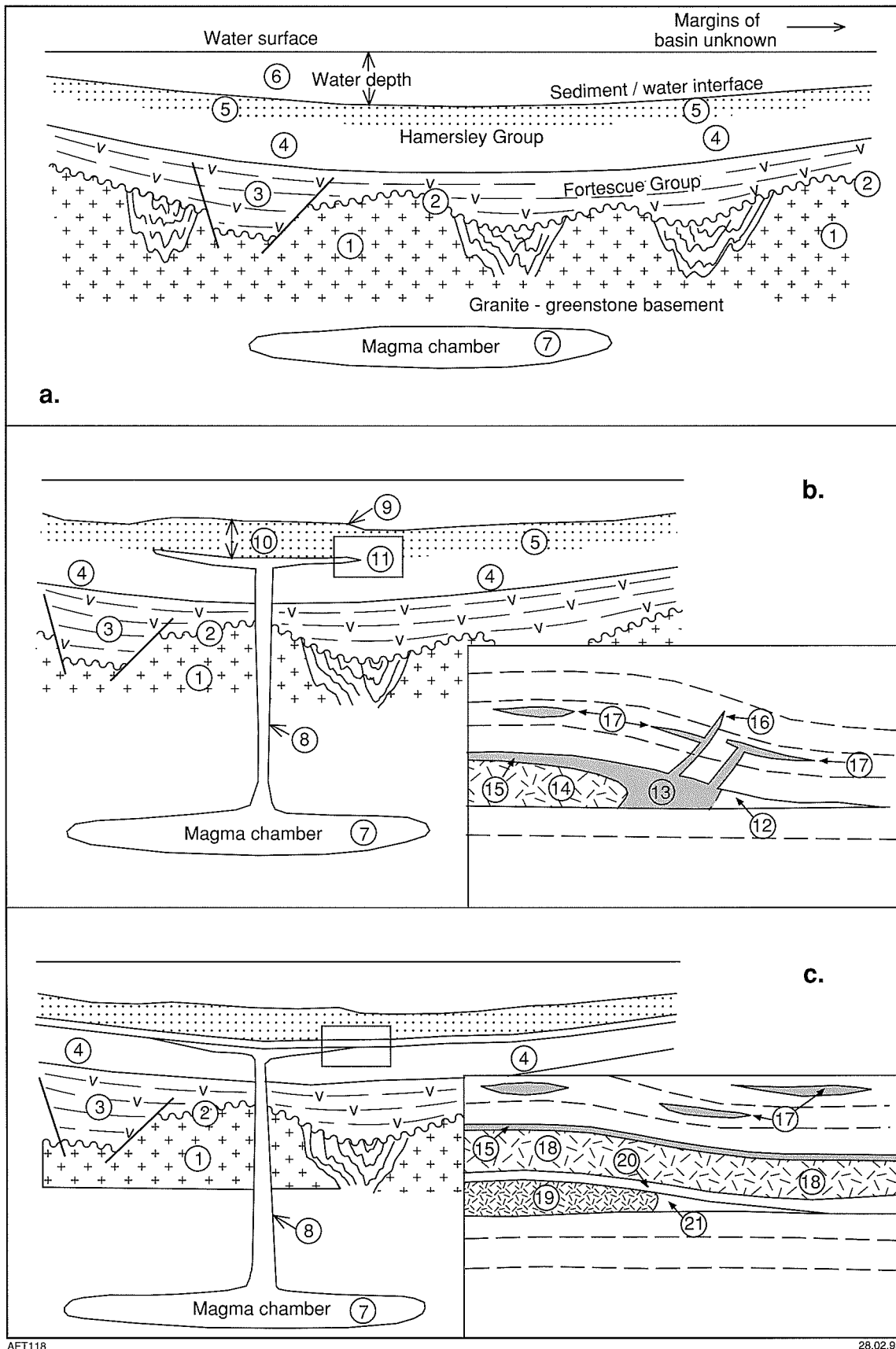
For reasons set out later, it is supposed that the columnar diapir, or feeder pipe, was relatively small, unique, and within the deeper central part of the basin. The depth below the sediment-water interface at which the column terminated (10), as well as the conditions at the spreading perimeter of the sill (11), shown in greater detail in the expanded diagram at the lower right-hand side of the section, are points that need detailed attention. But before addressing these it is necessary to deal with the question why the magma of the diapiric column should have spread out to form a sill rather than continued to the surface.

There is a substantial volume of literature on the theory of sill emplacement, but the great majority of papers are concerned with the commonest type of extensive sill: dolerite sheets, usually emplaced within epiblastic sedimentary rocks (e.g. Bradley, 1965; Leaman, 1975). The basic physics of a first-order model for the rise of magma in the crust, initially proposed by Gilbert (1877), is clearly described by Williams and McBirney (1979). In

this model (Williams and McBirney, 1979, figs 3–10) a diapiric column of mafic magma with a density about 2.7 g/cm<sup>3</sup> rises from a magma chamber that lies about 80 km below the surface, within rock with a density of about 3.3 g/cm<sup>3</sup>. While the hydrostatic pressure ( $P_m$ ) of the magma within the column decreases in direct proportion to height above the magma chamber, the lithostatic pressure (or vertical component of stress:  $\sigma_z$ ) in the wallrocks decreases in a more complex way. Within the lower, more dense, crustal layers it decreases faster than the magma pressure; but as successively lighter layers are traversed the rate of decrease at first becomes equal to, and finally, if the near-surface rocks are less dense than the magma, less than that of the magma pressure. According to Williams and McBirney (1979), for a simple model of continental crust, basaltic magma pressure at the surface may exceed lithostatic pressure (zero) by about 1 kb, to permit the construction of a volcanic cone about 3 km high. At depth, in their model, the difference between magma pressure and lithostatic pressure ( $P_m - \sigma_z$ ) increases from zero at about 60 km to a maximum at about 10 km depth. In Figure 39a–c a model similar to that of Williams and McBirney (1979) is shown, using their supposed crustal layer thicknesses and densities, as well as magma density, but differing in assuming that  $P_m$  is equal to  $\sigma_z$  in a magma chamber at a depth of 50 km, and also that the top of the magma column lies 1 km below the surface. Figure 39c illustrates the maximum in  $P_m - \sigma_z$  at a depth of 10 km.

Williams and McBirney (1979) wrote further: 'It is reasoned that magma will spread laterally at the level at which the difference between the hydrostatic pressure of magma and the lithostatic pressure of adjacent wallrocks reaches a maximum value. This is said to be where the relative densities of two columns are reversed and the magma is no longer lighter than the rocks it intrudes.' Francis (1982), in a thoughtful address directed towards understanding the thick-based saucer shapes of the Midland Valley Sill of Scotland and the Whin Sill of northern England, generally accepted the physical model of Williams and McBirney (1979), and reproduced their figure 3–10 with the words 'optimum level for sill emplacement' at a depth of 10 km, differing slightly from the text statement 'the optimum level would be less than 10 km where the density of the sediments becomes less than that of the magma'.

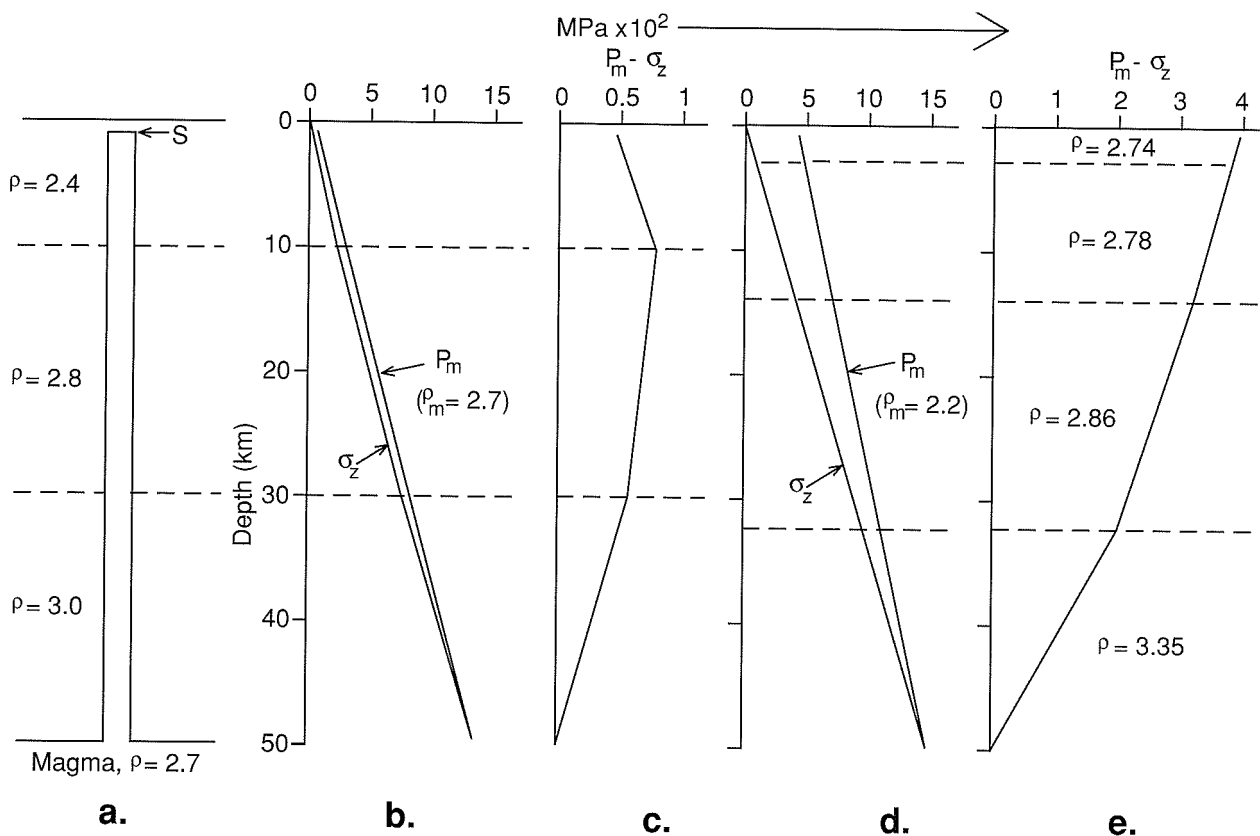
Walker (1989, fig. 3), in advocating a direct gravitational control on the movement of mafic magma in the crust, used a diagram similar to that of Williams and McBirney (1979). He introduced Ryan's (1987) concept of neutral buoyancy to argue that the stable crustal level 'in which magma is able to reside indefinitely is that at which the magma possesses neutral buoyancy', and that 'in a simple layered lithosphere, the level of neutral buoyancy (LNB) for any given magma density is the level below which the rocks are denser than the magma, and above which the rocks are less dense than the magma'. It does not matter whether the magma in the columnar diapir is lighter or heavier than the wallrock. The important issue is whether it is at a pressure, at any point in its ascent, capable of overcoming the combined vertical stress and the tensile strength of the contiguous rocks.



AFT118

28.02.95

Figure 38. Cartoon sequence summarizing the suggested emplacement mechanism of the Woongarra Rhyolite. Circled numbers are explained in the accompanying text. In (b) and (c) the cross-section of (a) has been offset slightly to the left to make space for the detailed sections of the advancing periphery of the upper unit (b) and lower unit (c)



AFT119

31.07.95

Figure 39. Cross-sections depicting hypothetical pressure and stress conditions within and adjacent to a diapiric column of magma. (a), (b), and (c) follow the model illustrated by Williams and McBirney (1979), but assume that the top of the column lies 1 km below the surface. (a) shows the assumed densities of the crustal layers, and of the mafic magma; the letter 's' is referred to in the text. (b) shows the variation with depth of the lithostatic pressure (vertical stress) in the wall rocks and the hydrostatic pressure of the mantle. (c) shows the variation of the difference between magma pressure and vertical stress. (d) and (e) show the same parameters as (b) and (c), using the central Hamersley Basin crustal layers of Drummond and Shelley (1981, p. 140, Gravity Model A) to a depth of 50 km; densities are shown in (e). The diapirically rising column is assumed to be occupied by silicic magma with a density of 2.2 g/cm<sup>3</sup>, and its top is again assumed to lie at a depth of 1 km. Note the x2 scale compression between (c) and (e)

It is not explicit in any of the theoretical discussions already cited why the level at which  $P_m - \sigma_z$  attains a maximum level should be the optimum level for sill emplacement. It may be assumed that the argument is one based on pressure gradient: a magma at a pressure  $P_m$  at that level will find the lithostatic pressure of its wallrocks *relatively* greater if it moves either higher or lower in the column. But this argument is not valid, since  $P_m$  will decrease upwards, not sideways, and if all other factors are equal, magma will move like any other liquid in response to a pressure gradient. Clearly, as Williams and McBirney (1979) noted, the classical model is simplistic, and not in accord with the geological observations on the depth of emplacement of sills. Mudge (1968) reviewed the geological evidence for the emplacement depth of sills at 54 localities, mainly in the U.S.A., and found a strong preference for depths between about 1 and 2.5 km; and emplacement of basaltic sills at a depth of less than one hundred metres has been documented by Einsele et al.

(1980) from the Gulf of California.

Mudge (1968) concluded that factors other than  $P_m - \sigma_z$  played significant roles in controlling the emplacement sites of the sills he reviewed. He identified these as the presence of planar zones of weakness, such as well-defined bedding planes or unconformities, and the existence of an overlying 'fluid barrier', such as a shale, which would hinder the continuing upward progress of the magma. The significance of these factors has also been identified by other authors. Thus Du Toit (1920, p. 5) emphasized both points in his review of the Karroo dolerites of South Africa. Bradley (1965, p. 39) not only suggested the need for an overlying 'impervious stratum' for sill initiation, but also suggested that the availability of pore water for steam generation was associated with sill initiation. Walker (1974) later revived this concept that the presence of groundwater in permeable rocks could constitute an effective barrier to the rise of magma, and

cause intrusion; and he also pointed out (Walker, 1989) that 'mechanically weak rocks at or near the LNB favour intrusion'. Gretener (1969) suggested that the crustal level of sill injection is stress controlled, and that dolerite sills will form immediately below strata in which the two horizontal stresses are different, and both higher than the vertical stress. Gretener's model seems simplistic in that it assumes that bedding planes have zero tensile strength (i.e. that they are 'surfaces of no cohesion'), but it should be noted that it predicts that 'sill intrusion is produced easier (sic) in shallow beds'.

In summary, although much thought has gone into the development of models for magma rise in the crust and its consequent emplacement as sills, the essential conclusions are that if rising magma is at a pressure sufficient to reach the surface, it will fail to do so only if and when restrained by an effective barrier of some kind; and if that barrier overlies a layer of low tensile strength a sill is likely to be formed\*.

The minor significance of either a level of maximum  $P_m - \sigma_z$  or an LNB for sill emplacement is increased, in the case of silicic magma, by the very different variation of these parameters with depth in crustal models such as that of Figure 39a–c in which silicic magma is substituted for basaltic magma. Such a model is depicted in Figure 39d,e. In Figure 39d, instead of using the crustal layers of Williams and McBirney (1979), the central Hamersley Basin crustal layers of Drummond and Shelley's (1981, p. 140) Gravity Model A are used to a depth of 50 km; their densities are shown in the figure. The diapirically rising column is assumed to be occupied by silicic magma with a density of 2.2 g/cm<sup>3</sup>, and its top is again assumed to lie at a depth of 1 km. In Figure 39e, in which the horizontal scale is compressed by a factor of two compared with Figure 39c, it is evident that there is no LNB, that  $P_m - \sigma_z$  reaches a maximum at the top of the column (and would continue to increase if the column rose), and that its magnitude is about four times higher than that in the model for mafic magma.

The intrusion hypothesis proposed here for the Woongarra Rhyolite essentially begins with the model of Figure 39a, coupled with the crustal layer and magma densities used for Figure 39d,e. When the top of the column reached the base of the zone of diagenesis and lithification (5 of Fig. 38), the rapid vapourization of the water that still remained in the rocks at the base of this zone led to their virtually explosive disintegration. Concurrent quenching and immediate hydroclastic shattering of the rising uppermost magma formed a potentially highly mobile, hot, fluidized mixture of rhyolitic and sedimentary (BIF) debris. This high-pressure fluidized mixture, the parent material of the peperites associated with the upper contact of the Woongarra Rhyolite, is referred to subsequently as 'proto-peperite' to distinguish it from the resultant cooled rock.

At this level, the precise position of which will be examined shortly, the proto-peperite was at an enormous pressure compared with the hydrostatic pressure resulting from the overlying rocks and basin water. This would have been most effectively released by breakthrough to the surface (or more correctly to the floor of the basin). But

the movement of the proto-peperite would have been controlled purely by the relative strength of the wet rocks of the immediately overlying zone of diagenesis, and that of the lithified BIF adjacent to the top of the plug. If the strength (shear and tensile) of the overlying 'lid' was sufficient, in combination with the effects of quenching and fluidization, to prevent further progress through it, and if the tensile strength of the lithified BIF was less than  $P_m - \sigma_z$ , as would clearly have been the case (Vutukuri et al., 1973), the top of the pipe would have forced up the overlying rocks to form a 'blister' on the floor of the basin, splitting apart the weakest bedding plane near the top of the pipe, so as to initiate a sill, now the *upper unit* of the Woongarra Rhyolite, at the level marked 'S' in Figure 39a; and the proto-peperite would have found pressure relief by forcing its way laterally along the fissure so formed. Its subsequent progress is examined below, after consideration of the depth below the sediment–water interface at which sill initiation occurred.

The process of fluidization envisaged to have taken place at the base of the zone of diagenesis has been vividly described by Kokelaar (1982), whose work permits further speculative constraints on the emplacement depth. Basing his argument on the liquid–vapour phase relationships of water in the pressure range 0–40 MPa and temperature range 0–600°C, Kokelaar (1982) argued that fluidization may not occur at pressures greater than 31.2 MPa, and his account suggests that the violence of water vapourization due to heating would increase dramatically at pressures below about 20 MPa. Now consider the model of Figure 39a,d, as the top of the magma column rises above a depth of 1 km, at the time of deposition of the Hamersley Group, as in section B of Figure 38. Under these circumstances a water depth of 1000 m, combined with an emplacement depth of 200 m below the sediment/water interface, will give a lithostatic pressure in the rock immediately overlying the column of about 14.3 MPa, while a water depth of 1500 m combined with an emplacement depth of 300 m will result in a lithostatic pressure of about 21.5 MPa; in both cases a density of 2.15 g/cm<sup>3</sup> is assumed for the overlying sediments, the mean of the primary precipitate and the lithified BIF, as discussed earlier. The intrusion depth of the Woongarra Rhyolite probably lay between these limits, and formed a suitable environment for fluidization.

The formation of marginal peperite during emplacement of sills at 'shallow' depths has been described by a number of authors apart from Kokelaar (1982), whose particular purpose was to emphasize the role of fluidization in suitable circumstances. A record of historical interest is that of Lyell (1865, p. 686), who referred to many places in the Auvergne where 'igneous rocks have been forced

\* The manuscript of this report was submitted for publication in December 1992. Concurrently with final editing, in November 1994, a debate on the dynamics of sill emplacement continues in the Australian Journal of Earth Sciences (Trendall, 1994; Francis, 1994; McPhie, 1994; Leaman, 1995; Kerr and Lister, 1995). It arose from McPhie's (1993) application of Francis' (1982) emplacement model to an extensive, silicic porphyry sheet in the Tennant Creek area. It is clear from this debate that the controls of sill formation are still incompletely understood.

by ... injection through (Eocene) clays and marly limestones, in such a manner that the whole has become blended in one confused and brecciated mass'; he illustrated an oblique dyke which 'cuts through the marly strata, ... producing ... great alteration and confusion in them for some distance from the point of contact'.

In more recent literature, Smedes (1956) noted the important role of water in the genesis of peperite at the margins of basaltic and andesitic sills intruded into wet Late Cretaceous sediments of the Elkhorn Mountains of Montana. In a more complete description of the peperites, Smedes (1966) noted that peperite occurs both at the margins of thicker sills and as the sole component of thinner sheets. His description of these Cretaceous peperites (Smedes, 1966, p. 42) as representing 'a thorough mixing of magma and country rock, with each retaining its identity even on a microscopic scale' applies well to many of the peperites associated with the Woongarra Rhyolite. He made no quantitative estimate of cover thickness, but stated that the sills 'were intruded into moist unconsolidated sediment [which] implies shallow cover at the time of intrusion and suggests that the intrusives were only a little younger than the enclosing strata'; their preferred injection into thin-bedded volcanic mudstone and siltstone nevertheless implies a sufficient degree of lithification for fissility.

Grapes et al. (1972) described a suite of shallow dolerite sills intruding Permo-Triassic strata in the Allan Hills region of Antarctica. The suite included a clastic sill some 650 m long and up to 7 m thick, consisting of 'an unsorted aggregate of sandstone, siltstone, carbonaceous shale, dolerite, amygdaloidal dolerite and tachylytic basalt in a fine, highly variable matrix composed of tachylyte with quartz and feldspar grains'; this sill was interpreted as a breccia-filled extension space. Hanson and Schweickert (1982) described localized pockets of peperite breccia, associated with hyaloclastite breccia, near the base of a rhyolite sill within the Upper Devonian volcanic sequence of the northern Sierra Nevada, California; they interpreted the peperite as resulting from intrusion into wet sediments, and suggested that 'a significant time did not elapse between deposition of the sediments and intrusion of the rhyolite'. Brooks et al. (1982) provided detailed descriptions of peperites of the same area, and Hanson (1991), in a further account of both andesitic and rhyolitic sills, noted that the intrusive silicic magmas often behaved in a way that suggested that their viscosity was comparable to that of basaltic magma.

Kokelaar et al. (1985) have described rocks formed by a complex sequence of syndepositional volcanic events within the Lower Ordovician marine succession of Ramsey Island, off the coast of South Wales. The contacts of minor rhyolitic intrusions are described as 'distinctively peperitic, with angular and irregular clasts of rhyolite supported in mudstone'; intrusion is believed to have occurred while the sediments were still wet and unlithified. A number of andesitic sheets within the Ordovician Borrowdale Group of northwest England, previously thought to be lavas, have recently been reinterpreted by Branney and Suthren (1988) as sills. These authors pointed to the presence of peperite at the upper contact of sills as a useful criterion for

distinction from lavas; the peperites are well described and illustrated, and are believed to have resulted from intrusion into wet sediments. Other published examples of high-level intrusions with marginal peperite include the 'very shallow' basaltic sills within Lower Cretaceous littoral carbonate and volcanoclastic rocks of Baja California described by Busby-Spera and White (1987), and the irregular 'shallow' andesitic bodies documented by Kano (1989) from the Neogene Shirahama Group of South Izu, Japan.

Many of the foregoing examples of high-level sheets intruded into wet sediments seem to be close to the 'synsedimentation sill' option considered by Cas (1978) for the porphyry sheets of the Merrions Tuff, and it seems pertinent to consider whether the admixture of porphyritic clasts and sediment at both margins of the Merrions Tuff porphyries may not be peperites similar to the ones described above, also resulting from intrusion into wet sediments.

In summary, although there are many published accounts of 'shallow' intrusion into wet sediments few authors commit themselves to a quantitative depth estimate; the depth range of 200–300 m arbitrarily proposed above, coupled with possible water depths of 1000–1500 m, will therefore have to serve for the purposes of further discussion. It is consistent with the maximum likely depth of 500 m proposed earlier by analogy with diagenesis of argillaceous sediments (Muller, 1967).

The evidence for vesiculation in the Woongarra Rhyolite is confined to small quartz-filled bubbles (either spherical or flattened) in quenched glass fragments of the upper unit (Fig. 16d,e) and to the presence of bubble-wall shards in some peperites (Figs 16c, 25). Although the degree of vesiculation might be thought of as providing some constraint on emplacement depth it is disappointing that this is not so. Fisher and Schmincke (1984, p. 55 on) have summarized recent work which highlights the complexity of the vesiculation process; and the fact that surface rhyolite flows without vesicles are of common occurrence emphasizes that depth is only one of an inter-related set of controls. Eichelberger et al. (1986) and Westrich et al. (1988) have recently proposed an ingenious mechanism by which they suggest water could have been removed from the rhyolitic magma of the 600-year-old Obsidian Dome (California) by early eruptive foaming, followed by reagglutination of the degassed lava. However, that explanation for the low level of vesiculation in the Woongarra Rhyolite is clearly not applicable.

At whatever depth lateral penetration was achieved, the proto-peperite would quickly have obtained increased mechanical leverage to assist its progress, and silicic magma would have forced its way behind it into the widening gap and increased the wedging effect (Anderson, 1938, p. 249; Bradley, 1965, p. 35; Pollard and Johnson, 1973, p. 340). The conditions at the advancing perimeter of the sill in the expanded diagram of the section in Figure 38b now need close examination.

The supposed cross-sectional shape of the advancing sill rim follows that proposed by Bradley (1965, figs 4 and 5) and Grapes et al. (1972, fig. 13). A thin steam-filled

'extension space' (12) led the way, followed closely by a zone of proto-peperite (13). This fluidized and highly mobile material probably had a density less than  $2 \text{ g/cm}^3$ , lower than the  $2.2 \text{ g/cm}^3$  of the silicic magma (14) which followed in its wake; the magma was therefore injected beneath the proto-peperite. As the whole complex front advanced, the foremost proto-peperite was forced against the roof by the advancing magma, and was quickly compacted and chilled to form the existing peperite (15). Immediately behind the advancing tip of the wedge, where the roof was first bent up, tension gashes (16) would have developed (Bradley, 1965; Grapes et al., 1972) up which the proto-peperite was injected to form overlying discontinuous sills and lenses (17) as the sill advanced (Figs 19a,c; 26–29); the tensions cracks closed as the roof curvature changed from convex inwards to concave inwards as the perimeter advanced, so that the supply routes of most such lenses were probably soon pinched out again, and their extent restricted. The mechanism of formation envisaged for the proto-peperite is very close to that proposed by Grapes et al. (1972) for the material of a clastic sill 'some 650 m long and as much as 7 m thick' composed of 'an unsorted aggregate of [wallrock], dolerite, amygdaloidal dolerite and tachylytic basalt' associated with dolerite sills in the Allan Hills region of Antarctica.

As the sill moved forward the magma at the base would have been quenched against the subjacent rocks, so that continuity of magma supply would have been achieved by flow in the central part of the magma sheet; internal movement of this type probably accounts for the abundant autobrecciation near the base of the upper unit of the type section (Fig. 20). Although Henry et al. (1990), in discussing the Bracks Rhyolite, asserted that 'basal breccia is probably the most diagnostic feature of a lava' this was written in the context of the problem of distinguishing lavas from ash-flow tuffs; there seems to be no reason why the structures developed at the base of a shallow sill should differ substantially from those at the base of a lava.

The advancing edge of the hot central part of the sill supplied heat to the perimeter, and resulted in the continuing generation of proto-peperite as the sill spread, probably from both the upper and lower stratigraphic surfaces of the expansion space. The proto-peperite did not itself flow laterally, but was continuously trapped and compressed by the moving magma below; this is why its constituent fragments are thin discs, rather than elongate, in plan.

The uppermost rhyolite magma, like that at the base, would also have been quenched and autobrecciated against the chilled marginal peperite. The wide textural variation in rocks from this zone reflects a complex sequence of physical events, which probably occurred in rapid succession during the initial emplacement of the advancing sill rim. Parts of the marginal magma fragments, which had developed vesicles while still plastic enough for these to be deformed, then developed perlitic cracks before brittle fragmentation, whereas other fragments in the same rock have undeformed vesicles (Fig. 16e). The genesis, composition, and physical behaviour of magma and proto-peperite at the top of the sill were quite different, a

distinction which remains reflected in the evident boundary between the uppermost rhyolite (often autobrecciated) and peperite (Fig. 26).

The regional extent and uniform lithology of the upper unit imply that this first sill spread out evenly, as described, over at least the present outcrop area of the Hamersley Group. The fact that it is always present, and that there is no sign of major rupture of the overlying Boolgeeda Iron Formation, accompanied by evasion of magma into the basin, suggest that it never reached the surface; its uniform lithology and composition also suggest that it was emplaced as a single continuous sheet, as a result of a single injection of magma that came from a unique source, or feeder pipe.

Ideally, a complete numerical model for the emplacement of this vast sill should be developed. However, there are so few firm constraints on any of the parameters needed for this that it is not yet possible. The unknowns include:

- temperature and viscosity of the magma;
- mechanical properties of the host rocks;
- depth of intrusion;
- properties of the fluidized proto-peperite;
- size and nature of the feeder pipe.

All that can be attempted here is to see whether it is possible to make estimates of such parameters as the rate of magma injection from the feeder pipe into the sill, the time required for sill emplacement, and the possible magma viscosity, temperature, and pressure within the sill during emplacement, which are all mutually consistent as well as credible in terms of what is known of the properties of rhyolitic magmas. The first two of these—time required for emplacement and rate of magma injection—are taken first.

The time required for emplacement of sills has not been extensively addressed in the literature. Bradley's (1965, p. 34) suggestions were purely suppositional. The most precise quantitative theories have been proposed for the formation of laccoliths, and insofar as sills are a special form of laccolith, those ideas provide a good starting point for discussion. In his reinvestigation of the laccoliths of the classic Henry Mountains region, Utah, Hunt (1953, p. 146–7) accepted the simple proposal that: 'The rate of intrusion of laccoliths perhaps is comparable to the rate of volcanic eruptions involving comparable quantities of material'; but because laccolith intrusion must have involved some resistance from the intruded strata Hunt suggested that laccolith formation was slower than the rate of eruption from volcanoes, and that a laccolith could be formed 'in a matter of days'. Hunt (1953) gave the average volume of Henry Mountains laccoliths as a quarter of a cubic mile ( $\sim 1 \text{ km}^3$ ), so that an intrusion rate of the order of  $10^3 \text{ m}^3/\text{s}$  would result in an intrusion time of 11–12 days. This is, in fact, substantially *higher* than the usual effusion rates of lavas, as listed for example by Cas and Wright (1987, tables 4.1 and 4.2); note that the highest value ( $5 \times 10^3 \text{ m}^3/\text{s}$ ) given by Cas and Wright (1987) on the

authority of Walker (1973) for the Laki 1783 flow in Iceland should be  $5 \times 10^2 \text{ m}^3/\text{s}$ . Although Tolan et al. (1989, p. 17) suggested flow rates of about  $1.2\text{--}3.6 \times 10^4 \text{ m}^3/\text{s}$  per linear kilometre of source fissure for great flows of the Columbia River Basalt Group, those lavas were of very low viscosity. The estimate by Henry et al. (1990, p. 129) of  $2.4 \times 10^2 \text{ m}^3/\text{s}$  for the Bracks Rhyolite of Trans-Pecos Texas depends on an assumed eruption time of 10 years, and may have been an order of magnitude greater if eruption only took one year.

Pollard and Johnson (1973, p. 348 on, and fig. 25) have given a more precisely quantified estimate of the emplacement time of one of the laccoliths of the Henry Mountains (the Black Mesa intrusion), based on their analysis of growth mechanics. Their estimates of 48 hours for that laccolith to reach its final diameter of 0.85 km (as a sill 50 m thick), and 'less than several weeks' for completion of intrusion (200 m thick), imply intrusion rates of the order of  $1.5\text{--}6.6 \times 10^2 \text{ m}^3/\text{s}$ . Dixon and Simpson's (1987) centrifuged models simulating laccolith intrusion gave intrusion rates of the same order: from their figure 8, rates of  $1.6\text{--}3.0 \times 10^2 \text{ m}^3/\text{s}$  can be estimated.

Contrary to Hunt's (1953) view that the rate of laccolith growth was likely to be slower than the rate of lava effusion, because of the greater pressure resisting intrusion, it can be argued that rhyolitic sills may grow faster than flows, since the rate of heat loss and the rate of volatile loss, both of which are conducive to increased viscosity, are likely to be less in intrusions. However that may be, a magma supply rate of  $10^3 \text{ m}^3/\text{s}$  for the Woongarra Rhyolite seems to be a reasonable one to accept for the purposes of further discussion.

A magma supply rate of  $10^3 \text{ m}^3/\text{s}$  for the upper unit of the Woongarra Rhyolite implies an intrusion time of  $7.5 \times 10^9 \text{ s}$ , or slightly less than 240 years. Whether that time is consistent with the driving pressure and viscosity of the magma, and also with retention of sufficient heat by the sill for peripheral fluidization in association with its extension, must now be considered. Johnson and Pollard (1973) examined in detail the different pressure distributions between sills which grow by thickening only and sills which grow by lengthening only, and concluded firstly that the latter probably never occur in nature, and secondly that most sills probably grow by a combination of thickening and lengthening. Although the Woongarra Rhyolite upper unit sill probably grew by both mechanisms, and probably also possessed a leading wedge with the structure suggested in Figure 38, it is adequate for first-order quantification of growth to consider it as having been elliptical in plan, with a 5:1 elongation, and a constant thickness of 100 m throughout its development. An elliptical plan shape is chosen purely because it reflects the present outcrop shape of the Woongarra Rhyolite; both Pollard and Johnson (1973, p. 328 on) and Dixon and Simpson (1987, p. 100) have drawn attention to problems in explaining laccolithic intrusions that are elliptical in plan, but study of the Woongarra Rhyolite has done nothing to resolve these. The initial peripheral spreading rate of such a sill would have been extremely fast, but with a constant magma supply rate of  $10^3 \text{ m}^3/\text{s}$  rim velocity would have decreased exponentially, as shown in Figure

40. Are the velocities shown in that figure consistent with the available driving pressure and likely magma viscosity?

Johnson and Pollard (1973, p. 296 on) examined the factors controlling the flow rates of Newtonian, pseudo-plastic and Bingham magmas in a tabular conduit. Applying their equation 10a (ibid., p. 299) to the major radii of the elliptical sill under discussion it can be shown that a Newtonian magma with a dynamic viscosity of about  $3.4 \times 10^{12}$  poises would fit with the parameters of Figures 39 and 40 throughout the life of the sill. In applying that equation it is adequate for the first-order result sought to assume that the sill was horizontal, and that the driving pressure at the feeder pipe was about equal to  $P_m - \sigma_z$  (Fig. 39D), decreasing to near zero at the leading edge of the sill (Pollard and Johnson, 1973, p. 350).

Compared to the relatively small intrusions of the Henry Mountains, towards which the modelling of Johnson and Pollard (1973) and Pollard and Johnson (1973) was largely directed, the upper unit of the Woongarra Rhyolite has a volume three orders of magnitude larger, and a source driving pressure two orders of magnitude greater, but the last parameter is combined with a slightly lower pressure gradient because of the much greater lateral extent. However, as both Anderson (1938, p. 250) and Pollard (1973, p. 253) have pointed out, the mechanical advantage of a sheet intrusion in brittle rock is such that it is more of a problem to explain why propagation ever stops, than why it continues. Provided that the thin overlying sheet of wet sediment was too strong to be penetrated by the spreading sill, the rhyolitic magma of the upper unit of the Woongarra Rhyolite had sufficient driving pressure to keep extending indefinitely. Dixon and Simpson (1987) suggested, from their centrifuged models, that 'magmatic driving pressure apparently affects primarily the rate of magmatic intrusion and has little effect on the form of the intrusion or its evolution'. The parameters proposed here for emplacement of the upper unit sill are consistent with Dixon and Simpson's (1987) findings that a shallow overburden is favourable for the development of a low aspect ratio, as well as with their suggestion that a well-laminated overburden with freely sliding interfaces leads to flat-roofed (i.e. constant thickness) intrusions; the BIF in the lower part, at least, of the zone of diagenesis would have had such a character. This latter idea was discussed more fully by Koch et al. (1981).

Is it credible that the rhyolitic magma of the upper unit had a viscosity no greater than  $3.4 \times 10^{12}$  poises (P) throughout the period of emplacement? Although no field determination of the viscosity of rhyolitic magma has ever been made there is general agreement in volcanological texts (e.g. Williams and McBirney, 1979; Cas and Wright, 1987) on two points: in the first place that there is an inverse exponential relationship between viscosity and temperature, and in the second place that, for any temperature, viscosity is substantially lowered by volatile content. In respect to rhyolite, this consensus is based mainly on data of Friedman et al. (1963), Shaw (1963), Murase (1962) and Murase and McBirney (1973). Between  $1000^\circ$  and  $800^\circ\text{C}$  the viscosity of dry rhyolite magma increases from about  $10^8$  to  $10^{11}$  P; with an  $\text{H}_2\text{O}$

content of about 1.5% these values decrease to  $10^7$  and  $10^9$  P respectively. Even at  $700^\circ\text{C}$ , rhyolitic magma with 1.5%  $\text{H}_2\text{O}$  probably has a viscosity little greater than  $10^{11}$  P. The present volatile content of the upper unit (Table 2) cannot be accepted as that of the intruding magma, but it is nonetheless credible that the magma had an  $\text{H}_2\text{O}$  content of that order. There is thus no difficulty with viscosity in the intrusion model under discussion for the upper unit of the Woongarra Rhyolite, provided that temperatures in excess of  $700^\circ\text{C}$  can be credibly sustained.

Williams and McBirney (1979, p. 28) listed estimated eruption temperatures of silicic lavas between  $790^\circ$  and  $925^\circ\text{C}$ . A slight fall in temperature is to be expected on eruption, and from data summarized by Carmichael et al. (1974) a granodioritic magma at  $1000^\circ\text{C}$  with about 1.5%  $\text{H}_2\text{O}$  would be above the liquidus, and thus have the potential to contain phenocrysts. Bonnicksen and Kauffman (1987) suggested an eruption temperature of 'around  $1000^\circ\text{C}$ ' for rhyolite lava flows from southwestern Idaho, and an intrusion temperature of  $1000^\circ\text{C}$  will be assumed here for the upper unit of the Woongarra Rhyolite. Jaeger (1959) considered the cooling of a tabular sheet intruded into wet sediments, and from his figure 2, which concerns the calculated cooling rates adjacent to a sheet with a fixed melting point (and intrusion temperature) of  $1000^\circ\text{C}$ , it can be estimated that the central part of a sheet 200 m thick will be at a temperature trivially below that of intrusion after 240 years, and only the outermost 30 m will have cooled below  $700^\circ\text{C}$ . It thus seems that an intrusive model for the upper unit of the Woongarra Rhyolite is credible in terms of the parameters noted above: magma supply rate ( $10^3$  m<sup>3</sup>/s), emplacement time ( $7.5 \times 10^9$  s), magma viscosity ( $<10^{13}$  P), source driving pressure (400 MPa), driving pressure gradient ( $2 \times 10^3$  Pa/m when the major axis of the ellipse was 200 km long), and temperature ( $1000^\circ$ – $700^\circ\text{C}$  over the period of emplacement), as well as in terms of rim velocity (Fig. 40).

This Report is not concerned with petrogenesis, and accepts without discussion the subsurface existence of a major volume of uniform rhyolitic magma at the start of the emplacement process, from which the feeder pipe rose. There is no clear evidence for the location of this pipe, but an assumption that it lay somewhere in the central part of the present outcrop area would be consistent with the model under discussion. As already discussed in connection with the supposed 5:1 elongation, there are difficulties with intrusive models involving asymmetric plan shapes, and it would certainly be hard to imagine why an intrusion related to the present elongate outcrop area should have developed from a pipe situated near either end. That only one feeder was involved seems likely from the consistent stratigraphic relationship, coupled with the equally consistent petrographic differences, of the upper and lower units. It might be expected that multiple sources would have produced locally overlapping injections at different stratigraphic levels. Greater local chemical variation might also be expected.

At the assumed magma supply rate of  $10^3$  m<sup>3</sup>/s, a feeder pipe of circular cross section and a diameter of

100 m would need an average flow velocity of 127.3 mm/s for the emplacement of the upper unit of the Woongarra Rhyolite in the suggested time of  $7.5 \times 10^9$  s; this seems unacceptably fast. The required velocity would decrease inversely with the square of the vent diameter, so that a pipe 1 km in diameter would need a magma velocity of 1.27 mm/s if other parameters remain the same. An average velocity of this order does not seem an unreasonable one to postulate, and a feeder pipe of about that size could easily be accommodated in the central part of the Woongarra Rhyolite outcrop area. It may be concealed either at depth below one of the synclines, or lie beneath superficial deposits in the anticlinal areas (Fig. 1).

It should be emphasized, first, that the model described above is a first-order one capable of refinement as additional data constrain its parameters, and second, that all such models imply a continuity which is likely to be hidden by the 'noise' implicit in the small-scale episodicity of natural events in the Earth.

In respect to the first of these points the arbitrarily selected depth of 50 km for the parent magma chamber is the critical control for the driving pressure. A shallower depth would decrease the driving pressure, so that it would be necessary to assume a lower viscosity (higher volatile content) to achieve emplacement within a time short enough to avoid cooling before completion of emplacement. The important point is that there is ample scope for adjustment in all of the interdependent parameters discussed, and that no factor has arisen which makes emplacement of the upper unit as a sill unacceptable.

On the second point it seems likely, in particular, that the rim velocities of Figure 40 must be considered only as time-integrated rates of the spasmodic advance of the periphery of the sill. This is suggested by the fine-grained, low-sediment peperites of the upper margin (Fig. 19c,d), which consist largely of close-packed shards, including bubble-wall shards, which are probably the result of sudden falls of pressure at the advancing tip, accompanied by abrupt magma vesiculation, as accumulated stress is relieved by the sudden opening of a roof crack (16 of Fig. 38b), or by enlargement of the extension space itself. Kokelaar (1982) has noted this phenomenon. Among the published descriptions, noted earlier, of peperites associated with shallow magma intrusion, few (e.g. Branney and Suthren, 1988) specifically noted the presence of bubble-wall shards.

The model described here is also deficient in that it is unlikely that the magma behaved as a Newtonian fluid during emplacement. However, alternative flow regimes, such as that of a Bingham fluid, do not at present justify detailed attention in the light of current doubts on the validity of experimental evidence for Bingham behaviour of magma (Kerr and Lister, 1991). Also, no published modelling of sill emplacement deals with temperature and viscosity relationships in a fully integrated way. Jaegers's (1957, 1959) thermal models were based on instantaneous emplacement of hot magma, and while more sophisticated cooling models have since appeared (Patchett, 1980; Delaney, 1988; Smith et al., 1991) none of the theoretical or analogue modelling

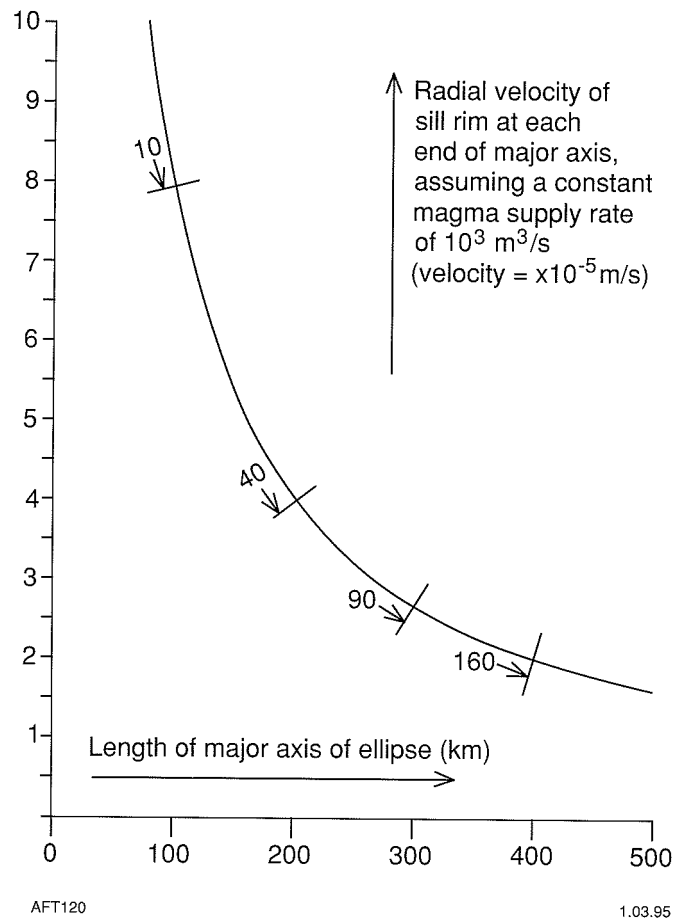


**Figure 40.** Relationship between radial velocity and length of major axis in a sill which has a uniform thickness of 200m and is an ellipse with a 5:1 elongation in plan. A constant magma supply rate is assumed. The numbered arrows along the curve show the approximate elapsed times in years after the start of intrusion when the major axis reached lengths of 100, 200, 300 and 400 km

of laccolith emplacement (Johnson and Pollard, 1973; Pollard and Johnson, 1973; Dixon and Simpson, 1987) takes temperature-related viscosity variations into account. A realistic model of Woongarra Rhyolite magma flow, which is beyond the scope of this report, would probably involve rapid flow of hot magma in the central part of the expanding sheet, so that continuous peripheral fluidization would be maintained, with the marginal parts of each sill acting as insulators. Such a mechanism might permit enhancement of magma transport within a sill in the same way that lava tubes facilitate the long-distance travel of erupted magma (Stephenson and Griffin, 1976).

Now that the mode of emplacement of the upper unit sill has been discussed in detail, the remaining history of the Woongarra Rhyolite can be covered more briefly. The upper sill reached its maximum extent, probably not far outside the present outcrop area of the Hamersley Group, when magma temperature fell to a point where the driving pressure could no longer overcome the increasing viscosity.

The cooling ('setting') of the upper unit sill effectively blocked the feeder pipe, for some unknown extent downwards, so that the deep magma chamber source was deprived of its pressure relief mechanism. After a further interval, silicic magma again rose up the feeder pipe, either reaming out the original channel, or establishing a contiguous parallel vent of similar size. As the rising magma approached the base of the upper unit sill, perhaps about 500 years after intrusion was complete (i.e. about 800 years after the start of sill formation), its pressure conditions would have been much the same as those of the first pulse of rising magma, but there would have been important differences in other factors controlling its further progress. In the first place the heat lost during cooling of the upper unit sill would have caused substantial heating of the adjacent sediments, and in particular an increase in temperature to  $>400^\circ\text{C}$  for a distance of 50 m below the sill (Jaeger, 1959, fig. 2). And in the second place the presence of the upper unit sill (18 of Fig. 38c), consisting at that time of cohesive rhyolitic glass still too hot for large-scale brittle failure but with a very high viscosity, would have presented a formidable mechanical barrier to

further upward progress. These two factors would have led to the initiation of a second sill (19 of Fig. 38c), now the lower unit of the Woongarra Rhyolite, below the first, but by an essentially analogous mechanism, in which an extension space (21 of Fig. 38c) at the periphery preceded the emplacement of rhyolite. In this case, however, the roof rocks were both hot and dry, so that explosive fluidization did not take place, and no proto-peperite formed; instead, the heated BIF and other rocks beneath the upper sill were close to their yield strength, so that a wide range of brittle and plastic deformation processes took place, to give the unusual mix of different structures (Fig. 12) in the median raft complex (20 of Fig. 38c).

The rhyolitic magma of the second sill, with essentially the same composition and temperature at intrusion as those of the first, would nevertheless have cooled more slowly because of its emplacement within pre-heated rocks. For the same reason its emplacement would have been faster, and its temperature at the end of emplacement higher. Do any petrographic or textural differences between the present upper and lower units of the Woongarra Rhyolite reflect these differences in the parameters of emplacement?

There are five principal differences between the chemically indistinguishable upper and lower units:

- the lower unit is characterized by abundant quartz paramorphs after tridymite;
- the snowflake (micropoikilitic) groundmass texture of the lower unit is coarser than that of the upper unit;
- spherulitic texture is characteristic of the lower unit;
- phenocrysts are fewer and smaller in the lower unit compared with the upper unit;
- although planar flow texture (sometimes plastically folded) and brittle autobrecciation occur in both units, flowage folds are relatively common in the lower unit, while autobrecciation is more typical of the upper unit.

All these differences can be argued to follow from the different temperatures and rates of emplacement, as well as from the different cooling rates suggested for the two bodies, although the relationship between these parameters and final rock textures is as yet poorly understood for rhyolitic glasses generally.

Eales (1974) reviewed the occurrence of quartz paramorphs after tridymite, and concluded that in intrusive rocks the crystallization of tridymite is a reliable index of high temperature (>870°C) and low pressure. If groundmass crystallization (or devitrification) of the two sills of the Woongarra Rhyolite did not begin until injection was completed, then this would have occurred at about 800°C in the upper sill, but possibly at 900°C in the more rapidly emplaced lower sill. Inhibition of crystal nucleation by magma movement is a phenomenon that does not appear to have been discussed in the literature, but it would account for the pervasive presence of tridymite paramorphs in the lower sill and their rarity or absence in the upper. It is possible that tridymite crystallized above 870°C in the upper sill before the end of magma movement, but there

is no textural evidence for its earlier presence in the present rocks; in the lower sill it is clear that no movement (strain) of the magma took place after tridymite crystallization (Fig. 9).

Snyder (1962) first introduced the name 'snowflake' texture as a petrographic term for the appearance of the matrix of porphyritic rhyolitic rocks from the Central Davis Mountains of Texas, and suggested that it formed by devitrification of a glass. Anderson (1969) studied the same rocks in closer detail, and identified the texture as consisting of 'more or less randomly oriented laths of alkali feldspar poikilitically enclosed by small patches of optically continuous silica, commonly alpha-quartz'. He also suggested that it was characteristic of the devitrification of welded ash-flow tuffs. This proposition can be discounted in the light of later discussion (Green, 1970; Anderson, 1970) and the studies of Lofgren (1971b), who showed that the identical texture, for which (following Haworth, 1888) he preferred the name 'micropoikilitic', could be formed by laboratory devitrification of natural rhyolite glass. Lofgren found that the texture developed best at temperatures between 400° and 650°C, and at pressures less than 300 MPa. The poikilitic quartz crystals formed in his experimental work were generally equidimensional, and between 0.2 and 1.5 mm in diameter; their boundaries were irregular in detail, and the crystals were 'choked with feldspar fibers'.

Lofgren (1971a) reviewed the formation of spherulites and suggested that they can form in any silicate melt (or glass) of appropriate composition under specific physical conditions; he concluded that 'the presence of spherulites does not uniquely define the mode of formation of the original material'. Lofgren, (1971b) was also able to produce spherulitic textures in rhyolitic glass under similar conditions to those which resulted in snowflake texture, and (ibid., fig. 3B) illustrated a micropoikilitic quartz patch that encloses several spherulites, presumably implying that the spherulites formed first.

On the third point, Figure 7 is taken as definitive textural evidence that, in the crystallization of the lower unit sill, the snowflake (micropoikilitic) texture developed later than the spherulites. It is consistent with Lofgren's (1971b) experimental results that the spherulites crystallized in the temperature range 650° to 700°C or higher, while the snowflake texture developed between 400° and 650°C. As the basic fabric of the snowflake texture is a fine-grained quartz mosaic, it would be reasonable to expect that during slow cooling the average grain size might increase through annealing, with a consequent decrease in free energy; faster cooling would result in less time for annealing. Both the absence of spherulites in the upper unit sill, and the smaller grain size of its snowflake texture (cf. Figs 7 and 15) are consistent with initiation of crystallization in the upper unit sill at a lower temperature (<800°C) as well as with its faster cooling.

Slower cooling of the lower unit sill is also consistent with the smaller size of the phenocrysts and their greater degree of resorption, which is presumed to have taken place partly during, but principally after, sill emplacement. The retention of the corroded material within the cooling

glass accounts for the lack of any chemical differences related to phenocryst size or abundance.

On the fifth point, the greater abundance of flowage folding in the lower unit is taken as evidence of irregular turbulent flow in the hotter and less viscous magma. Flow layering of this type is an earlier structure, which created compositional irregularities which were emphasized by irregularities in growth of the later spherulites (Fig. 6).

The final point of evidence consistent with an intrusive emplacement of the Woongarra Rhyolite is the probable stratigraphic discordance at the upper margin, the evidence for which was summarized at the beginning of this discussion. It probably provides the most critical single item of evidence for discrimination between silicic lava flows and sills, not only for the Woongarra Rhyolite but for all similar GLFSs.

At the conclusion of this discussion it needs to be emphasized that, in spite of the excellent exposure and relatively slight metamorphism and deformation of the Woongarra Rhyolite, its mode of emplacement has been an enigma since it was first formally defined by MacLeod et al. (1963). Although the study reported here has not produced a definitive resolution of this, it has shown that intrusion is the only emplacement mechanism consistent with all the evidence so far available; all other hypotheses involve the need to discount particular lines of evidence as irrelevant, equivocal, or coincidental. And yet the case has been built by integration of many lines of argument, rather than by establishment of one or two diagnostic features. The lesson to be learned from this for palaeo-volcanological interpretation is that the intrusive option is one which should be more strongly borne in mind than has hitherto been the case in many investigations of Precambrian rocks, particularly where exposure is poor; and also that interpretations based on a few supposedly diagnostic textural criteria should be made with extreme caution.

## Tests of the proposed hypothesis

Although it is clear from the foregoing discussion that there are strong grounds for preferring intrusion as the most likely emplacement mechanism for the Woongarra Rhyolite there are at least four areas in which additional evidence would provide useful further tests: these include zircon geochronology, detailed stratigraphy, search for sections which expose the lower margin, and further study of the dolerite sills within and below the Woongarra Rhyolite.

Recent progress in zircon geochronology, particularly using single-crystal methods, has brought error limits in favourable circumstances to about  $\pm 1$  m.y. The intrusion hypothesis described here predicts that the immediately overlying rocks should be older than the rhyolite of the upper unit, which should in turn be older than the lower unit; the demonstration of any other age sequence would require major changes to the emplacement mechanism suggested here. This test is a practical one, since a thin zircon-bearing tuffaceous band has been observed in

sample 60234 from the overlying shale at Woongarra Gorge (Fig. 21). Both the upper and lower units are known to contain abundant zircon, so that the feasibility of the test is mainly dependent on whether a resolution of  $\pm 1$  m.y. is small enough relative to the real time differences involved. The model examined in the preceding discussion postulates an intrusion depth of 200–300 m. If the depositional rate of the overlying rocks was as low as the 3–4 m/m.y. suggested as possible by Arndt et al. (1991) for the lower part of the Hamersley Group, there should be an easily measurable difference in age between the upper unit and the immediately overlying sediments. With depositional rates an order of magnitude greater the test should still be feasible. The model predicts that no age differences should be detectable between the two units of the Woongarra Rhyolite.

It has been argued that there may be slight stratigraphic discordance at the upper margin, based on observed lithological differences in the immediately overlying rocks (Fig. 21). However, insufficient work was done to exclude the possibility that these differences may be due to lateral facies changes. It would be useful to evaluate these alternatives by reconstructing a sedimentary stratigraphy of the upper Hamersley Group without the Woongarra Rhyolite, and determining its regional variation.

## The Kaapvaal connection

Striking similarities between aspects of the geological evolution of the Kaapvaal Craton (KC) of southern Africa and of the Pilbara Craton (PC) of northwestern Australia have been noted by many authors. Thus Trendall (1968) emphasized the similarities between the BIFs of the Transvaal Supergroup (KC) and those of the Hamersley Group (PC); and Button (1976) extended this comparison further to embrace the broader evolution of the two depositional basins. Grobler and Meakins (1988) made a detailed comparison of the Ventersdorp Supergroup (KC) with the Fortescue Group (PC), while Cheney et al. (1988) looked at the possible equivalence of unconformity-bounded sequences in the two cratons. Trendall et al. (1990) made a chronological comparison of the lithostratigraphically similar sequences of the two cratons between about 3.1 and 2.4 Ga.

During the preparation of this publication, the literature relating to the Kaapvaal Craton was reviewed to check whether any stratigraphic unit comparable to the Woongarra Rhyolite had been described within its supracrustal sequence. Although no closely comparable unit exists within the Chuniespoort Group, the BIF-rich lithostratigraphic analogue of the Hamersley Group, it is evident that the Rooiberg Felsite, within the Rooiberg Group of the Transvaal Supergroup, is similar in a number of ways to the Woongarra Rhyolite.

Figure 41 shows simplified stratigraphic columns of the relevant parts of the supracrustal sequences of the two cratons. The lowest units shown in that figure, the Ventersdorp Supergroup (KC) and Fortescue Group (PC) show compelling lithostratigraphic similarities (Grobler and Meakins, 1988) and substantial temporal

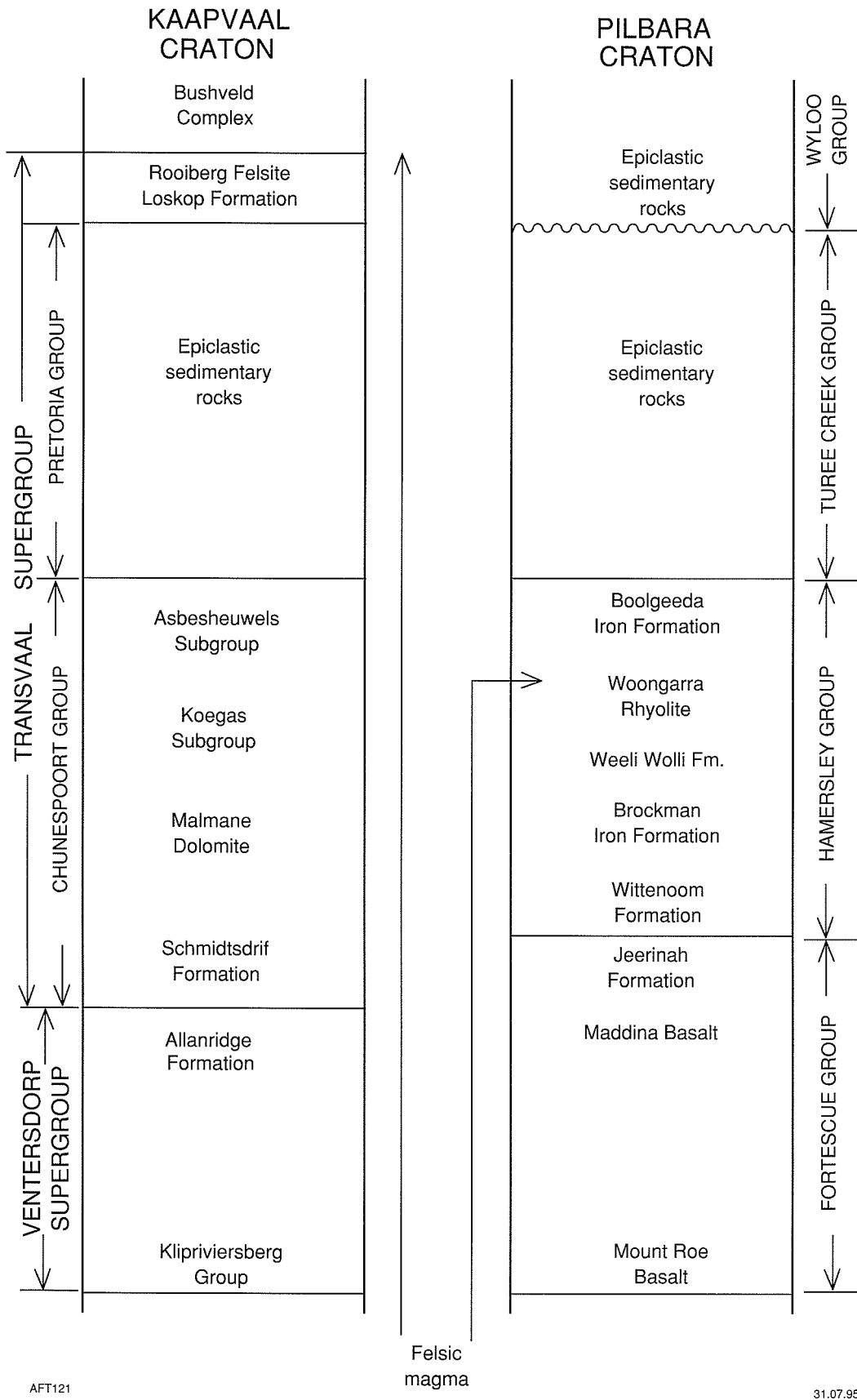


Figure 41. Simplified lithostratigraphic equivalence of part of the Precambrian supracrustal successions of the Kaapvaal (left) and Pilbara (right) Cratons. Only selected formal names are included, and the purpose of the diagram is purely to illustrate the text suggestion that equivalent magmas rising from depth at about the same time may have given rise to the Rooiberg Felsite and the Woongarra Rhyolite

overlap (Trendall et al., 1990). The thick carbonate-rich Campbellrand Subgroup may be correlative with the thinner dolomite of the Wittenoom Formation, while the overlying units, the BIF-rich Asbesheuwels and Koegas Subgroups (KC) and Hamersley Group (PC), are both lithologically and temporally equivalent. Immediately above these units the Pretoria Group (KC) and the Turee Creek Group (PC) both consist mainly of epiclastic sediments, although there are substantial lithological dissimilarities. The largely volcanic Rooiberg Group (KC) and Loskop Formation (KC) have no immediately apparent analogues in the Hamersley Basin, but closer examination reveals a possible relationship between the Woongarra Rhyolite and the Rooiberg Group (=Rooiberg Felsite).

Although the Rooiberg Felsite has not been extensively studied a summary review was given by Twist and French (1983). Twist (1985) provided a detailed account of the 3500+ m section in the immediate vicinity of Loskop Dam, while Walraven (1985, fig. 2) showed the relationship of the unit to other similar (and possibly related) silicic rocks of the Bushveld Complex. Twist and Harmer (1987) provided a detailed geochemical comparison of Rooiberg Felsite and Bushveld granites, building on the earlier work of Rhodes (1974).

From the descriptions in those papers the following similarities between the Woongarra Rhyolite and the Rooiberg Felsite may be listed:

- lavalike lithologies of the rhyolites/felsites;
- enormous volumes compared with other known occurrences of lavalike silicic rocks;
- very large outcrop areas;
- sheet-like form of individual felsite/rhyolite units;
- raft-like separation of felsite/rhyolite units by waterlain sedimentary rocks;
- general groundmass textures typically microcrystalline quartz and feldspar, often spherulitic, and commonly with undeformed quartz paramorphs after tridymite;
- close chemical similarity.

This last point has not been specifically made in the text above, but it is clear from comparison of Twist and Harmer's (1987) plots that rhyolites of the Woongarra Rhyolite fall generally within the more silicic part of the fields of low-Mg Rooiberg felsites on most diagrams. Another possible similarity may be the presence in the Rooiberg Felsite of peperites, since Twist and French

(1983) described, under the name agglomerate, rocks consisting of mixed sedimentary and felsitic clasts; and Rhodes and Du Plessis (1976) described a zone of large quartzite xenoliths whose emplacement is 'difficult to attribute ... to normal processes of volcanic eruption'. However, peperites resulting from the intrusion of rhyolitic magma have not yet been specifically described from the Rooiberg Felsite. This may be because the possibility of intrusion has not been seriously considered for any of its sheet-like igneous units. The criteria cited by Twist and French (1983) for their identification as lavas — the presence of planar and contorted flow banding, amygdalae, vesicles, lithophysae, and spherulites — may all be found in silicic intrusions, and in the light of earlier discussion the possibility of intrusion, even in part, seems to remain open. Certainly the arguments already set out against the identification of the Woongarra Rhyolite as subaerial lavas apply equally to the igneous units of the Rooiberg Felsite.

If Rooiberg Felsite sheets are intrusive then it is possible that they closely resemble the rocks that might have formed in the Hamersley Basin if the Woongarra Rhyolite had broken through the BIFs of the Hamersley Group, into the higher levels of the Turee Creek Group. Further evaluation of this speculative concept would be assisted by determination of the precise age of the Rooiberg Felsite. While the SACS (1980) age of 2150 Ma is accepted by all authors cited above as the best estimate of this, a substantially older real age is necessary if the Rooiberg Felsite is to be realistically considered as an analogue of the Woongarra Rhyolite.

## Acknowledgements

Dr R. C. Horwitz kindly supplied details of the location of sample No. W101, used by Pidgeon and Horwitz (1991) for their geochronological work. Thanks are also due to Dr R. C. Morris for supplying a pre-publication copy of a paper in press. Among many past and present colleagues in the Geological Survey of Western Australia who have helped me to understand aspects of the geology of the Woongarra Rhyolite, special thanks are due to Mr R. T. (Bob) Halligan, for introducing me to the Duck Creek section.

## References

- ANDERSON, E. M., 1938, The dynamics of sheet intrusion: Proceedings of the Royal Society of Edinburgh, v. B58, p. 242–251.
- ANDERSON, J. E., 1969, Development of snowflake texture in a welded tuff, Davis Mountains, Texas: Geological Society of America, Bulletin, v. 80, p. 2075–2080.
- ANDERSON, J. E., 1970, Snowflake texture not diagnostic of devitrified ash-flow tuffs: Reply: Geological Society of America, Bulletin, v. 81, p. 2529–2530.
- ARNDT, N. T., NELSON, D. R., COMPSTON, W., TRENDALL, A. F., and THORNE, A. M., 1991, The age of the Fortescue Group, Hamersley Basin, Western Australia, from ion microprobe zircon U–Pb results: Australian Journal of Earth Sciences, v. 38, p. 261–281.
- ARRIENS, P. A., 1975, Geochronological studies of some Proterozoic rocks in Australia: Geological Society of Australia, First Convention (Adelaide), Abstracts Volume, p. 63.
- AUSTRALIAN CODE OF STRATIGRAPHIC NOMENCLATURE, 1973 (4th edition, reprinted with corrigenda and additional notes): Geological Society of Australia Journal, v. 20, p. 105–112.
- BONNICHSEN, B., and KAUFFMAN, D. F., 1987, Physical features of rhyolite lava flows in the Snake River Plain volcanic province, southwestern Idaho, in The emplacement of silicic domes and lava flows edited by J. H. FINK: Geological Society of America, Special Paper, 212, p. 119–145.
- BRADLEY, J., 1965, Intrusion of major dolerite sills: Transactions of the Royal Society of New Zealand, v. 3, p. 27–55.
- BRANNEY, M. J., 1986, Letter discussing “Isolated pods of subaqueous welded ash-flow tuff: a distal facies of the Capel Curig Volcanic Formation (Ordovician), North Wales”, by Howells, M. F., Campbell, S. D. G., and Reedman, A. J., 1985, Geological Magazine, v. 122, p. 175–180: Geological Magazine, v. 123, p. 589–590.
- BRANNEY, M. J., and SUTHREN, R. J., 1988, High-level peperitic sills in the English Lake District: distinction from block lavas, and implications for Borrowdale Volcanic Group stratigraphy: Geological Journal, v. 23, p. 171–187.
- BROOKS, E. R., WOOD, M. M., and GARBUTT, P. L., 1982, Origin and metamorphism of peperite and associated rocks in the Devonian Elwell Formation, northern Sierra Nevada, California: Geological Society of America, Bulletin, v. 93, p. 1208–1231.
- BUSBY-SPERA, C. J., and WHITE, J. D. L., 1987, Variation in peperite textures associated with differing host-sediment properties: Bulletin of Volcanology, v. 49, p. 765–775.
- BUTTON, A., 1976, Transvaal and Hamersley Basins — review of basin development and mineral deposits: Minerals Science and Engineering, v. 8, p. 262–293.
- CARMICHAEL, I. S. E., TURNER, F. J., and VERHOOGEN, J., 1974, Igneous Petrology: New York, McGraw-Hill Book Company.
- CAS, R. A. F., 1977, Basin characteristics of the Early Devonian part of the Hill End Trough, New South Wales, based on a stratigraphic analysis of the Merriams Tuff: Journal of the Geological Society of Australia, v. 24, p. 381–401.
- CAS, R. A. F., 1978, Silicic lavas in Paleozoic flyschlike deposits in New South Wales, Australia: behavior of deep subaqueous silicic flows: Geological Society of America, Bulletin, v. 89, p. 1708–1714.
- CAS, R. A. F., and WRIGHT, J. V., 1987, Volcanic successions, modern and ancient: London, Allen and Unwin.
- CHENEY, E. S., ROERING, C., and STETTLER, E., 1988, Vaalbara: Geological Society of South Africa, Geocongress 88, Abstracts Volume, p. 85–88.
- COLE, R. B., and DeCELLES, P. G., 1991, Subaerial to submarine transitions in Early Miocene pyroclastic flow deposits, southern San Joaquin basin, California: Geological Society of America, Bulletin, v. 103, p. 221–235.
- COMPSTON, W., and ARRIENS, P. A., 1968, The Precambrian geochronology of Australia: Canadian Journal of Earth Sciences, v. 5, p. 561–583.
- COMPSTON, W., WILLIAMS, I. S., McCULLOCH, M. T., FOSTER, J. J., ARRIENS, P. A., and TRENDALL, A. F., 1981, A revised age for the Hamersley Group in Sediments through the ages edited by D. I. GROVES, K. McNAMARA, R. G. BROWN, and M. H. JOHNSTONE: Geological Society of Australia, 5th Convention, Perth, WA, Abstracts series no.3, p. 40.
- CREASER, R. A., and WHITE, A. J. R., 1991, Yardea Dacite — large-volume, high-temperature felsic volcanism from the Middle Proterozoic of South Australia: Geology, v. 19, p. 48–51.
- DANIELS, J. L., 1968, Turee Creek, W.A.: Western Australia Geological Survey, 1:250 000 Geological Series Explanatory Notes, 18p.
- DANIELS, J. L., 1970, Wylloo, W.A.: Western Australia Geological Survey, 1:250 000 Geological Series Explanatory Notes, 20p.
- DANIELS, J. L., and MacLEOD, W. N., 1965, Newman, W.A.: Western Australia Geological Survey, 1:250 000 Geological Series Explanatory Notes, 24p.
- DAVIES, D. K., QUEARRY, M. W., and BONIS, S. B., 1978, Glowing avalanches from the 1974 eruption of volcano Fuego, Guatemala: Geological Society of America, Bulletin, v. 89, p. 369–384.
- DAVY, R., 1992, Mineralogy and chemical composition of a core from the Weeli Wollli Formation in the Hamersley Basin: Western Australia Geological Survey, Record 1991/6, 103p.
- de la HUNTY, L. E., 1965, Mount Bruce, W.A.: Western Australia Geological Survey, 1:250 000 Geological Series Explanatory Notes, 28p.
- de la HUNTY, L. E., 1969, Robertson, W.A.: Western Australia Geological Survey, 1:250 000 Geological Series Explanatory Notes, 27p.
- DELANEY, P. T., 1988, FORTRAN 77 programs for conductivity cooling of dikes with temperature-dependent thermal properties and heat of crystallization: Computers and Geosciences, v. 14, p. 181–212.
- De ROSEN-SPENCE, A. F., PROVOST, G., DIMROTH, E., GOCHNAUER, K., and OWEN, V., 1980, Archean subaqueous felsic flows, Rouyn-Noranda, Quebec, Canada, and their Quaternary equivalents: Precambrian Research, v. 12, p. 43–77.

- DIXON, J. M., and SIMPSON, D. G., 1987, Centrifuge modelling of laccolith intrusion: *Journal of Structural Geology*, v. 9, p. 87–103.
- DRUMMOND, B. J., and SHELLEY, H. M., 1981, Isostasy and structure of the lower crust and upper mantle in the Precambrian terrains of northwest Australia, from regional gravity studies: *BMR Journal of Australian Geology and Geophysics*, v. 6, p. 137–143.
- DU TOIT, A. I., 1920, The Karroo Dolerites: *Transactions of the Geological Society of South Africa*, v. 33, p. 1–42.
- EALLES, H. V., 1974, The occurrence and geological significance of quartz paramorphs after tridymite in the north-eastern Cape: *Transactions of the Geological Society of South Africa*, v. 77, p. 37–51.
- EICHELBERGER, J. C., CARRIGAN, C. R., WESTRICH, H. R., and PRICE, R. H., 1986, Non-explosive silicic volcanism: *Nature*, v. 323, p. 598–602.
- EINSELE, G., GEISKES, J. M., CURRAY, J., MOORE, D. M., AGUAYO, E., AUBRY, M., FORNARI, D., GUERRERO, J., KASTNER, M., KELTS, K., LYLE, M., MATOBA, Y., MOLLINA-CRUZ, A., NIEMITZ, J., RUEDA, J., SAUNDERS, A., SCHRADER, H., SIMONEIT, B., and VACQUIER, V., 1980, Intrusion of basaltic sills into highly porous sediments, and resulting hydrothermal activity: *Nature*, v. 283, p. 441–445.
- EKREN, E. B., McINTYRE, D. H., and BENNETT, E. H., 1984, High-temperature, large-volume, lavalike ash-flow tuffs without calderas in southwestern Idaho: *United States Geological Survey, Professional Paper 1272*.
- EWERS, W. E., and MORRIS, R. C., 1981, Studies on the Dales Gorge Member of the Brockman Iron Formation, Western Australia: *Economic Geology*, v. 76, p. 1929–1953.
- FARQUHARSON, R. A., 1920, Part V. Petrology of the district, *in* The geology and mineral resources of the North-West, Central and Eastern Divisions between Long. 119° and 122°E and Lat. 22° and 28°S: *Western Australia Geological Survey, Bulletin 83*, p. 169–214.
- FISHER, R. V., and DIMROTH, E., 1978, Subaqueous volcanic rocks are examined: *Geotimes*, v. 23, p. 16–18.
- FISHER, R. V., and SCHMINCKE, H.-U., 1984, *Pyroclastic rocks*: Berlin, Springer-Verlag, 472p.
- FISKE, R. S., and MATSUDA, T., 1964, Submarine equivalents of ash flows in the Tokiwa Formation, Japan: *American Journal of Science*, v. 262, p. 76–106.
- FRANCIS, E. H., 1982, Magma and sediment — I Emplacement mechanism of late Carboniferous tholeiite sills in northern Britain: *Journal of the Geological Society of London*, v. 139, p. 1–20.
- FRANCIS, E. H., 1994, The Tennant Creek porphyry revisited: a synsedimentary sill with peperite margins, Early Proterozoic, Northern Territory — Reply to discussion by Trendall: *Australian Journal of Earth Sciences*, v. 41, p. 392.
- FRANCIS, E. H., and HOWELLS, M. F., 1973, Transgressive welded ash-flow tuffs among the Ordovician sediments of NE Snowdonia, North Wales: *Journal of the Geological Society of London*, v. 129, p. 621–641.
- FRIEDMAN, I., LONG, W., and SMITH, R. L., 1963, Viscosity and water content of rhyolite glass: *Journal of Geophysical Research*, v. 68, p. 6523–6535.
- GASS, I. G., HARRIS, P. G., and HOLDGATE, M. W., 1963, Pumice eruption in the area of the South Sandwich Islands: *Geological Magazine*, v. 100, p. 321–330.
- GEOLOGICAL SURVEY OF WESTERN AUSTRALIA, 1990, *Geology and mineral resources of Western Australia*: Western Australia Geological Survey, Memoir 3, 827p.
- GIBBON, D. L., 1969, Origin and development of the Star Mountain rhyolite: *Bulletin of Volcanology*, v. 33, p. 438–474.
- GILBERT, G. K., 1877, Report on the geology of the Henry Mountains: *United States Geographical and Geological Survey of the Rocky Mountains Region* (Powell).
- GRAPES, R. H., REID, D. L., and McPHERSON, J. G., 1972, Shallow dolerite intrusion and phreatic eruption in the Allan Hills region, Antarctica: *New Zealand Journal of Geology and Geophysics*, v. 17, p. 563–577.
- GREEN, J. C., 1970, Snowflake texture not diagnostic of devitrified ash-flow tuffs: Discussion: *Geological Society of America, Bulletin*, v. 81, p. 2527–2528.
- GRETENER, P. E., 1969, On the mechanics of the intrusion of sills: *Canadian Journal of Earth Sciences*, v. 6, p. 1415–1419.
- GROBLER, N. J., and MEAKINS, A., 1988, Comparison between the Fortescue Group and the Ventersdorp Supergroup: *Geological Society of South Africa, Geocongress 88, Abstracts Volume*, p. 211–214.
- GUEST, J. E., and SANCHEZ, J., 1969, A large dacitic lava flow in northern Chile: *Bulletin of Volcanology*, v. 33, p. 778–790.
- HANSON, R. E., 1991, Quenching and hydroclastic disruption of andesitic to rhyolitic intrusions in a submarine island-arc sequence, northern Sierra Nevada, California: *Geological Society of America, Bulletin*, v. 103, p. 804–816.
- HANSON, R. E., and SCHWEICKERT, R. A., 1982, Chilling and brecciation of a Devonian rhyolite sill intruded into wet sediments, northern Sierra Nevada, California: *Journal of Geology*, v. 90, p. 717–724.
- HAUSBACK, B. P., 1987, An extensive, hot, vapor-charged rhyodacite flow, Baja California, Mexico, *in* The emplacement of silicic domes and lava flows *edited by* J. H. FINK: *Geological Society of America, Special Paper 212*, p. 111–118.
- HAWORTH, E., 1888, A contribution to the Archaean geology of Missouri: *American Geology*, v. 1, p. 280–297, 363–382.
- HENRY, C. D., PRICE, J. G., RUBIN, J. N., PARKER, D. F., WOLFF, J. A., SELF, S., FRANKLIN, R., and BARKER, D. S., 1988, Widespread, lavalike silicic volcanic rocks of Trans-Pecos Texas: *Geology*, v. 16, p. 509–512.
- HENRY, C. D., PRICE, J. G., RUBIN, J. N., and LAUBACH, S. E., 1990, Case study of an extensive silicic lava: the Bracks Rhyolite, Trans-Pecos Texas: *Journal of Volcanology and Geothermal Research*, v. 43, p. 113–132.
- HORWITZ, R. C., 1978, The Lower Proterozoic of the Wyloo Anticline: *Australia CSIRO, Minerals Research Laboratories, Division of Mineralogy, Report FP 20*.
- HOWELLS, M. F., CAMPBELL, S. D. G., and REEDMAN, A. J., 1985, Isolated pods of subaqueous welded ash-flow tuff: a distal facies of the Capel Curig Volcanic Formation (Ordovician), North Wales: *Geological Magazine*, v. 122, p. 175–180.
- HOWELLS, M. F., and LEVERIDGE, B. E., 1980, The Capel Curig Volcanic Formation: *Institute of Geological Sciences, Report 80/6*.
- HOWELLS, M. F., LEVERIDGE, B. E., ADDISON, R., EVANS, C. D. R., and NUTT, M. J. C., 1979, The Capel Curig Volcanic Formation, Snowdonia, North Wales; variations in ash-flow tuffs related to emplacement environments, *in* The Caledonides of the British Isles — reviewed *edited by* A. L. HARRIS, C. H. HOLLAND, and B. E. LEAKE: *Geological Society of London, Special Publication No. 8*, p. 611–618.
- HOWELLS, M. F., LEVERIDGE, B. E., and EVANS, C. D. R., 1973, Ordovician ash-flow tuffs in eastern Snowdonia: *Institute of Geological Sciences, Report 73/3*.
- HOWELLS, M. F., REEDMAN, A. J., and CAMPBELL, S. D. G., 1986, The submarine eruption and emplacement of the Lower Rhyolitic Tuff Formation (Ordovician), N Wales: *Journal of the Geological Society of London*, v. 143, p. 411–423.

- HULME, G., 1974, The interpretation of lava flow morphology: *Geophysical Journal of the Royal Astronomical Society*, v. 39, p. 361–383.
- HUNT, C. B., 1953, *Geology and geography of the Henry Mountains region, Utah*: United States Geological Survey, Professional Paper 228.
- JAEGER, J. C., 1957, The temperature in the neighbourhood of a cooling intrusive sheet: *American Journal of Science*, v. 255, p. 306–318.
- JAEGER, J. C., 1959, Temperatures outside a cooling intrusive sheet: *American Journal of Science*, v. 257, p. 44–54.
- JENSEN, L. S., 1976, A new cation plot for classifying subalkalic volcanic rocks: Ontario Division of Mines, Miscellaneous Paper 66.
- JOHNSON, A. M., and POLLARD, D. D., 1973, Mechanics of growth of some laccolithic intrusions in the Henry Mountains, Utah – I. Field observations, Gilbert's model, physical properties and flow of the magma: *Tectonophysics*, v. 18, p. 261–309.
- JONES, J. G., 1967, A lacustrine volcano of central France, and the nature of peperites: *Proceedings of the Geologists' Association*, v. 80, p. 177–188.
- JONES, J. G., 1969, Pillow lavas as depth indicators: *American Journal of Science*, v. 267, p. 181–195.
- KANO, K., 1989, Interactions between andesitic magma and poorly consolidated sediments: examples in the Neogene Shirahama Group, South Izu, Japan: *Journal of Volcanology and Geothermal Research*, v. 37, p. 59–75.
- KERR, R. C., and LISTER, J. R., 1991, The effects of shape on crystal settling and on the rheology of the magma: *Journal of Geology*, v. 99, p. 457–467.
- KERR, R. C., and LISTER, J. R., 1995, The lateral intrusion of silicic magmas into unconsolidated sediments: the Tennant Creek porphyry revisited: *Australian Journal of Earth Sciences*, v. 42, p. 223–224.
- KIEFFER, S. W., 1981, Fluid dynamics of the May 18 blast at Mount St. Helens: United States Geological Survey, Professional Paper 1250, p. 379–400.
- KOCH, F. G., JOHNSON, A. M., and POLLARD, D. D., 1981, Monoclinical bending of strata over laccolithic intrusions: *Tectonophysics*, v. 74, p. T21–T31.
- KOKELAAR, B. P., 1982, Fluidization of wet sediments during the emplacement and cooling of various igneous bodies: *Journal of the Geological Society of London*, v. 139, p. 21–33.
- KOKELAAR, B. P., BEVINS, R. E., and ROACH, R. A., 1985, Submarine silicic volcanism and associated sedimentary and tectonic processes, Ramsey Island, SW Wales: *Journal of the Geological Society of London*, v. 152, p. 591–613.
- KRIEVALDT, M. K., and RYAN, G. R., 1967, Pyramid, W.A.: Western Australia Geological Survey, 1:250 000 Geological Series Explanatory Notes.
- KRONER, A., THORPE, R. I., and HICKMAN, A. H., in prep., Geochronological comparison of the evolution of the granite–greenstone terranes of the Pilbara and Kaapvaal Cratons: *Geology*.
- LEAMAN, D. E., 1975, Form, mechanism and control of dolerite intrusion near Hobart, Tasmania: *Journal of the Geological Society of Australia*, v. 22, p. 175–186.
- LEAMAN, D. E., 1995, Mechanics of sill emplacement: comments based on the Tasmanian dolerites: *Australian Journal of Earth Sciences*, v. 42, p. 151–155.
- LEGGO, P. J., COMPSTON, W., and TRENDALL, A. F., 1965, Radiometric ages of some Precambrian rocks from the North West Division of Western Australia: *Journal of the Geological Society of Australia*, v. 12, pt. 1, p. 53–66.
- LE MAITRE, R. W. (editor), BATEMAN, P., DUDEK, A., KELLER, J., LAMEYRE, J., LE BAS, M. J., SABINE, P. A., SCHMID, R., SORENSEN, A., STRECKEISEN, A., WOOLLEY, A. R., and ZANETTIN, B., 1989, A classification of igneous rocks and glossary of terms — Recommendations of the International Union of Geological Sciences Subcommittee on the Systematics of Igneous Rocks: Oxford, Blackwells Scientific Publications.
- LOFGREN, G., 1971a, Spherulitic textures in glassy and crystalline rocks: *Journal of Geophysical Research*, v. 76, p. 5635–5648.
- LOFGREN, G., 1971b, Experimentally produced devitrification textures in natural rhyolitic glass: *Geological Society of America, Bulletin*, v. 82, p. 111–124.
- LOFGREN, G., 1980, Experimental studies on the dynamic crystallization of silicate melts, in *Physics of magmatic processes edited by R. B. HARGRAVES*: Princeton, New Jersey, Princeton University Press, p. 487–551.
- LOWMAN, R. D. W., and BLOXAM, T. W., 1981, The petrology of the Lower Palaeozoic Fishguard Volcanic Group and associated rocks east of Fishguard, north Pembrokeshire (Dyfed), South Wales: *Journal of the Geological Society of London*, v. 138, p. 47–68.
- LYELL, C., 1865, *Elements of geology* (6th Edition): London, John Murray.
- MACLEOD, W. N., 1966, The geology and iron deposits of the Hamersley Range area: Western Australia Geological Survey, Bulletin 117.
- MACLEOD, W. N., and de la HUNTY, L. E., 1966, Roy Hill, W.A.: Western Australia Geological Survey, 1:250 000 Geological Series Explanatory Notes.
- MACLEOD, W. N., de la HUNTY, L. E., JONES, W. R., and HALLIGAN, R., 1963, A preliminary report on the Hamersley Iron Province, North-West Division: Western Australia Geological Survey, Annual Report for 1962, p. 44–54.
- MANLEY, C. R., 1992, Extended cooling and viscous flow of large, hot rhyolite lavas: implications of numerical modeling results: *Journal of Volcanology and Geothermal Research*, v. 53, p. 27–46.
- MARSHALL, P., 1935, Acid rocks of the Taupo–Rotorua volcanic district: *Transactions of the Royal Society of New Zealand*, v. 64, p. 323–366.
- MARTIN, B. S., 1989, The Roza Member, Columbia River Basalt Group; chemical stratigraphy and flow distribution, in *Volcanism and tectonism in the Columbia River Flood-Basalt Province edited by S. P. REIDEL, and P. R. HOOPER*: Geological Society of America, Special Paper 239, p. 85–104.
- McBIRNEY, A. R., and MURASE, T., 1984, Rheological properties of magmas: *Annual Reviews of Earth and Planetary Science*: v. 12, p. 337–357.
- McPHIE, J., 1993, The Tennant Creek porphyry revisited: a synsedimentary sill with peperite margins, Early Proterozoic, Northern Territory: *Australian Journal of Earth Sciences*, v. 40, p. 545–558.
- McPHIE, J., 1994, The Tennant Creek porphyry revisited: a synsedimentary sill with peperite margins, Early Proterozoic, Northern Territory — Reply to discussion by A. F. Trendall: *Australian Journal of Earth Sciences*, v. 41, p. 393–394.
- MILLWARD, D., and LAWRENCE, D. J. D., 1985, The Stockdale (Yarlside) Rhyolite — a rheomorphic ignimbrite?: *Proceedings of the Yorkshire Geological Society*, v. 45, p. 299–306.
- MINAKAMI, T., 1950, Recent activities of Volcano Usu (V). Topographical deformation during the 1943–1945 eruption: *Bulletin of the Earthquake Research Institute*, v. 28, p. 143–153.
- MOORE, J. G., 1965, Petrology of deep-sea basalt near Hawaii: *American Journal of Science*, v. 263, p. 40–52.

- MORRIS, R. C., 1993, Genetic modelling for banded iron-formation of the Hamersley Group, Pilbara Craton, Western Australia: *Precambrian Research*, v. 60, Special Issues, Nos 1–4, p. 243–286.
- MORRIS, R. C., and HORWITZ, R. C., 1983, The origin of the BIF-rich Hamersley Group of Western Australia — deposition on a platform: *Precambrian Research*, v. 21, p. 273–297.
- MUDGE, M. R., 1968, Depth control of some concordant intrusions: *Geological Society of America, Bulletin*, v. 79, p. 315–332.
- MULLER, G., 1967, Diagenesis in argillaceous sediments: *in Diagenesis in sediments edited by G. LARSEN and G. V. CHILINGAR*: Amsterdam, Elsevier.
- MURASE, T., 1962, Viscosity and related properties of volcanic rocks at 800° to 1400°C: *Hokkaido University Faculty of Science Journal, Series 7*, v. 1, p. 487–584.
- MURASE, T., and MCBIRNEY, A. R., 1973, Properties of some common igneous rocks and their melts at high temperatures: *Geological Society of America, Bulletin*, v. 84, p. 3563–3592.
- MYERS, J. S., and HOCKING, R. M. (compilers), 1988, *Geological Map of Western Australia, 1:2 500 000*: Western Australia Geological Survey.
- ORTON, G., 1987, Discussion on the submarine eruption and emplacement of the Lower Rhyolitic Tuff Formation (Ordovician), North Wales: *Journal of the Geological Society of London*, v. 144, p. 523–525.
- PAIGE, S., 1913, The bearing of progressive increase of viscosity during intrusion on the form of laccoliths: *Journal of Geology*, v. 21, p. 541–549.
- PATCHETT, P. J., 1980, Thermal effects of basalt on continental crust and crustal contamination of magma: *Nature*, v. 283, p. 559–561.
- PICHLER, H., 1975, Acid hyaloclastites: *Bulletin of Volcanology*, v. 28, p. 293–310.
- PIDGEON, R. T., and HORWITZ, R. C., 1991, The origin of olistoliths in Proterozoic rocks of the Ashburton Trough, Western Australia, using zircon U–Pb isotopic characteristics: *Australian Journal of Earth Sciences*, v. 38(1), p. 55–63.
- POLLARD, D. D., 1973, Derivation and evaluation of a mechanical model for sheet intrusions: *Tectonophysics*, v. 19, p. 233–269.
- POLLARD, D. D., and JOHNSON, A. M., 1973, Mechanics of growth of some laccolithic intrusions in the Henry Mountains, Utah – II. Bending and failure of overburden layers and sill formation: *Tectonophysics*, v. 18, p. 311–354.
- PRICE, N. J., 1975, Rates of deformation: *Journal of the Geological Society of London*, v. 131, p. 553–575.
- REEDMAN, A. J., HOWELLS, M. F., ORTON, G., and CAMPBELL, D. G., 1987, The Pitts Head Tuff Formation: a subaerial to submarine ash-flow tuff of Ordovician age, North Wales: *Geological Magazine*, v. 124, p. 427–439.
- RHODES, R. C., 1974, Petrochemical characteristics of Bushveld Granite and Rooiberg Felsite: *Transactions of the Geological Society of South Africa*, v. 77, p. 93–98.
- RHODES, R. C., and Du PLESSIS, M. D., 1976, Notes on some stratigraphic relations in the Rooiberg Felsite: *Transactions of the Geological Society of South Africa*, v. 79, p. 183–185.
- ROBERTS, J. R., 1970, The intrusion of magma into brittle rocks, *in Mechanism of igneous intrusion edited by G. NEWALL and N. RAST*: *Geological Journal, Special Issue No. 2*, p. 287–338.
- ROSS, G. S., and SMITH, R. L., 1961, Ash-flow tuffs, their origin, geological relations and identification: *United States Geological Survey, Professional Paper 366*.
- RYAN, M. P., 1987, Neutral buoyancy and the mechanical evolution of magmatic systems, *in Magmatic Processes: Physico-chemical Principles edited by B. O. MYSON*: *Geochemical Society, Special Publication 1*, p. 259–287.
- SACS (SOUTH AFRICAN COMMITTEE FOR STRATIGRAPHY), 1980, *Lithostratigraphy of the Republic of South Africa, South West Africa/Namibia, and the Republics of Bophuthatswana, Transkei and Venda compiled by L. E. KENT*: *Geological Survey of South Africa, Handbook 8*.
- SCHMINCKE, H-U., 1967, Fused tuff and peperites in South-Central Washington: *Geological Society of America, Bulletin*, v. 78, p. 319–330.
- SCROPE, J. P., 1862, *Volcanoes. The character of their phenomena, their share in the structure and composition of the globe, and their relation to its internal forces*, (2nd edition): London, Longman, Green, Longmans and Roberts, 490p.
- SEYMOUR, D. B., THORNE, A. M., and BLIGHT, D. F., 1988, Wyloo, W.A. (2nd edition): *Western Australia Geological Survey, 1:250 000 Geological Series Explanatory Notes*.
- SHAW, H. R., 1963, Obsidian–H<sub>2</sub>O viscosities at 1000 and 2000 bars in the temperature range 700° to 900°C: *Journal of Geophysical Research*, v. 68, p. 6337–6343.
- SHAW, H. R., and SWANSON, D. A., 1970, Eruption and flow rates of flood basalts: *Proceedings of the Second Columbia River Basalt Symposium*, Cheney, Eastern Washington State College Press, p. 271–299.
- SHERATON, J. W., and SIMONS, L., 1988, *Geochemical data analysis system reference manual: Australia BMR, Record 1988/45*.
- SMEDES, H., 1956, Peperites as contact phenomena of sills in the Elkhorn Mountains, Montana (Abstract): *Geological Society of America, Bulletin*, v. 67, p. 1783.
- SMEDES, H., 1966, *Geology and igneous petrology of the Northern Elkhorn Mountains, Jefferson and Broadwater Counties, Montana: United States Geological Survey, Professional Paper 510*.
- SMITH, B., BONNEVILLE, A., and HAMZAOUI, R., 1991, Flow duration of a dike constrained by palaeomagnetic data: *Geophysical Journal International*, v. 106, p. 621–634.
- SNYDER, J. L., 1962, *Geological investigations, central Davis Mountains, Texas: Texas Journal of Science*, v. 14, p. 197–215.
- SPARKS, R. S. J., 1978, The dynamics of bubble formation and growth in magmas: a review and analysis: *Journal of Volcanology and Geothermal Research*, v. 3, p. 1–37.
- SPARKS, R. S. J., SIGURDSSON, H., and CAREY, S. N., 1980a, The entrance of pyroclastic flows into the sea, I. Oceanographic and geologic evidence from Dominica, Lesser Antilles: *Journal of Volcanology and Geothermal Research*, v. 7, p. 87–96.
- SPARKS, R. S. J., SIGURDSSON, H., and CAREY, S. N., 1980b, The entrance of pyroclastic flows into the sea, II. Theoretical considerations on subaqueous emplacement and welding: *Journal of Volcanology and Geothermal Research*, v. 7, p. 97–105.
- SPARKS, R. S. J., WILSON, L., and HULME, G., 1978, Theoretical modelling of the generation, movement and emplacement of pyroclastic flows by column collapse: *Journal of Geophysical Research*, v. 83, p. 1727–1739.
- STAINES, H. R. E., 1985, *Field geologist's guide to lithostratigraphic nomenclature in Australia: Australian Journal of Earth Science*, v. 32, p. 83–106.
- STEPHENSON, P. J., and GRIFFIN, T. J., 1976, Some long basaltic lava flows in north Queensland, *in Volcanism in Australia edited by R. W. JOHNSON*: Amsterdam, Elsevier, p. 41–51.
- STEVEN, T. A., and LIPMAN, P. W., 1976, *Calderas of the San Juan volcanic field, southwestern Colorado: United States Geological Survey, Professional Paper 958*.

- STIX, J., 1991, Subaqueous, intermediate to silicic-compositions explosive volcanism: a review: *Earth Science Reviews*, v. 31, p. 21–53.
- SUN, S. S., and McDONOUGH, W. F., 1989, Chemical and isotope systematics of oceanic basalts: implications for mantle composition and processes, in *Magmatism in the ocean basins* edited by A. D. SAUNDERS and M. J. NORRY: Geological Society of London, Special Publications no. 42, p. 313–345.
- TALBOT, H. W. B., 1920, The geology and mineral resources of the North-West, Central and Eastern Divisions between Long. 119° and 122°E and Lat. 22° and 28°S: Western Australia Geological Survey, Bulletin 83, 218p.
- THORNE, A. M., and TYLER, I. M., 1991, Turee Creek, W.A. (2nd edition): Western Australia Geological Survey, 1:250 000 Geological Series Explanatory Notes, 29p.
- TOLAN, T. L., REIDEL, S. P., BEESON, M. H., ANDERSON, J. L., FECHT, K. R., and SWANSON, D. A., 1989, Revisions to the estimates of the areal extent and volume of the Columbia River Basalt Group, in *Volcanism and tectonism in the Columbia River Flood-Basalt Province* edited by S. P. REIDEL and P. R. HOOPER: Geological Society of America, Special Paper 239, p. 1–20.
- TRENDALL, A. F., 1963, Some Proterozoic volcanic rocks from the North West Division: Western Australia Geological Survey, Annual Report 1962, p. 106–108.
- TRENDALL, A. F., 1968, Three great basins of iron-formation deposition: *Geological Society of America, Bulletin*, v. 79, p. 1527–1544.
- TRENDALL, A. F., 1972, An unusual eutaxitic rock from the Precambrian Hamersley Group, Western Australia: Western Australia Geological Survey, Annual Report for 1971, p. 65–68.
- TRENDALL, A. F., 1973, Varve cycles in the Weeli Wolli Formation of the Precambrian Hamersley Group, Western Australia: *Economic Geology*, v. 68, p. 1089–1097.
- TRENDALL, A. F., 1975, Hamersley Basin in *The Geology of Western Australia*: Western Australia Geological Survey, Memoir 2, p. 118–141.
- TRENDALL, A. F., 1976, Geology of the Hamersley Basin: *International Geological Congress, 25th, Sydney, N.S.W., Excursion Guide 43A*.
- TRENDALL, A. F., 1983, The Hamersley Basin, in *Iron-formation: facts and problems* edited by A. F. TRENDALL and R. C. MORRIS: Elsevier, Amsterdam, p. 69–129.
- TRENDALL, A. F., 1990, Hamersley Basin, in *Geology and mineral resources of Western Australia*: Western Australia Geological Survey, Memoir 3, p. 163–189.
- TRENDALL, A. F., 1994, The Tennant Creek porphyry revisited: a synsedimentary sill with peperite margins, Early Proterozoic, Northern Territory — Discussion of McPhie, 1993: *Australian Journal of Earth Sciences*, v. 41, p. 391–392.
- TRENDALL, A. F., and BLOCKLEY, J. G., 1970, The iron formations of the Precambrian Hamersley Group, Western Australia: Western Australia Geological Survey, Bulletin 119, 366p.
- TRENDALL, A. F., COMPSTON, W., WILLIAMS, I. S., ARMSTRONG, R. A., ARNDT, N. T., McNAUGHTON, N. J., NELSON, D. R., BARLEY, M. E., BEUKES, N. J., de LAETER, J. R., RETIEF, E. A., and THORNE, A. M., 1990, Precise zircon U–Pb chronological comparison of the volcano-sedimentary sequences of the Kaapvaal and Pilbara Cratons between about 3.1 and 2.4 Ga: *Third International Archaean Symposium, Perth, Abstracts Volume*, p. 81–83.
- TRENDALL, A. F., and de LAETER, J. R., 1972, Apparent age, and origin, of black porcelanite of the Joffre Member: Western Australia Geological Survey, Annual Report 1971, p. 68–74.
- TWIST, D., 1985, Geochemical evolution of the Rooiberg silicic lavas in the Loskop Dam area, southeastern Bushveld: *Economic Geology*, v. 80, p. 1153–1165.
- TWIST, D., and BRISTOW, J. W., 1990, Extensive lava-like siliceous flows in southern Africa: a review of occurrences: *Research Reports of the Institute for Geological Research on the Bushveld Complex (University of Pretoria)*, No.82, 35p.
- TWIST, D., and FRENCH, B. M., 1983, Voluminous acid volcanism in the Bushveld Complex: a review of the Rooiberg Felsite: *Bulletin of Volcanology*, v. 46, p. 225–242.
- TWIST, D., and HARMER, R. E. J., 1987, Geochemistry of contrasting siliceous magmatic suites in the Bushveld Complex: genetic aspects and implications for tectonic discrimination diagrams: *Journal of Volcanology and Geothermal Research*, v. 32, p. 83–98.
- TYLER, I. M., HUNTER, W. M., and WILLIAMS, I. R., 1991, Newman, W.A. (2nd edition): Western Australia Geological Survey, 1:250 000 Geological Series Explanatory Notes, 36p.
- VUTUKURI, V. S., LAMA, R. D., and SALUJA, S. S., 1974, *Handbook on mechanical properties of rocks*, v. 1: Clausthal, Trans Tech Publications, 280p.
- WAGER, L. R., WEEDON, D. S., and VINCENT, E. A., 1953, A granophyre from Coire Uaigneich, Isle of Skye, containing quartz paramorphs after tridymite: *Mineralogical Magazine*, v. 24, p. 263–276.
- WALKER, B. H., and FRANCIS, E. H., 1987, High-level emplacement of an olivine-dolerite sill into Namurian sediments near Cardenden, Fife: *Transactions of the Royal Society of Edinburgh, Earth Sciences*, v. 77, p. 295–307.
- WALKER, G. P. L., 1973, Lengths of lava flows: *Philosophical Transactions of the Royal Society of London*, v. 274, p. 107–118.
- WALKER, G. P. L., 1974, Eruptive mechanisms in Iceland, in *Geodynamics of Iceland and the North Atlantic area* edited by L. KRISTJANSSON: Dordrecht, Reidel, p. 189–201.
- WALKER, G. P. L., 1989, Gravitational (density) controls on volcanism, magma chambers and intrusions: *Australian Journal of Earth Sciences*, v. 36, p. 149–165.
- WALRAVEN, F., 1985, Genetic aspects of the granophyric rocks of the Bushveld Complex: *Economic Geology*, v. 80, p. 1166–1180.
- WESTRICH, H. R., STOCKMAN, H. W., and EICHELBERGER, J. C., 1988, Degassing of rhyolitic magma during ascent and emplacement: *Journal of Geophysical Research*, v. 93, p. 6503–6511.
- WILLIAMS, H., 1927, *The Geology of Snowdon (North Wales)*: Quarterly Journal of the Geological Society of London, v. 83, p. 133–140.
- WILLIAMS, H., and McBIRNEY, A. R., 1979, *Volcanology*: San Francisco, Freeman, Cooper and Company, 397p.
- WILLIAMS, I. R., 1968, Yarraloola, W.A.: Western Australia Geological Survey, 1:250 000 Geological Series Explanatory Notes, 30p.
- WILLIAMS, I. R., and TYLER, I. M., 1989, Robertson, W.A. (2nd edition): Western Australia Geological Survey, 1:250 000 Geological Series Explanatory Notes, 36p.
- WILSON, L., SPARKS, R. S. J., and WALKER, G. P. L., 1980, Explosive volcanic eruptions – IV. The control of magma properties and conduit geometry on eruption column behaviour: *Geophysical Journal of the Royal Astronomical Society*, v. 63, p. 117–148.